11 Granular Filtration

MWH's Water Treatment: Principles and Design, Third Edition
John C. Crittenden, R. Rhodes Trussell, David W. Hand, Kerry J. Howe and George Tchobanoglous

Copyright © 2012 John Wiley & Sons, Inc.

Terminology for Granular Filtration

Term	Definition
Air scour	Optional feature during backwash in which air is introduced into filter underdrains along with backwash water; the vigorous scouring action helps clean deep-bed filters.
Backwash	Process for removing accumulated solids from a filter bed by reversing the water flow.
Bag and cartridge filtration	Pressure driven separation processes that remove particles larger than 1 μm using an engineered porous filtration media consisting of fabric or self-supporting filter elements.
Conventional treatment	Process train consisting of coagulation, flocculation, sedimentation, and filtration.
Contact filtration	Process train consisting of coagulation and filtration.
Depth filtration	Filtration mechanism in which particles accumulate throughout the depth of a granular filter bed by colliding with and adhering to the media. Captured particles can be many times smaller than the pore spaces in the bed.
Diatomaceous earth	Granular material of nearly pure silica, mined from natural deposits of fossilized diatoms that is used as a filtration media in precoat filtration.

Term	Definition
Direct filtration	Process train consisting of coagulation, flocculation, and filtration.
Effective size (ES)	Measure of the size of granular media; the size at which 10 percent of the media has a smaller diameter (d_{10}) as determined by a sieve analysis.
Filtration	Removal of particles (solids) from a suspension (two-phase system containing particles and liquid) by passage of the suspension through a porous medium. In granular filtration, the porous medium is a bed of granular material.
Filtration rate	Key process variable; the superficial water velocity through the filter bed, calculated as the flow rate divided by the cross-sectional area of the bed.
In-line filtration	Contact filtration.
Precoat filtration	Granular filtration process in which a fine granular material is introduced into the filter module and collects as a thin cake against a support septum; filtration occurs by straining at the surface of this cake layer.
Rapid filtration	Granular filtration process engineered to achieve filtration rates about 100 times greater than slow sand filtration. Key requirements include coagulation pretreatment, granular media sieved for greater uniformity, and backwashing to remove accumulated particles.
Ripening	Process of granular media conditioning at the beginning of a filter run during which clean media captures particles and becomes more efficient at capturing additional particles. During ripening filter effluent water may not meet quality requirements and must be wasted; typically it is recycled to the head of the plant.
Schmutzdecke	Layer of particles and microorganisms that forms in the top few centimeters of a slow sand filter.
Slow sand filtration	Granular filtration process during which water passes slowly down through a bed of sand. Filtration occurs primarily by straining at the surface of the Schmutzdecke located at the top of the bed.
Specific deposit	Mass of accumulated particles in a filter per unit of filter volume
Straining	Filtration mechanism in which particles are captured at the surface of a filter because they are too large to fit through the pore spaces in the filter.

Term	Definition
Underdrain	Components installed at the base of a filter bed. Underdrains must support the media and evenly collect filter effluent and distribute backwash water (and air) to avoid channeling in the filter bed.
Uniformity coefficient (UC)	Measure of the uniformity of granular media; the ratio of the 60th percentile (d_{60}) to the 10th percentile (d_{10}) media sizes as determined by a sieve analysis.
Unit filter run volume (UFRV)	Quantity of water that passes through a filter over the course of an entire filter run.

Filtration is widely used for removing particles from water. Filtration can be defined as any process for the removal of solid particles from a suspension (a two-phase system containing particles in a fluid) by passage of the suspension through a porous medium. In granular filtration, the porous medium is a thick bed of granular material such as sand. The most common granular filtration technology in water treatment is *rapid filtration*. The term is used to distinguish it from *slow sand filtration*, an older filtration technology with a filtration rate 50 to 100 times lower than rapid filtration. Key features of rapid filtration include granular media sieved for greater uniformity, coagulation pretreatment, backwashing to remove accumulated particles, and a reliance on *depth filtration* as the primary particle removal mechanism. In depth filtration, particles accumulate throughout the depth of the filter bed by colliding with and adhering to the media. Captured particles can be many times smaller than the pore spaces in the bed.

Nearly all surface water treatment facilities and some groundwater treatment facilities use filtration. Most surface waters contain algae, sediment, clay, and other organic or inorganic particles. Filtration improves the clarity of water by removing these particles. All surface waters also contain microorganisms that can cause illness, and filtration is nearly always required in conjunction with chemical disinfection to assure that water is free of these pathogens. Groundwater is often free of significant concentrations of microorganisms or particles, but may require filtration when other treatment processes (such as oxidation or softening) generate particles that must be removed.

This chapter presents a brief history of granular filtration, a description of the rapid filtration process, properties of filter media, hydraulics of flow through granular media, particulate removal in rapid filtration, and design of rapid filters. A variety of other filtration options and technologies are used in water treatment, including pressure filtration, slow sand filtration, greensand filtration, biologically active filtration, diatomaceous earth filtration, and cartridge or bag filtration. These technologies are introduced

briefly at the end of this chapter. Membrane filtration is another common filtration technology used in water treatment but will be discussed in a different chapter (Chap. 12) because of the substantial differences between granular and membrane filtration technologies. Granular media filters are still the most common type of filters in use today.

11-1 Brief History of Filtration

Filters have been used to clarify water for thousands of years. Medical lore written in India, dating to perhaps 2000 BC, mentions filtration through sand and gravel as a method of purifying water. Hippocrates advocated filtration through cloth bags in the fourth century BC. The Romans dug channels parallel to lakes to take advantage of natural filtration through soil when using lakes for water supplies. Venice, Italy, stored rainwater in cisterns but drew the fresh water from wells in sand that surrounded the cisterns (Baker, 1948).

The commercialization and patenting of filtration technologies started in France around 1750, using various filter media such as sponges, charcoal, wool, sand, crushed sandstone, or gravel. The practice of filtering surface water through engineered systems and distributing it on a municipal scale began in England and Scotland around 1800. Various filtration concepts were tested, including flow direction (downflow, upflow, and horizontal flow), sand and gravel media graded from smaller to larger sizes, and backwashing by reverse flow. The first modern slow sand filter, designed by James Simpson for the Chelsea Water Works Company in London in 1829, incorporated an underdrain system, graded gravel and sand media, a filtration rate of about 0.12 m/h (0.05 gpm/ft^2), and cleaning by scraping (Baker, 1948). These design features are still used today.

The first regulation mandating filtration, passed in 1852, required all river water supplied by the Metropolitan District of London to be filtered. The regulation was prompted by rampant pollution in the Thames River and suspicions that cholera was transmitted by water (Fuller, 1933), a suspicion confirmed by Dr. John Snow in his famous investigation of a cholera outbreak in London just 2 years later.

Interest in filtration grew as people realized that it prevented waterborne disease. In 1892, the city of Altona, Germany, largely escaped a cholera epidemic that ravaged neighboring Hamburg. Both cities used the Elbe River as a water supply, but Altona was protected by its slow sand filters even though its water was withdrawn downstream of Hamburg and was contaminated with Hamburg's waste (Hamburg had no filtration system). Similarly, a dramatic reduction in typhoid cases resulted when filters were installed in Lawrence, Massachusetts. Many communities in the United States first began filtering their water supplies during the first couple of decades of the twentieth century.

Rapid filtration originated in the United States during the 1880s. The first municipal plant employing coagulation and other critical elements of rapid filtration was in Somerville, New Jersey, in 1885 (Fuller, 1933). Both slow sand and rapid filters were common in early filter installations (Fuller, 1933), but by the middle of the twentieth century, rapid filters were commonplace and slow sand filters were rarely used.

By the latter part of the twentieth century, most surface waters were filtered before municipal distribution, with rapid filters used in almost all cases (99 percent). Nevertheless, the Surface Water Treatment Rule (SWTR), passed in 1989, was the first regulation in the United States requiring widespread (but not universal) mandatory filtration of municipal water (U.S. EPA, 1989), with the recognition that chemical disinfection alone was insufficient for protozoa such as *Giardia lamblia* and *Cryptosporidium parvum*. Surface water treatment regulations have continued to get more stringent, particularly the remaining utilities with unfiltered surface water supplies that have been under increasing pressure to install filtration. In short, filtration is and will continue to be a central feature in surface water treatment plants.

11-2 Principal Features of Rapid Filtration

Rapid filtration has several features that allow it to operate at rates up to 100 times greater than slow sand filtration. The most important of these features are (1) a filter bed of granular material that has been processed to a more uniform size than typically found in nature, (2) the use of a coagulant to precondition the water, and (3) mechanical and hydraulic systems to efficiently remove collected solids from the bed.

Uniformity of Filter Media

The filter material in rapid filters is processed to a fairly uniform size. Media uniformity allows the filters to operate at a higher hydraulic loading rate with lower head loss but results in a filter bed with void spaces significantly larger than the particles being filtered. As a result, straining is not the dominant removal mechanism. Instead, particles are removed when they adhere to the filter grains or previously deposited particles. Particles are removed throughout the entire depth of the filter bed by a process called depth filtration, which gives the filter a high capacity for solids retention without clogging rapidly.

Coagulation Pretreatment

Coagulation pretreatment is required ahead of rapid filtration. If particles are not properly destabilized, the natural negative surface charge on the particles and filter media grains cause repulsive electrostatic forces that prevent contact between particles and media. The origin of surface charge on particles in nature and the proper use of coagulants for destabilizing

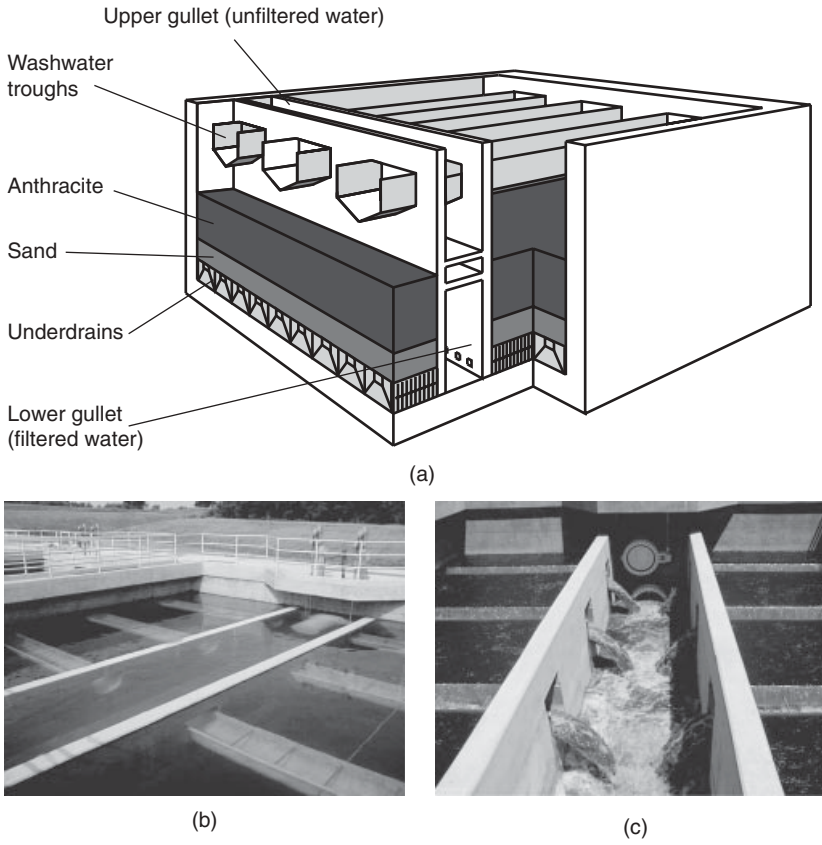

Figure 11-1
Typical dual-media rapid filter. (a) Schematic representation of dual-media filter. (b) View of an operating rapid filter. Washwater troughs are visible below the water surface. Influent water enters through the central channel, flows through the wall openings for the washwater troughs, and then down through the filter media, which is below the water surface. (c) Rapid filter during the backwash cycle. Washwater flows up through the media, pours over into the troughs, and then runs into the central channel.

particles were discussed in detail in Chap. 9. Properly designed and operated rapid filters can fail quickly if the coagulant feed breaks down or the raw-water quality changes and the coagulant dose is not adjusted accordingly.

Basic Process Description

A typical configuration for rapid filters is illustrated on Fig. 11-1. The filter bed is contained in a deep structure that is typically constructed of reinforced concrete and open to the atmosphere. The rapid filtration cycle consists of two stages: (1) a filtration stage, during which particles accumulate, and (2) a backwash stage, during which the accumulated material is flushed from the system. During the filtration stage, water flows downward through the filter bed and particles collect within the bed. The filtration stage typically lasts from 1 to 4 days.

During the backwash stage, water flows in the direction opposite to remove the particles that have collected in the filter bed. Efficient removal of collected solids is a key component of rapid filtration systems, so while the backwashing stage is very short compared to the filtration stage, it is a very important part of the filtration cycle.

The physical steps that occur during the backwashing stage include the following: (1) the filter influent and effluent lines are isolated with valves and the backwash supply and waste washwater valves are opened; (2) backwash water, which is potable water produced by the plant, is directed upward through the filter bed; (3) the upward flow flushes captured particles up and away from the bed; and (4) after backwash, the valve positions are reversed and the filter is placed back in service.

Most filters also contain supplemental systems to assist the backwashing process. One option is the surface wash system, which is a fixed grid or rotating system of nozzles that blast the surface of the filter bed to break up any mat of solids that may have formed. Another option is to introduce pressurized air underneath the media with the backwash water. Often the air is introduced while the backwash water flows at a low rate, and the consequent pulsing efficiently scours retained solids from the media. For deep filter beds, both air and surface wash are often provided. The backwashing step typically takes 15 to 30 min.

Filtration Effectiveness During the Filtration Stage

The efficiency of particle capture as reflected by effluent turbidity and head loss varies during the filtration stage (also called a filter run), as illustrated on Fig. 11-2. Filter effluent turbidity during the filter run follows a characteristic pattern with three distinct segments. During the first segment (immediately after backwash), the filter effluent turbidity rises to a peak and then falls. This segment is called filter ripening (or maturation). Ripening is the process of media conditioning and occurs as clean media captures particles and becomes more efficient at collecting additional particles. Some studies indicate that 90 percent of the particles that pass through a well-operating filter do so during the initial stage of filtration (Amirtharajah, 1988). The ripening curve sometimes contains two distinct peaks, the first corresponding to residual backwash water being flushed from the media and the second corresponding to particles from the water column above the backwashed filter. Ripening periods of 15 min to 2 h are possible. The magnitude and duration of the ripening peak can be sizable but can be substantially reduced by proper backwashing procedures, such as minimizing the duration of the backwash stage or using filter aid polymers in the backwash water. Modern filtration plants are designed with a filter-to-waste line, and the water produced during ripening is discharged to waste or recycled to the head of the plant.

The particles captured during ripening improve the overall efficiency of the filter by providing a better collector surface than uncoated media grains. After ripening, effluent turbidity typically can be maintained at a steady-state value below 0.1 NTU. Even though effluent turbidity is essentially constant after ripening, head loss through the filter continuously increases because of the collection of particles in the filter bed. After the period of effective filtration, the filter can experience breakthrough. During breakthrough,

the filter contains so many particles than it can no longer filter effectively and the effluent turbidity increases.

Several events can trigger the end of the filter run and lead to backwash. First, if the filter reaches breakthrough, it must be backwashed to prevent high-turbidity water from entering the distribution system. Second, the head loss can increase beyond the available head through the process. Rapid filters typically operate by gravity and are designed with 1.8 to 3 m (6 to 10 ft) of available head. When head loss exceeds this available head (also called the limiting head), the filter must be backwashed even if it has not reached breakthrough. Some filters do not reach breakthrough or the limiting head within several days. In these cases, utilities backwash filters after a set period to maintain a convenient schedule for plant operators, even though the filter has additional usable capacity.

On Fig. 11-2, the filter reaches breakthrough before reaching the available head, but these events can occur in either order depending on the filter design and raw-water quality. A filter design is optimized when both events occur simultaneously.

Classifications of Rapid Filtration Systems

Rapid filtration is classified by the level of pretreatment, as presented on Fig. 11-3. The most important factors that determine the required level of pretreatment are the raw-water quality and the preference and resources of the operating utility. Rapid filters are also classified by the number of layers of filter material, as shown in Table 11-1. The common filter materials are sand, anthracite, granular activated carbon (GAC), garnet, and ilmenite. Some are used alone, and others are used only in combination with other media. Additional information on the use and characteristics of these media materials is presented later in the chapter.

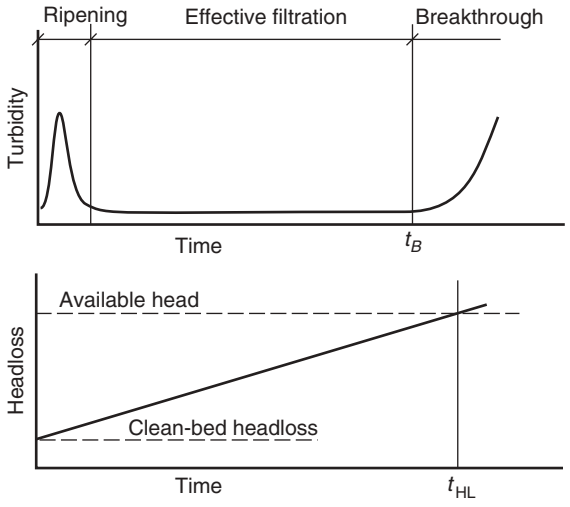

Figure 11-2
Operation of a rapid filter: (a) effluent turbidity versus time and (b) head loss development versus time.

Conventional filtration.
Most common filtration system. Used with any surface water, even those with very high or variable turbidity. Responds well to rapid changes in source water quality.

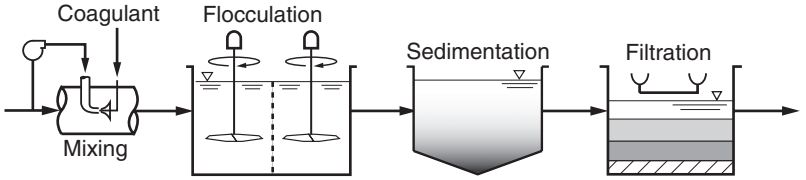

Direct filtration.
Good for surface waters without high or variable turbidity. Typical source waters are lakes and reservoirs, but usually not rivers. Raw-water turbidity < 15 NTU.

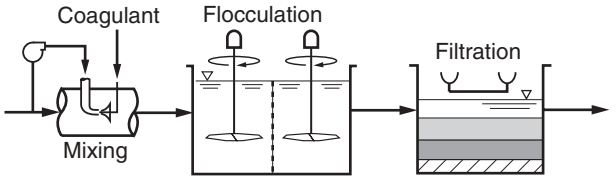

In-line filtration (also called contact filtration).
Requires high-quality surface water with very little variation and no clay or sediment particles. Raw-water turbidity < 10 NTU.

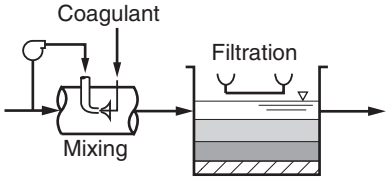

Two-stage filtration.
Preengineered systems used in small treatment plants (also called package plants). Raw-water turbidity < 100 NTU.

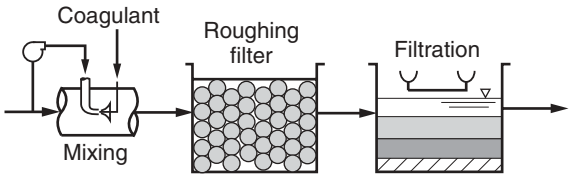

Figure 11-3
Classification of rapid filtration by pretreatment level.

Table 11-1
Classification of rapid filtration by media type

Filter Classification	Description
Monomedia	One layer of filter material, usually sand. Sand monomedia filters are typically about 0.6–0.76 m (24–30 in.) deep. Sand monomedia filters are an older design and have been largely superseded by other designs.
Deep-bed monomedia	One layer of filter material, usually anthracite or granular activated carbon. Deep-bed monomedia filters are typically 1.5–1.8 m (5–6 ft) deep. They are used to provide greater filtration capacity (longer run time) when feed water of consistent quality can be provided.
Dual media	Two layers of filter media. The older design is 0.45–0.6 m (18–24 in.) of anthracite over 0.23–0.3 m (9–12 in.) of sand, with filtration in the downflow direction. Deep-bed dual-media filters using 1.5–1.8 m (5–6 ft) of anthracite in the top layer are now common. GAC is sometimes used instead of anthracite in the top layer. Dual-media filters are more robust than monomedia filters.
Trimedia or mixed media	Three media, typically anthracite as the top layer, sand as the middle layer, and garnet or ilmenite as the bottom layer. The anthracite layer is typically 0.45–0.6 m (18–24 in.) deep, the sand layer is typically 0.23–0.3 m (9–12 in.) deep, and the garnet or ilmenite layer is 0.1–0.15 m (4–6 in.) deep. These have sometimes been called mixed-media filters when the media properties were selected to promote intermixing rather than the formation of distinct layers.

11-3 Properties of Granular Filter Media

Granular media filtration is affected by properties of the filter media and the filter bed, including grain size and size distribution, density, shape, hardness, bed porosity, and specific surface area. The types of media used in water filtration and their properties are addressed below.

Materials Used for Rapid Filtration Media

Naturally occurring granular minerals are mined and processed specifically for use as filter media. The common materials are sand, anthracite coal, garnet, and ilmenite. Anthracite is harder and contains less volatile material than other types of coal. Garnet and ilmenite are heavier than sand and

are used as the bottom layer in trimedia filters. Garnet is comprised of a group of minerals containing a variety of elements, often appearing reddish or pinkish, and ilmenite is an oxide of iron and titanium. In addition to these four minerals, GAC is sometimes used as a filter material when adsorption and filtration are combined in a single unit process. Standard requirements for filtering materials are described in *ANSI/AWWA B100-01 Standard for Filtering Material* (AWWA, 2001a). Additional information on GAC is provided in Chap. 15.

Effective Size and Uniformity Coefficient

Filter materials are found in a granular state in nature or must be crushed to the desired size. Naturally occurring granular materials have nearly a lognormal size distribution, meaning that the distribution plots roughly as a straight line on lognormal graph paper. The size distribution is determined by sieve analysis (ASTM, 2001a), in which a sample of material is sifted through a stack of calibrated sieves (ASTM, 2001b), the weight of material retained on each sieve is measured, and the cumulative weight retained is plotted as a function of sieve size. The results of sieve analyses for naturally occuring sand and processed filter media are illustrated on Fig. 11-4. The size distribution of naturally occurring material is broader than desirable for rapid filter media. Thus, rapid filter media is processed to remove the largest (by sieving) and smallest (by washing) grain sizes, producing a narrower size distribution.

In North America, the standard method for characterizing the media size distribution is by effective size and uniformity coefficient. The *effective size* (ES or d_{10}) is the media grain diameter at which 10 percent of the media by weight is smaller, as determined by a sieve analysis. The *uniformity coefficient* (UC) is the ratio of the 60th percentile media grain diameter (the diameter at which 60 percent of the media by weight is smaller) to the

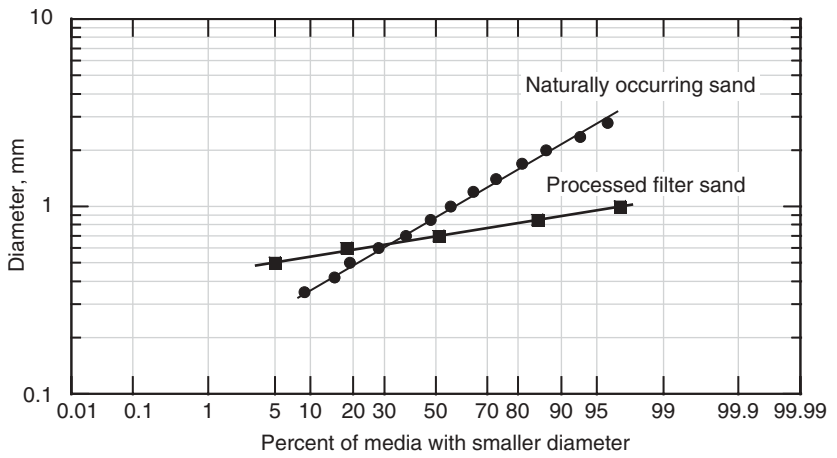

Figure 11-4
Size distribution of typical naturally occurring and processed filter sand.

effective size, as shown in the equation

$$\text{UC} = \frac{d_{60}}{d_{10}} \tag{11-1}$$

where UC = uniformity coefficient, dimensionless
d_{10} = 10th percentile media grain diameter, mm
d_{60} = 60th percentile media grain diameter, mm

The concept of the effective size was proposed by Allen Hazen in the 1890s because the hydraulic resistance of an unstratified granular bed tends to be unaffected by size variation as long as the effective size remains constant (Fair et al., 1971). Filter media tends to stratify during backwash. Fine grains collect at the top of the filter bed, where they cause excessive head loss and reduce overall effectiveness of the filter bed. Large grains settle to the bottom of the bed and are difficult to fluidize during backwash. A low UC can minimize these effects and is an important factor in the design of rapid filters. The ES and UC of typical filtration materials are provided in Table 11-2, along with typical values of other material properties. Granular activated carbon is typically specified by the maximum and minimum sieve sizes. For instance, an 8 × 20 mesh GAC refers to media that passes through a No. 8 sieve but is retained by a No. 20 sieve. Determination of the ES and UC from sieve data is demonstrated in Example 11-1.

Grain Shape

Mathematical models often assume that particles and filter grains are spherical for simplicity, but actual filter grains are not spherical, as shown on Fig. 11-5. The shape of individual grains affects filter design and performance in at least three ways. First, shape affects the size determined by sieve analysis. For spheres, the sieve opening will correspond to the diameter, but for nonspherical media, the sieve opening theoretically corresponds to the largest dimension of the smallest particle cross section (visualize rods going through a sieve lengthwise; the sieve opening corresponds to the largest rod diameter). The grain diameter determined by sieve

Table 11-2
Typical properties of filter media used in rapid filters[a]

Property	Unit	Garnet	Ilmenite	Sand	Anthracite	GAC
Effective size, ES	mm	0.2–0.4	0.2–0.4	0.4–0.8	0.8–2.0	0.8–2.0
Uniformity coefficient, UC	UC	1.3–1.7	1.3–1.7	1.3–1.7	1.3–1.7	1.3–2.4
Density, ρ_p	g/mL	3.6–4.2	4.5–5.0	2.65	1.4–1.8	1.3–1.7
Porosity, ε	%	45–58	N/A	40–43	47–52	N/A
Hardness	Moh	6.5–7.5	5–6	7	2–3	Low

[a]N/A = not available.

Example 11-1 Determination of effective size and uniformity coefficient

Determine the effective size and uniformity coefficient of the processed filter sand shown on Fig. 11-4.

Solution

1. Find the 10th percentile line on the *x* axis and follow it up to the intersection of the line for the processed filter sand. The corresponding value on the *y* axis is 0.54 mm.
2. The size (*y* axis) corresponding to the 60th percentile (*x* axis) for the processed filter sand is 0.74 mm.
3. The effective size is ES $= d_{10} = 0.54$ mm. The uniformity coefficient is UC $= d_{60}/d_{10} = 0.74/0.54 = 1.37$.

Comment

Probability paper is not required to determine the effective size and uniformity coefficient. Either an arithmetic scale or a probability scale can be used on the *x* axis. As long as a smooth curve can be drawn through the data, the d_{10} and d_{60} values can be determined. In addition, some spreadsheet software has functions for determining standard deviations and probability functions that can assist with the process of determining ES and UC.

analysis is typically smaller than the diameter of an ''equivalent-volume'' sphere. Cleasby and Woods (1975) compared size determinations from sieve analysis to equivalent-volume spheres and found that the equivalent-volume sphere diameter was 5 to 10 percent larger than the sieve size for sand and anthracite and 2 percent larger for garnet. Second, shape affects

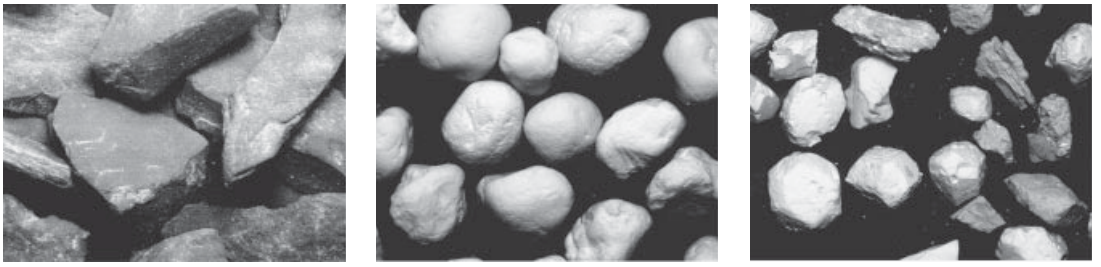

(a) (b) (c)

Figure 11-5
Typical filter media: (a) anthracite coal, (b) sand, and (c) garnet. The sand shown is a worn river sand; suppliers may provide worn or crushed sand, depending on the source, which would change the shape factor.

how filter grains pack together in a bed. The porosity (defined below) of a randomly packed bed of spherical beads is typically about 38 percent, but the porosity of beds of filter grains typically ranges from 40 to 60 percent. Third, the hydraulics of flow through a bed of grains with sharp, angular surfaces is different from that through a bed of spherical beads.

Although grain shape has important implications in filter design, there is no easy way to account for it. Throughout filtration literature, grain shape is often characterized by either sphericity (ψ) or shape factor (ξ), which are interrelated as follows:

$$\psi = \frac{\text{surface area of equivalent-volume sphere}}{\text{actual surface area of grain}} \tag{11-2}$$

$$\xi = \frac{6}{\psi} \tag{11-3}$$

where ψ = sphericity, dimensionless
ξ = shape factor, dimensionless

For spherical grains, $\psi = 1$ and $\xi = 6$. Because a sphere has the minimum surface area of any geometric shape with the same volume, other shapes will have $\psi < 1$ and $\xi > 6$ based on the definitions in Eqs. 11-2 and 11-3.

Unfortunately, ψ and ξ have limited value in actual practice for several reasons. First, filter media is routinely measured and specified using the diameter determined by sieve analysis, not by equivalent-volume diameter. The equivalent-volume diameter can be determined by counting and weighing a representative number of media grains and calculating volume from the weight and density (Cleasby and Woods, 1975), a tedious procedure that is not done for commercially available filter media. Second, sphericity and shape factors are difficult to measure directly, and indirect means are normally used. The literature values for sphericity of common filter materials, such as the values available in Carman (1937), Cleasby and Fan (1981), and Dharmarajah and Cleasby (1986), were calculated from head loss experiments with the implicit assumption that the head loss equation coefficients (discussed in Sec. 11-4, see Eqs. 11-11 and 11-13) are independent of grain shape characteristics. As a result, many of the sphericity values for filter media available in the literature are really just empirical fitting parameters for head loss rather than true independent measurements of shape. Finally, other variables such as porosity have more impact on design, and arbitrary selection of a value for sphericity does little to improve the accuracy of design equations.

Material Density

The fluidization and settling velocities of filter media during and after backwash are influenced by material density. Backwash flow requirements are higher for denser materials of equal diameter. In addition, multimedia filters are constructed in a reverse-graded fashion (larger filter grains are near the top of the bed after backwashing) by using materials of

different density. In a dual-media filter, anthracite is above sand because of differences in density. In a trimedia filter, the media are arranged from top to bottom as anthracite, sand, and garnet or ilmenite.

Material Hardness

Hardness affects the abrasion and breakdown of filter material during the backwash cycle. Hardness is ranked on the Moh table, a relative ranking of mineral hardness (talc = 1, diamond = 10). Sand, garnet, and ilmenite are hard enough to be unaffected by abrasion, but anthracite and GAC are friable, and design specifications must identify minimum hardness values to avoid excessive abrasion. A minimum Moh hardness of 2.7 is often specified for anthracite. The hardness of GAC is evaluated with procedures (the stir-ring abrasion test or the Ro-Tap abrasion test) outlined in *ANSI/AWWA B604-96 Standard for Granular Activated Carbon* (AWWA, 1996).

Granular Bed Porosity

The filter bed porosity (not porosity of the individual grains) has a strong influence on the head loss and filtration effectiveness in a filter bed. Porosity, or fraction of free space, is the ratio of void space volume to total bed volume and is calculated using the expression

$$\varepsilon = \frac{V_V}{V_T} = \frac{V_T - V_M}{V_T} \tag{11-4}$$

where ε = porosity, dimensionless
V_V = void volume in media bed, m^3
V_T = total volume of media bed, m^3
V_M = volume of media, m^3

Filter bed porosity ranges from 40 to 60 percent, depending on the type and shape of the media and how loosely it is placed in the filter bed.

Granular Bed Specific Surface Area

The specific surface area of a granular bed is defined as the total surface area of the filter material divided by the bed volume and is described by the expression

$$S = \frac{(\text{number of grains})\,(\text{surface area of each grain})}{\text{bulk volume of filter bed}} \tag{11-5}$$

where S = specific surface area, m^{-1}

For a uniform bed of monodisperse spheres, the specific surface area is given by the expression

$$S = \frac{6(1-\varepsilon)}{d} \tag{11-6}$$

where d = diameter of sphere, m

For nonspherical media, Eq. 11-6 is written as

$$S = \frac{6(1-\varepsilon)}{\psi d} = \frac{\xi(1-\varepsilon)}{d} \tag{11-7}$$

where d = equivalent-volume diameter, m

Equation 11-7 is useful only when the equivalent-volume diameter is known.

11-4 Hydraulics of Flow through Granular Media

The head loss through a clean filter bed and the flow rate needed to fluidize the filter bed during backwashing are discussed in this section. The increase in head loss as particles are captured during filtration is discussed in Sec. 11-5.

An important aspect of hydraulic behavior is the flow regime. The flow regime in granular media is identified by the Reynolds number for flow around spheres, which uses the media grain diameter for the length scale:

$$\mathrm{Re} = \frac{\rho_W v d}{\mu} \tag{11-8}$$

where Re = Reynolds number for flow around a sphere, dimensionless
ρ_W = fluid density, kg/m^3
v = filtration rate (superficial velocity), m/s
d = media grain diameter, m
μ = dynamic viscosity of fluid, kg/m·s

Flow in granular media does not experience a rapid transition from laminar to turbulent, as observed in pipes, but can be divided into four flow regimes (Trussell and Chang, 1999). The low end, called Darcy flow or creeping flow, occurs at Reynolds numbers less than about 1 and is characterized entirely by viscous flow behavior. The next regime, called Forchheimer flow after the first investigator to describe it, occurs at Reynolds numbers between about 1 and 100. Both Darcy flow and Forchheimer flow can be described as steady laminar flow because dye studies demonstrate that the fluid follows distinct streamlines. Forchheimer flow, however, is influenced by both viscous and inertial forces. In purely viscous flow, momentum is transferred between streamlines solely via molecular interactions. In twisting, irregular voids of a granular media bed, however, the fluid must accelerate and decelerate as void spaces turn, contract, and expand. The complex fluid motion through passageways of varying dimensions complicates the momentum transfer between streamlines, leading to an additional component of head loss that can be ascribed to inertial forces. Head loss due to viscous forces is proportional to v and head loss due to inertial forces is proportional to v^2. The third regime, a transition zone, has an upper limit Reynolds number between 600 and 800, and full turbulence occurs at higher Reynolds numbers.

Typical rapid filters have Reynolds numbers ranging from 0.5 to 5, straddling the transition between the Darcy and Forchheimer flow regimes. High-rate rapid filters have been designed with filtration rates as high as 33 m/h (13.5 gpm/ft^2), resulting in a Reynolds number of about 18. Backwashing of rapid filters occurs between Reynolds numbers of 3 and 25, completely in the Forchheimer flow regime.

Head Loss through Clean Granular Filters

The head loss through a filter increases as particles are retained. The net head available for particle retention is the difference between the available head and the clean-bed head loss.

FILTRATION RATE

The filtration rate is the flow rate through the filter divided by the area of the surface of the filter bed. The filtration rate has units of volumetric flux (reported as m/h in SI units, gpm/ft^2 in U.S. customary units) and is sometimes referred to as the superficial velocity because it is the velocity the water would have in an empty filter box (actual average velocity within the bed is higher due to the volume taken up by the filter grains).

DARCY FLOW REGIME

In 1856, Henry Darcy published a report stating the relationship between velocity, head loss, and bed depth in granular media under creeping-flow conditions (Darcy, 1856):

$$v = k_p \frac{h_L}{L} \tag{11-9}$$

where v = superficial velocity (filtration rate), m/s
k_p = coefficient, known as hydraulic permeability, m/s
h_L = head loss across media bed, m
L = depth of granular media, m

Darcy's law contains no mathematical descriptors of the porous material and therefore has no predictive value for filter system design. In 1927, Kozeny (1927a,b) developed an equation to relate granular media hydraulics to properties of the media by postulating an analogy between a bed of granular media and a system of parallel cylindrical channels. Laminar flow through cylindrical tubes is described by Poiseuille's law (Poiseuille, 1841), which can be written as

$$\frac{h_L}{L} = \frac{32\mu v}{\rho_W g d^2} \tag{11-10}$$

where g = acceleration due to gravity, 9.81 m/s^2

By equating the bed void volume to total internal channel volume and the media surface area to internal channel surface area, the Kozeny equation can be developed:

$$\frac{h_L}{L} = \frac{\kappa_k \mu S^2 v}{\rho_W g \varepsilon^3} \tag{11-11}$$

where κ_k = Kozeny coefficient, unitless
S = specific surface area from Eq. 11-5, m^{-1}
ε = porosity from Eq. 11-4, dimensionless

The Kozeny coefficient is an empirical coefficient introduced to fit the model results to experimental data. Other experimenters determined the value of κ_k to be about 5 (Carman, 1937; Fair and Hatch, 1933) for spherical media. Carman (1937) and Fair and Hatch (1933) proposed that the value of κ_k was independent of media properties and introduced a correction factor to account for the nonspherical nature of filter grains, Carman using sphericity and Fair and Hatch using the shape factor. Carman's correction factors were calculated from head loss data, which suggests that they might not be independent of κ_k. The origin of Fair and Hatch's shape factors was not clear, and their factors were based on diameter determined by sieve analysis rather than equivalent volume.

FORCHHEIMER FLOW REGIME

Subsequent studies demonstrated that head loss in granular media was greater than predicted by Eq. 11-11 when the Reynolds number was greater than 1. Forchheimer (1901) proposed a nonlinear equation that more accurately described head loss with higher velocity or larger media:

$$\frac{h_L}{L} = \kappa_1 v + \kappa_2 v^2 \tag{11-12}$$

where κ_1 = permeability coefficient for linear term, s/m
κ_2 = permeability coefficient for square term, s^2/m^2

Ahmed and Sunada (1969) showed that an equation with the form of Eq. 11-12 could be derived from the Navier–Stokes equation with only two assumptions: (1) the medium and the fluid are homogeneous and isotropic and (2) thermodynamic and chemical effects are small.

Ergun (1952) developed an equation with this form to describe head loss through granular media under Forchheimer flow conditions. The result was

$$h_L = \kappa_V \frac{(1-\varepsilon)^2}{\varepsilon^3} \frac{\mu L v}{\rho_W g d^2} + \kappa_I \frac{1-\varepsilon}{\varepsilon^3} \frac{L v^2}{g d} \tag{11-13}$$

where κ_V = head loss coefficient due to viscous forces, unitless
κ_I = head loss coefficient due to inertial forces, unitless

Equation 11-13 is known as the Ergun equation. Ergun (1952) compiled data from 640 experiments covering a range of Reynolds numbers between about 1 and 2000 when the diameter d was an effective diameter based on specific surface, and proposed values of $\kappa_V = 150$ and $\kappa_I = 1.75$ to fit the experimental data. The first term of the Ergun equation is identical to Eq. 11-11 (with substitution of Eq. 11-6) with the exception of the numerical

value of the coefficient. Ergun proposed that the first term in Eq. 11-13 represented viscous energy losses and the second term represented kinetic energy losses, which is consistent with the mathematical construct of the equation. The dependence on μ, L, v, ρ_W, g, and d in the first term is consistent with the Poiseuille equation (i.e., laminar flow), while the dependence on these six variables in the second term is consistent flow under turbulent conditions, where kinetic energy losses predominate (Streeter and Wylie, 1979).

PRACTICAL CONSIDERATIONS FOR CALCULATION OF CLEAN-BED HEAD LOSS

Although some filters may operate in the Darcy flow regime, the transition between Darcy flow and Forchheimer flow is gradual. Based on past experience, it has been found that equations based on the Forchheimer flow regime can be used to determine the clean-bed head loss over the full range of values of interest in rapid filtration; therefore, Eq. 11-13 is the recommended equation for clean-bed head loss in rapid filters.

An important issue is the selection of values for each parameter in the clean-bed head loss equation. The coefficients proposed by Ergun are based on an effective diameter that is not easily measured. A more recent study has reexamined head loss through granular media (Chang et al., 1999; Trussell and Chang, 1999; Trussell et al., 1999). For spherical glass beads, the values proposed by Ergun were found to be reasonable. Different values are proposed for sand and anthracite, as shown in Table 11-3 (Trussell and Chang, 1999). The values for the head loss coefficients and porosity in Table 11-3 are based on the use of the effective size as determined by sieve analysis for the diameter (e.g., $d = \text{ES}$) and take media shape into account so that a separate shape factor is not needed. In the absence of pilot data or other site-specific information, the midpoint values in Table 11-3 are recommended for model use.

The sensitivity of clean-bed head loss to filtration rate, porosity, and media diameter is illustrated on Fig. 11-6. The significant impact of filtration rate is evident. In addition, clean-bed head loss doubles as the effective size of anthracite decreases from 1.2 to 0.8 mm, and increases by about 65 percent as porosity declines from 0.52 to 0.47. Head loss is also dependent on temperature because fluid viscosity increases as temperature decreases. The clean-bed head loss at 5°C is 60 to 70 percent higher than at 25°C.

Table 11-3
Recommended parameters for use with Eq. 11-13[a]

Medium	κ_V	κ_I	ε_I,
Sand	110–115	2.0–2.5	40–43
Anthracite	210–245	3.5–5.3	47–52

[a]When effective size as determined by sieve analysis is used for the diameter.

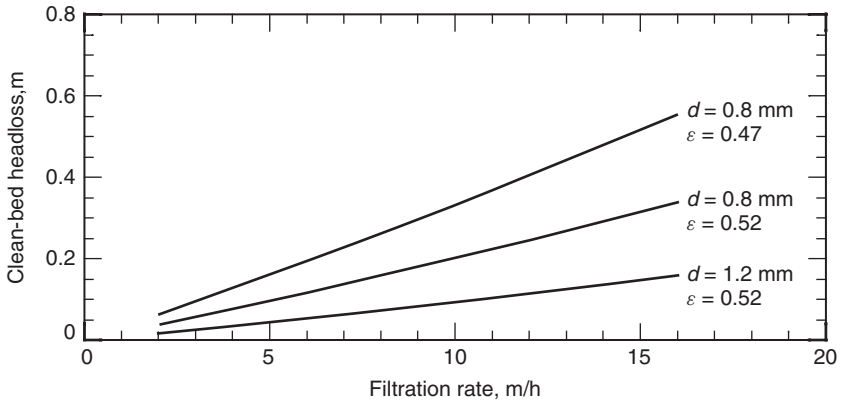

Figure 11-6
Effect of media size, bed porosity, and filtration rate on head loss through a clean granular filter bed. Calculated using Eq. 11–13 for anthracite ($L = 1$ m, $T = 15°C$, $\kappa_V = 228$, $\kappa_I = 4.4$).

Fortunately, it is common for water treatment plants to operate at a lower capacity during the winter than during the summer, and the reduction in filtration rate typically counteracts the increase in viscosity. Calculation of clean-bed head loss is demonstrated in Example 11-2.

Example 11-2 Clean-bed head loss through rapid filter

Calculate the clean-bed head loss through a deep-bed anthracite filter with 1.8 m of ES = 0.95 mm media at a filtration rate of 15 m/h and a temperature of 15°C.

Solution

The head loss through anthracite is calculated first using Eq. 11-13.

1. No pilot or site-specific information is given, so midpoint values are selected from Table 11-3; $\kappa_V = 228$, $\kappa_I = 4.4$, and $\varepsilon = 0.50$. Values of ρ_W and μ are available in Table C-1 in App. C ($\rho_W = 999$ kg/m^3 and $\mu = 1.14 \times 10^{-3}$ kg/m · s).
2. Calculate the first term in Eq. 11-13:

$$\frac{(228)(1-0.50)^2(1.14\times10^{-3}\ \text{kg/m}\cdot\text{s})(1.8\ \text{m})(15\ \text{m/h})}{(0.50)^3(999\ \text{kg/m}^3)(9.81\ \text{m/s}^2)(0.95\ \text{mm})^2(10^{-3}\ \text{m/mm})^2(3600\ \text{s/h})}$$

$$= 0.44\ \text{m}$$

3. Calculate the second term in Eq. 11-13:

$$\frac{(4.4)(1-0.50)(1.8\ \text{m})(15\ \text{m/h})^2}{(0.50)^3(9.81\ \text{m/s}^2)(0.95\ \text{mm})(10^{-3}\ \text{m/mm})(3600\ \text{s/h})^2} = 0.06\ \text{m}$$

4. Add the two terms together:

$$h_L = 0.44 \text{ m} + 0.06 \text{ m} = 0.50 \text{ m} \quad (1.6 \text{ ft})$$

Comments

A relatively small contribution to head loss comes from the inertial term. The inertial term becomes more important for the larger media and higher velocities used in high-rate rapid filters. If the filter is designed with 2.5 m (8.2 ft) of available head, the clean-bed head loss consumes about 20 percent of the available head. Note that if multiple layers of media are present, the head loss through each layer is additive.

Backwash Hydraulics

At the end of a filter run, rapid filters are backwashed by filtered water flowing upward through the filter bed. The backwash flow rate must be great enough to flush captured material from the bed, but not so high that the media is flushed out of the filter box. To prevent loss of media, it is important to determine the bed expansion that occurs as the filter media is fluidized, which is a function of the backwash flow rate and can be calculated using head loss equations for fixed beds.

FORCES ON PARTICLES

The forces on an individual particle (either a particle from the influent or a media grain) in upward-flowing water are exactly the same as were developed for the terminal settling velocity in Chap. 10 (see the free-body diagram on Fig 10-2). The particle will settle (or fail to fluidize) when downward forces predominate, be washed away when upward forces predominate, and remain suspended (fluidized) when the forces are balanced. The downward force is equal to the buoyant weight of the media and the upward force is the drag caused by the backwash flow. As noted in Chap. 10, the sum of forces on a particle is given by the expression

$$\sum F = F_g - F_b - F_d \tag{10-1}$$

where F_g = gravitational force on a particle, N
F_b = buoyant force on a particle, N
F_d = drag force on a particle, N

Combining Eqs. 10-1 through 10-4 from Chap. 10 yields the equation

$$\sum F = \rho_P V_p g - \rho_W V_p g - C_d \rho_W A_p \frac{v_s^2}{2} \tag{11-14}$$

where ρ_P = particle density, kg/m^3
ρ_W = water density, kg/m^3
V_p = volume of particle, m^3
A_p = projected area of particle in direction of flow, m^3
C_D = drag coefficient, unitless
g = acceleration due to gravity, 9.81 m/s^2
v_s = settling velocity of the particle, m/s

The drag coefficient is dependent on the flow regime (Clark, 1996). As noted in Chap. 10, the drag coefficient is described by the following expressions:

$$C_d = \frac{24}{\text{Re}} \quad \text{for Re} < 2 \quad \text{(laminar flow)} \tag{10-10}$$

$$C_d = \frac{18.5}{\text{Re}^{0.6}} \quad \text{for } 2 \le \text{Re} \le 500 \quad \text{(transition flow)} \tag{10-11}$$

The fluid velocity required to keep an individual particle suspended can be determined by substituting Eq. 10-10 or Eq. 10-11 into Eq. 11-14 and solving for velocity. As was shown in Chap. 10, the fluid velocity is given as Stokes' law (Eq. 10-13) for laminar flow, and the following expression for transition flow:

$$v_s = \frac{g\,(\rho_P - \rho_W)\,d_p^2}{18\mu} \quad \text{(laminar flow)} \tag{10-13}$$

$$v_s = \left[\frac{g\,(\rho_P - \rho_W)\,d_p^{1.6}}{13.9\rho_W^{0.4}\mu^{0.6}}\right]^{1/1.4} \quad \text{(transition flow)} \tag{10-14}$$

The velocity required to suspend an isolated particle in a uniform flow field (i.e., above the filter bed, away from the influences of the bed) may be determined using Eqs. 10-13 or 10-14, as appropriate. Within a filter bed, velocities (and therefore drag forces) are higher due to the volume taken up by the media. The balance of forces on an individual particle is demonstrated in Example 11-3.

Example 11-3 Forces on suspended particle

A filter is backwashed at 50 m/h at 15°C. Determine whether a 0.1-mm diameter particle of sand will be washed from the filter.

Solution

1. Calculate the gravitational force on the particle using the F_g term from Eq. 10-1. The value for ρ_P is available in Table 11-2:

$$F_g = \rho_P V_p g = (2650\ \text{kg/m}^3)\left(\frac{\pi}{6}\right)\left(\frac{0.1\ \text{mm}}{10^3\ \text{mm/m}}\right)^3 (9.81\ \text{m/s}^2)$$

$$= 1.36 \times 10^{-8}\ \text{kg} \cdot\ \text{m/s}^2 = 1.36 \times 10^{-8}\ \text{N}$$

2. Calculate the buoyant force on the particle using the F_b term from Eq. 10-1. The value for ρ_W is available in Table C-1 in App. C:

$$F_g = \rho_W V_p g = (999\ \text{kg/m}^3)\left(\frac{\pi}{6}\right)\left(\frac{0.1\ \text{mm}}{10^3\ \text{mm/m}}\right)^3 (9.81\ \text{m/s}^2)$$

$$= 5.13 \times 10^{-9}\ \text{kg} \cdot \text{m/s}^2 = 5.13 \times 10^{-9}\ \text{N}$$

3. Calculate the Reynolds number using Eq. 11-8 to determine in what flow regime the particle is:

$$\text{Re} = \frac{\rho_W v d}{\mu} = \frac{(999\ \text{kg/m}^3)(50\ \text{m/h})(0.1\ \text{mm})}{(1.139 \times 10^{-3}\ \text{kg/m} \cdot \text{s})(3600\ \text{s/h})(10^3\ \text{mm/m})} = 1.22$$

4. The Reynolds number is less than 2, so Eq. 10-10 can be used to calculate drag forces:

$$C_d = \frac{24}{\text{Re}} = \frac{24}{1.22} = 19.7$$

$$F_d = C_d \rho_W A_p \frac{v_s^2}{2} = \frac{19.7(999\ \text{kg/m}^3)}{2}\left(\frac{\pi}{4}\right)\left(\frac{0.1\ \text{mm}}{10^3\ \text{mm/m}}\right)^2\left(\frac{50\ \text{m/h}}{3600\ \text{s/h}}\right)^2$$

$$= 1.49 \times 10^{-8}\ \text{N}$$

5. Calculate the sum of the forces:

$$\sum F = F_g - F_b - F_d = 1.36 \times 10^{-8}\ \text{N} - 5.13 \times 10^{-9}\ \text{N} - 1.49 \times 10^{-8}\ \text{N}$$

$$= -6.43 \times 10^{-9}\ \text{N}$$

The net force is negative (upward), so the particle will be flushed away with the backwash water.

BED EXPANSION AND POROSITY

A state of equilibrium between gravitational and drag forces is established in the filter bed. During backwash, the velocity in a filter bed is higher than for an isolated particle due to the presence of the media, causing higher drag forces that lift the media. As the media rises, increasing porosity reduces the velocity until the drag force is balanced by the gravitational force. The relationship between bed expansion and porosity is described in the following equation and on Fig. 11-7:

$$\frac{L_E}{L_F} = \frac{1 - \varepsilon_F}{1 - \varepsilon_E} \tag{11-15}$$

where L_E = depth of expanded bed, m
L_F = depth of bed at rest (fixed bed), m
ε_E = porosity of expanded bed, dimensionless
ε_F = porosity of bed at rest (fixed bed), dimensionless

The drag force on the media exerts an equal and opposite force on the water, which is manifested as head loss. Head loss through a fluidized bed is calculated as the gravitational force (fluidized weight) of the entire bed, as shown in the expression

$$F_g = mg = (\rho_p - \rho_w)(1 - \varepsilon)aLg \tag{11-16}$$

where F_g = weight of the entire filter bed, N
a = cross-sectional area of filter bed, m^2

The weight of the bed must be divided by the filter area to convert the weight of the bed to units of pressure (i.e., convert N to N/m^2) and divided by $\rho_w g$ to convert units of pressure (N/m^2) to units of head (m) as follows:

$$h_L = \frac{F_g}{a\rho_w g} = \frac{(\rho_p - \rho_w)(1 - \varepsilon)L}{\rho_w} \tag{11-17}$$

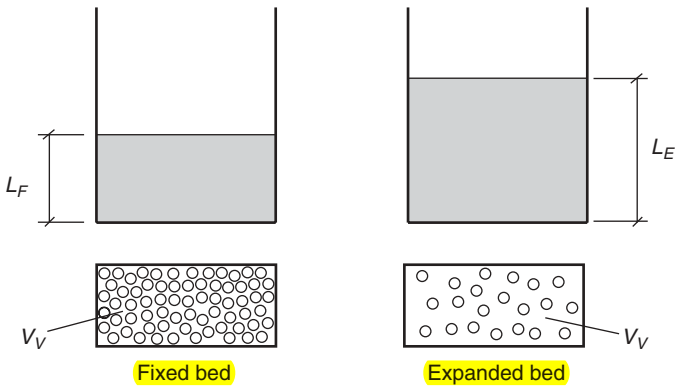

Figure 11-7
Fixed and expanded beds during backwashing of rapid filters. During filtration, the media grains are touching each other, but when media are fluidized during backwashing, the void volume increases, causing an overall expansion of the bed.

Akgiray and Saatçi (2001) demonstrated that the Eq. 11-13 is equally valid for fixed and expanded beds. Thus, in a fluidized bed, the head loss due to the weight of the media is equal to the head loss calculated from Eq. 11-13. Equating Eqs. 11-13 and 11-17 yields the expression

$$\kappa_V \frac{(1-\varepsilon)^2}{\varepsilon^3}\frac{\mu L v}{\rho_w g d^2} + \kappa_I \frac{1-\varepsilon}{\varepsilon^3}\frac{L v^2}{g d} = \frac{(\rho_p - \rho_w)(1-\varepsilon)L}{\rho_w} \tag{11-18}$$

An analytical solution for Eq. 11-18 in terms of v would allow the backwash velocity to be calculated directly for any set of filter conditions. Equation 11-18 can be seen to be a quadratic equation in v with a multitude of other terms, but it can be solved directly by making use of the Reynolds number. Equation 11-18 can be rearranged as follows after incorporating Eq. 11-8:

$$\kappa_I/\mathrm{Re}^2 + \kappa_V(1-\varepsilon)\mathrm{Re} - \beta = 0 \tag{11-19}$$

$$\beta = \frac{g\rho_w(\rho_p - \rho_w)\,d^3\varepsilon^3}{\mu^2} \tag{11-20}$$

where β = backwash calculation factor, dimensionless

Equation 11-19 is a quadratic equation in terms of Re. One root of Eq. 11-19 is necessarily negative because both κ_I and κ_V are positive. The remaining meaningful solution of the quadratic equation is

$$\mathrm{Re} = \frac{-\kappa_V(1-\varepsilon) + \sqrt{\kappa_V^2(1-\varepsilon)^2 + 4\kappa_I\beta}}{2\kappa_I} \tag{11-21}$$

Once the Reynolds number is obtained from Eq. 11-21, the velocity that will maintain the bed in an expanded state corresponding to a specific porosity value can be determined from Eq. 11-8. The minimum fluidization flow rate can be calculated by determining the velocity that produces head loss equal to the buoyant weight of the media at the fixed-bed porosity. The minimum fluidization velocity is a function of grain size, with smaller particles fluidizing at lower velocity. The backwash rate must be above the minimum fluidization velocity of the largest media, typically taken as the d_{90} diameter (Cleasby and Logsdon, 1999). After fluidization, head loss may decrease slightly because the media grains are no longer in contact and extremely small or dead-end void spaces disappear. Akgiray and Saatçi (2001) performed an analysis using equivalent-volume diameters and sphericity factors and recommended Ergun's values of $\kappa_I = 150$ and $\kappa_V = 1.75$ for fixed beds but that $\kappa_V = 1.0$ fit the data better for expanded beds. The problems associated with equivalent-volume diameters and sphericity factors have been discussed previously. Thus, the values of κ_I and κ_V from Table 11-3 are recommended for backwash expansion calculations. Calculation of the backwash flow rate to achieve a certain level of bed expansion is illustrated in Example 11-4.

Example 11-4 Backwash flow rate for bed expansion

Find the backwash flow rate that will expand an anthracite bed by 30 percent given the following information: $L_F = 2$ m, $d = 1.3$ mm, $\rho_p = 1700$ kg/m^3, $\varepsilon = 0.52$, and $T = 15^\circ$C.

Solution

1. Calculate L_E that corresponds to a 30 percent expansion:

$$L_E = L_F + 0.3L_F = 2\text{ m} + 0.3(2\text{ m}) = 2.6\text{ m}$$

2. Calculate ε_E using Eq. 11-15:

$$\varepsilon_E = 1 - \left[\frac{L_F}{L_E}(1-\varepsilon_F)\right] = 1 - \left[\left(\frac{2\text{ m}}{2.6\text{ m}}\right)(1-0.52)\right] = 0.63$$

3. Calculate β using Eq. 11-20. Values of ρ_W and μ are available in Table C-1 in App. C.

$$\beta = \frac{g\rho_w(\rho_p - \rho_w)d^3\varepsilon^3}{\mu^2}$$

$$= \frac{(9.81\text{ m/s}^2)(999\text{ kg/m}^3)(1700 - 999\text{ kg/m}^3)(0.0013\text{ m})^3(0.63)^3}{(1.139\times10^{-3}\text{ kg/m}\cdot\text{s})^2}$$

$$= 2910$$

4. Calculate Re using Eq. 11-21. Because no pilot or site-specific data are given, use values of κ_V and κ_I from midpoint values from Table 11-3 (e.g., $\kappa_V = 228$ and $\kappa_I = 4.4$):

$$\text{Re} = \frac{-\kappa_V(1-\varepsilon) + \sqrt{\kappa_V^2(1-\varepsilon)^2 + 4\kappa_I\beta}}{2\kappa_I}$$

$$= \frac{-228(1-0.63) + \sqrt{(228)^2(1-0.63)^2 + 4(4.4)(2910)}}{2(4.4)} = 17.9$$

5. Calculate v using Eq. 11-8:

$$v = \frac{\mu\,\text{Re}}{\rho_W d} = \frac{(1.139\times10^{-3}\text{ kg/m}\cdot\text{s})(17.9)(3600\text{ s/h})}{(999\text{ kg/m}^3)(0.0013\text{ m})}$$

$$= 56.5\text{ m/h} \quad (22.6\text{ gpm/ft}^2)$$

Alternatively, it is frequently necessary to determine the bed expansion that occurs for a specific backwash rate. Equation 11-18 is a cubic equation in porosity, which was analytically solved by Akgiray and Saatçi (2001). Akgiray and Saatçi showed that two roots of the cubic equation are complex numbers, leaving only one meaningful solution as follows:

$$\varepsilon = \sqrt[3]{X + (X^2 + Y^3)^{1/2}} + \sqrt[3]{X - (X^2 + Y^3)^{1/2}} \qquad (11\text{-}22)$$

where X = backwash calculation factor, dimensionless
Y = backwash calculation factor, dimensionless

The factors X and Y are defined as

$$X = \frac{\mu v}{2g(\rho_p - \rho_w)d^2}\left(\kappa_V + \frac{\kappa_I \rho_w v d}{\mu}\right) \qquad (11\text{-}23)$$

$$Y = \frac{\kappa_V \mu v}{3g(\rho_p - \rho_w)d^2} \qquad (11\text{-}24)$$

The targeted expansion rate is about 25 percent for anthracite and about 37 percent for sand (Kawamura, 2000). The procedure for calculating the expansion of media during backwashing is demonstrated in Example 11-5.

Example 11-5 Filter bed expansion during backwash

Find the expanded bed depth of a sand filter at a backwash rate of 40 m/h given the following information: $L = 0.9$ m, $d = 0.5$ mm, $\rho_P = 2650$ kg/m^3, and $T = 15°$C.

Solution

1. Calculate X using Eq. 11-23. Values of ρ_W and μ are available in Table C-1 in App. C. Because no pilot or site-specific data are given, use values of κ_V and κ_I from midpoint values in Table 11-3 (e.g., $\kappa_V = 112$ and $\kappa_I = 2.25$):

$$X = \frac{\mu v}{2g(\rho_p - \rho_w)d^2}\left(\kappa_V + \frac{\kappa_I \rho_w v d}{\mu}\right)$$

$$= \frac{(1.14 \times 10^{-3}\ \text{kg/m} \cdot \text{s})[(40\ \text{m/h})/(3600\ \text{s/h})]}{2(9.81\ \text{m/s}^2)(2650 - 999\ \text{kg/m}^3)[0.5\ \text{mm}/(10^3\ \text{mm/m})]^2}$$

$$\times \left[112 + \frac{(2.25)(999\ \text{kg/m}^3)[(40\ \text{m/h})/(3600\ \text{s/h})][0.5\ \text{mm}/(10^3\ \text{mm/m})]}{1.14 \times 10^{-3}\ \text{kg/m} \cdot \text{s}}\right]$$

$$= 0.1921$$

2. Calculate Y using Eq. 11-24:

$$Y = \frac{k_V \mu v}{3g(\rho_p - \rho_w)d^2}$$

$$= \frac{(112)(1.14 \times 10^{-3}\ \text{kg/m} \cdot \text{s})(40\ \text{m/h})(10^3\ \text{mm/m})^2}{3(9.81\ \text{m/s}^2)(2650 - 999\ \text{kg/m}^3)(0.5\ \text{mm})^2(3600\ \text{s/h})} = 0.1168$$

3. Calculate porosity using Eq. 11-22:

$$\varepsilon_E = \sqrt[3]{X + (X^2 + Y^3)^{1/2}} + \sqrt[3]{X - (X^2 + Y^3)^{1/2}}$$

$$= \sqrt[3]{0.1921 + [(0.1921)^2 + (0.1168)^3]^{1/2}}$$

$$+ \sqrt[3]{0.1921 - [(0.1921)^2 + (0.1168)^3]^{1/2}} = 0.57$$

4. Calculate the expanded bed depth using Eq. 11-15. Because no site-specific porosity value is given, the fixed-bed porosity is taken from Table 11-3 and is assumed to be $\varepsilon_F = 0.42$.

$$L_E = L_F \frac{1 - \varepsilon_F}{1 - \varepsilon_E} = 0.9\ \text{m}\left(\frac{1 - 0.42}{1 - 0.57}\right) = 1.21\ \text{m}$$

5. Calculate the percent expansion of the bed:

$$\left(\frac{L_E}{L_F} - 1\right) \times 100 = \left(\frac{1.21\ \text{m}}{0.9\ \text{m} - 1}\right) \times 100 = 34\%$$

Comment

The bed expansion under the example conditions is 34 percent, which is about equal to the desired expansion rate of 37 percent for sand.

Backwash hydraulics depends on the viscosity of water, which varies with temperature. To achieve the same expansion, it is necessary to use a higher backwash rate in summer, when the water is warmer, than the backwash rate used when the water is cold.

Several aspects of rapid filter design and operation result directly from requirements for effective backwashing. These include selection of a low uniformity coefficient to minimize stratification, skimming to remove fines, and selecting media for dual- and multimedia filters.

STRATIFICATION

Stratification is an important side effect of backwashing of rapid media filters. As shown in Eq. 10-14, the settling velocity of individual grains of filter media depends on diameter, with larger grains requiring a larger

fluidization velocity. When a graded media filter bed (of constant grain density) is backwashed at a uniform rate, the smallest particles fluidize most and rise to the top of the filter bed, while the largest particles collect near the bottom of the bed.

Stratification has several adverse effects on filter performance. First, the accumulation of small grains near the top of the bed causes excessive head loss in the first few centimeters of bed depth (because head loss is a function of grain size). Second, the ability of a filter to remove particles is also a function of grain size (as will be presented subsequently), so small grains at the top of a bed cause all particles to be filtered in the first few centimeters of bed depth, which means the entire bed depth is not being used effectively.

The method for minimizing stratification is proper selection of filter media. The uniformity coefficient determines the stratification of the media. Low values of the uniformity coefficient are recommended specifically to minimize stratification of the filter bed during backwashing. A uniformity coefficient less than 1.4 is recommended for all rapid filter media, and uniformity coefficient values less than 1.3 are becoming common.

REMOVAL OF FINES

Stratification is particularly problematic if the media has excessive fines (particles considerably smaller than the effective size), even if a low uniformity coefficient has been specified. Fines are normally removed by backwashing and skimming immediately after the installation of new media. After media installation, backwashing normally proceeds at a low rate, just above the minimum fluidization velocity to bring as many fines as possible to the top of the bed, which are then skimmed with a flat-bladed shovel after the filter is drained. It is usually necessary to repeat the backwashing and skimming several times to remove the fines. Multimedia filters should be backwashed and skimmed after each layer of media is installed.

MULTIMEDIA FILTERS

Backwash hydraulics have important implications for the selection of media in dual- and trimedia filters. The media in multimedia filters must be matched so that all media fluidize at the same backwash rate. Otherwise, one media may be washed out of the filter during attempts to fluidize the other media, or alternatively, one media may fail to fluidize. Fluidization of media can be balanced by selecting a ratio of grain sizes that is matched to the ratio of grain densities. During backwash, the settling velocity is in the transition flow regime. Equating an equivalent fluidization velocity for two media in Eq. 10-14 and solving for the ratio of particle sizes yield the expression

$$\frac{d_1}{d_2} = \left(\frac{\rho_2 - \rho_w}{\rho_1 - \rho_w}\right)^{0.625} \tag{11-25}$$

where d_1 = grain diameter of one filter medium, m
d_2 = grain diameter of a second filter medium, m
ρ_1 = density of medium with diameter d_1, kg/m^3
ρ_2 = density of medium with diameter d_2, kg/m^3

If the two media have approximately the same uniformity coefficient, the effective size can be used in Eq. 11-25.

INTERMIXING

Proper selection of media and proper backwashing procedures result in the layers of media staying segregated, with only a few centimeters of intermixing. Two layers of media tend to stay segregated when the bulk densities of the two layers are different. Bulk density is a function of the grain density, water density, and bed porosity (Cleasby and Woods, 1975), as shown in the expression

$$\rho_B = \rho_p(1 - \varepsilon) + \rho_w\varepsilon \tag{11-26}$$

where ρ_B = bulk density of bed, kg/m^3

The vigorous agitation of media during backwashing can cause intermixing. Segregation of media types is maintained by reducing the backwash rate gradually at the end of the backwash cycle, which allows the media to segregate before the backwash cycle is terminated.

The size and uniformity coefficient of media for trimedia filters are sometimes selected to encourage intermixing rather than segregation. Filters with media that is intermixed are called *mixed-media filters* and are thought to have a better distribution of media, from coarse grains on the top of the bed to fine grains at the bottom, which would minimize the porosity of the filter bed, sacrificing head loss but improving removal.

11-5 Particle Removal in Rapid Filtration

Filters can remove particles from water by several mechanisms. When particles are larger than the void spaces in the filter, they are removed by straining. When particles are smaller than the voids, they can be removed only if they contact and stick to the grains of the media. Transport to the media surface occurs by interception, sedimentation, and diffusion, and attachment occurs by attractive close-range molecular forces such as van der Waals forces.

Straining causes a cake to form at the surface of the filter bed, which can improve particle removal but also increases head loss across the filter. Rapid filters quickly build head loss to unacceptable levels if a significant cake layer forms. In addition, filtration at the surface leaves the bulk of the rapid filter bed unused. Consequently, rapid filters are designed to minimize straining and encourage depth filtration.

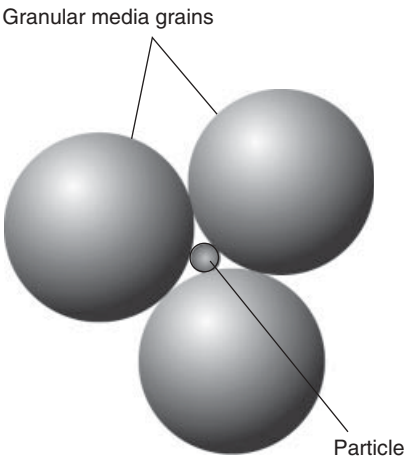

Figure 11-8
Capture of spherical particle by spherical media grains. If the ratio of particle diameter to media diameter is greater than 0.15, the particle will be strained by the media. If it is smaller, straining is not possible and particle capture must occur by other means. For typical rapid filtration, straining is limited to particles about 80 μm and larger.

Straining

A bed of granular media can strain particles smaller than the grain size. For spherical media, a close-packed arrangement will cause straining when the ratio of particle diameter to grain diameter is greater than 0.15; smaller particles can pass through the media, as shown on Fig. 11-8. The effective size of the smallest media specified in rapid filters is typically around 0.5 mm, although some trimedia filters use garnet or ilmenite with an effective size as small as 0.2 mm. With the use of engineered media that minimizes the quantity of finer grains, straining becomes insignificant for particles smaller than about 30 to 80 μm, depending, of course, on the shape and variability of the media and how it packs together. The vast majority of particles in the influent to rapid filters are smaller, particularly when sedimentation is used ahead of filtration. For example, viruses can be more than 1000 times smaller than particles that would be strained in a conventional filter, and clearly would not be removed without transport and attachment mechanisms.

Depth Filtration

In depth filtration, particles are removed continuously throughout the filter through a process of transport and attachment to the filter grains. Particle removal within a filter is dependent on the concentration of particles, similar to a first-order rate equation (Iwasaki, 1937), as described by

$$\frac{\partial C}{\partial z} = -\lambda C \tag{11-27}$$

where λ = filtration coefficient, m^{-1}
C = mass or number concentration of particles, mg/L or L^{-1}
z = depth in filter, m

If the filtration coefficient was known, it would be possible to calculate the effluent particle concentration from a filter. Unfortunately, filtration

is a complex process, and the filtration coefficient can vary in both time and depth in the filter and depend on properties of the filter bed (grain shape and size distribution, porosity, depth), influent suspension (turbidity, particle concentration, particle size distribution, particle and water density, water viscosity, temperature, level of pretreatment), and operating conditions (filtration rate).

Two types of models have evolved to explain rapid filter behavior. Fundamental (or microscopic) models examine the importance of actual transport and attachment mechanisms. Phenomenological (or macroscopic) models attempt to explain the physical progression of the filtration cycle, through ripening, effective filtration, and breakthrough, though they do so with empirical parameters obtained from site-specific pilot studies rather than fundamental mechanisms. Phenomenological models are useful for evaluating pilot data and can be used to predict filter performance for conditions that were not specifically addressed within a pilot study. Because of the complexity of filtration mechanisms and the wide variation in source water properties, neither type of model can predict filter performance without site-specific pilot studies; nevertheless, they provide insight and understanding into the filtration process.

Fundamental Depth Filtration Theory

Fundamental filtration models examine the relative importance of mechanisms that cause particles to contact media grains. They can explain how particles are removed during depth filtration and the importance of various design and operating parameters under time-invariant conditions. For instance, fundamental filtration models are used later in this section to demonstrate the advantages of dual-media over monomedia filters and the importance of a low uniformity coefficient. Fundamental filtration models can also be used to examine the relative impact of varying other parameters on filter performance, such as porosity, filtration rate, or temperature. For these reasons, fundamental filtration models are valuable to a student acquiring a conceptual understanding of the filtration process.

Although they assist with conceptual understanding, fundamental filtration models are not very effective at quantitatively predicting the effluent turbidity in actual full-scale filters for the following reasons: (1) the models are based on an idealized system in which spherical particles collide with spherical filter grains; (2) the hydrodynamic variability and effect on streamlines introduced by the use of angular media are not addressed; (3) the models predict a single value for the filtration coefficient, which does not change as a function of either time or depth, whereas in real filters the filtration coefficient changes with both time and depth as solids collect on the media; and (4) the models assume no change in grain dimensions or bed porosity as particles accumulate. For these reasons, fundamental depth filtration models are often called clean-bed filtration models, and experimental validation generally focuses on the initial performance of laboratory filters (with spherical particles and media grains).

Yao Filtration Model

The basic model for water treatment applications was presented by Yao et al. (1971). Yao et al.'s theory is based on the accumulation of particles on a single filter grain (termed a ''collector''), which is then incorporated into a mass balance on a differential slice through a filter. The accumulation on a single collector is defined as the rate at which particles enter the region of influence of the collector multiplied by a transport efficiency factor and an attachment efficiency factor. The transport efficiency η and the attachment efficiency α are ratios describing the fraction of particles contacting and adhering to the media grain, respectively, as described by the equations

$$\eta = \frac{\text{particles contacting collector}}{\text{particles approaching collector}} \tag{11-28}$$

$$\alpha = \frac{\text{particles adhering to collector}}{\text{particles contacting collector}} \tag{11-29}$$

where η = transport efficiency, dimensionless
α = attachment efficiency, dimensionless

The mass flow of particles approaching the collector is the mass flux through the cross-sectional area of the collector:

$$\text{Mass flow to one collector} = vC\frac{\pi}{4}d_c^2 \tag{11-30}$$

where v = superficial velocity, m/s
C = concentration of particles, mg/L
d_c = diameter of collector (media grain), m

The model development was based on an isolated single collector in a uniform-flow field, so the velocity in Eq. 11-30 is the filtration rate.

The accumulation of particles on a single collector is applied to a mass balance in a filter using a differential element of depth as the control volume, as shown on Fig. 11-9. The number of collectors in the control volume must be determined, which is the total volume of media within the control volume divided by the volume of a single collector:

$$\text{Number of collectors} = \frac{(1-\varepsilon)\,a\Delta z}{(\pi/6)\,d_c^3} \tag{11-31}$$

where ε = porosity
a = cross-sectional area of filter bed, m^2
Δz = incremental unit of depth in filter, m

The total accumulation of particles within the control volume is the product of the number of collectors and the accumulation on a single isolated collector. These terms can then be applied to a mass balance on the differential element:

$$[\text{accum}] = [\text{mass in}] - [\text{mass out}] \pm [\text{rxn}] \tag{11-32}$$

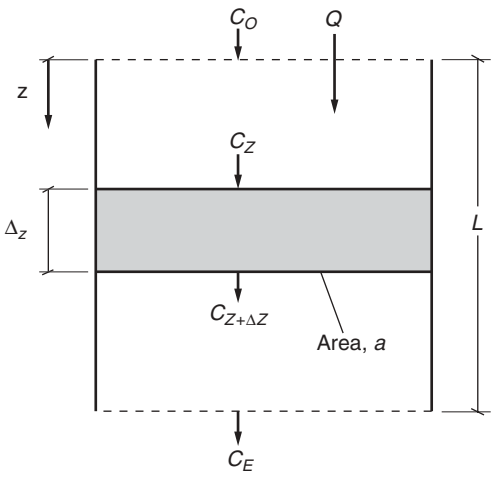

Figure 11-9
Differential element of filter bed for filtration models.

Generation or loss of particles due to reactions (i.e., production of biomass or consumption of particles via chemical or biological activity) is not included in the model. Diffusion is negligible compared to convective flux, so the mass balance can be written as

$$\left(vC\frac{\pi}{4}d_c^2\eta\alpha\right)\left[\frac{(1-\varepsilon)a\Delta z}{(\pi/6)d_c^3}\right] = QC_Z - QC_{Z+\Delta Z} = -va\,(C_{Z+\Delta Z} - C_Z) \tag{11-33}$$

where Q = flow through filter, m^3/s

Taking the limit as Δz goes to zero, Eq. 11-33 can be rearranged as

$$\frac{dC}{dz} = \frac{-3(1-\varepsilon)\eta\alpha C}{2d_c} \tag{11-34}$$

Equation 11-34 has the same form as Eq. 11-27 and defines the filter coefficient as

$$\lambda = \frac{3(1-\varepsilon)\eta\alpha}{2d_c} \tag{11-35}$$

If the parameters in Eq. 11-35 ($\varepsilon, \eta, \alpha$, and d_c) are constant with respect to depth in the filter, Eq. 11-34 can be integrated to yield the expression

$$C = C_O \exp\left[\frac{-3(1-\varepsilon)\eta\alpha L}{2d_c}\right] \tag{11-36}$$

where C_O = particle concentration in filter influent, mg/L
L = depth of filter, m

The next step in the development of the Yao model is to evaluate the mechanisms that influence the transport of particles to the media surface and the forces that influence attachment to the media.

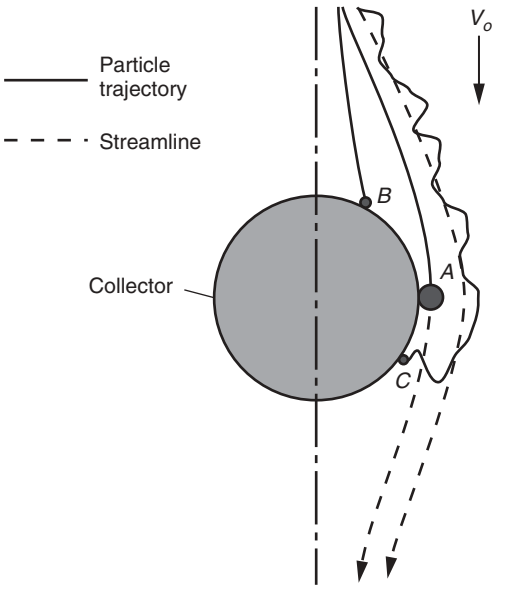

Figure 11-10
Particle transport mechanisms in fundamental filtration theory: (a) interception, particle A follows streamline but collides with the collector because of the proximity between the streamline and the collector; (b) sedimentation, particle B deviates from the streamline and collides with the collector because of gravitational forces; (c) diffusion, particle C collides with collector due to random Brownian motion.

Transport Mechanisms

The mechanisms for transporting particles to media grains are shown on Fig. 11-10. Water approaching a spherical collector in a uniform-flow field under laminar flow conditions follows streamlines to either side of the collector. Some particles will contact the collector because they follow a fluid streamline that passes close to the grain, while others must deviate from their fluid streamline to reach the collector surface. Details for each transport mechanism are as follows.

INTERCEPTION

Particles remaining centered on fluid streamlines that pass the collector surface by a distance of half the particle diameter or less will be intercepted. For laminar flow, spherical particles, and spherical collectors, particle transport by interception is given by the following expression (Yao et al., 1971):

$$\eta_I = \frac{3}{2}\left(\frac{d_p}{d_c}\right)^2 \tag{11-37}$$

where η_I = transport efficiency due to interception, dimensionless
d_p = diameter of particle, m

As shown in Eq. 11-37, interception increases as the ratio of particulate size to collector size increases. For 10-μm particles passing through a filter with 0.5-mm sand, $\eta_I < 10^{-3}$. In other words, only about one of a thousand possible collisions with a single collector due to interception will actually occur. However, a particle will pass thousands of collectors during its passage through a filter bed, increasing the chance of being removed somewhere in the filter bed.

SEDIMENTATION

Particles with a density significantly greater than water tend to deviate from fluid streamlines due to gravitational forces. The collector efficiency due to gravity has been shown to be the ratio of the Stokes settling velocity (see Chap. 10) to the superficial velocity (Yao et al., 1971), as shown in the expression

$$\eta_G = \frac{v_S}{v_F} = \frac{g(\rho_p - \rho_w)\, d_p^2}{18\mu\, v_F} \tag{11-38}$$

where η_G = transport efficiency due to gravity, dimensionless
v_S = Stokes' settling velocity, m/s
v_F = filtration rate (superficial velocity), m/s

DIFFUSION

Particles move by Brownian motion and will deviate from the fluid streamlines due to diffusion. The transport efficiency due to diffusion is given by the following expression (Levich, 1962):

$$\eta_D = 4\,\mathrm{Pe}^{-2/3} \tag{11-39}$$

$$\mathrm{Pe} = \frac{3\pi\mu\, d_p d_C v}{k_B T} \tag{11-40}$$

where η_D = transport efficiency due to diffusion, dimensionless
Pe = Peclet number, dimensionless
k_B = Boltzmann constant, 1.381×10^{-23} J/K
T = absolute temperature, K (273 + °C)

The Peclet number is a dimensionless parameter describing the relative significance of advection and dispersion in mass transport and is discussed further in Chap. 6. For physically similar systems, a lower value of the Peclet number implies greater significance of diffusion. The formulation of the Peclet number in Eq. 11-40 uses the Stokes–Einstein equation (see Chap. 7) to relate the diffusion coefficient to the diameter of a spherical particle. In rapid filtration, diffusion is most significant for particles less than about 1 μm in diameter.

TOTAL TRANSPORT EFFICIENCY

The relative importance of these various mechanisms for transporting the particle to the surface depends on the physical properties of the filtration system. The Yao model assumes that the transport mechanisms are additive:

$$\eta = \eta_I + \eta_G + \eta_D \tag{11-41}$$

where η = total transport efficiency, dimensionless

The importance of each mechanism can be evaluated as a function of system properties. The effect of particle diameter on the importance of

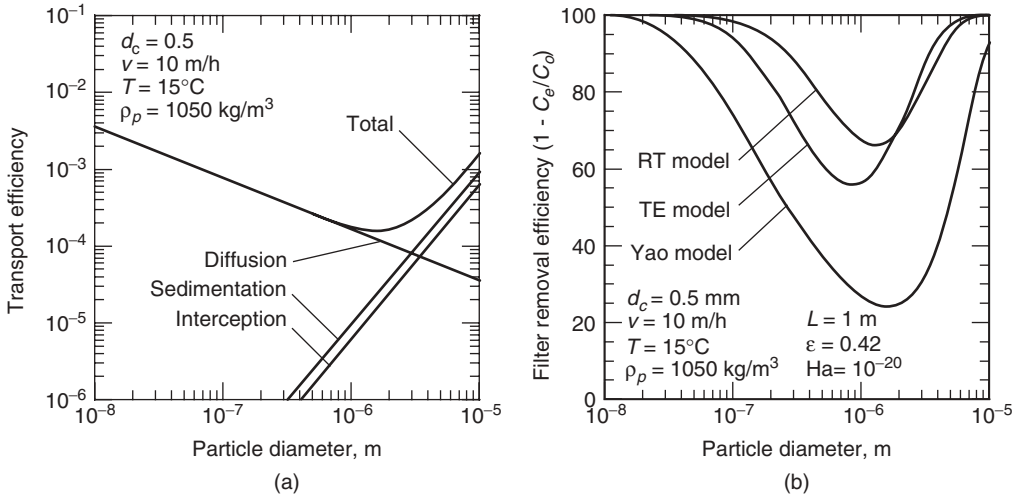

Figure 11-11
Predictions of fundamental filtration models: (a) importance of each transport mechanism on particles of different size as predicted by the Yao model and (b) comparison of predictions by each model for removal efficiency.

each mechanism is shown on Fig. 11-11a. Small particles are efficiently removed by diffusion, whereas larger particles are removed mainly by sedimentation and interception. The Yao model predicts that the lowest removal efficiency occurs for particles of about 1 to 2 μm in size, which has been verified experimentally (Yao et al., 1971).

Advanced Fundamental Filtration Models

The Yao filtration model frequently underpredicts the number of collisions between particles and collectors when compared to experimental data. Several groups of researchers have tried to refine the Yao model by using a different flow regime or incorporating addition transport mechanisms. Rajagopalan and Tien (1976) developed a fundamental depth filtration model (the RT model) that (1) used a sphere-in-cell model of granular media, (2) accounted for the attraction between the collectors and particles caused by van der Waals forces (for interception and sedimentation only), and (3) accounted for reduced collisions due to viscous resistance of the water between the particle and collector. Following Rajagopalan and Tien's work, Tufenkji and Elimelech (2004) expanded the correlation further (the TE model) and more fully integrated van der Waal forces and hydrodynamic interactions into all transport mechanisms. The RT and TE models are semiempirical expressions that were correlated with the results of a numerical simulation model. The equations for the individual transport mechanisms in the Yao, RT, and TE models, along with the underlying expressions, are summarized in Table 11-4. In each case, the total transport efficiency is expressed by Eq. 11-41. The filter removal

Table 11-4
Transport mechanism equations in the Yao, RT[a], and TE fundamental filtration models

Mechanism	Yao, Habibian, and O'Melia		Rajagopalan and Tien[a]		Tufenkji and Elimelech	
Interception	$\eta_I = \frac{3}{2} N_R^2$	(11-37)	$\eta_I = A_S \left(\frac{4}{3} N_A\right)^{1/8} N_R^{15/8}$	(11-43)	$\eta_I = 0.55\, A_S N_A^{1/8} N_R^{1.675}$	(11-46)
Sedimentation	$\eta_G = N_G$	(11-42)	$\eta_G = 0.00338 A_S N_R^{-0.4} N_G^{1.2}$	(11-44)	$\eta_G = 0.22 N_R^{-0.24} N_{vdW}^{0.053} N_G^{1.11}$	(11-47)
Diffusion	$\eta_D = 4\text{Pe}^{-2/3}$	(11-39)	$\eta_D = 4 A_S^{1/3} \text{Pe}^{-2/3}$	(11-45)	$\eta_D = 2.4 A_S^{1/3} N_R^{-0.081} N_{vdW}^{0.052} \text{Pe}^{-0.715}$	(11-48)

$$N_R = \frac{d_p}{d_c} \quad (11\text{-}49)$$

$$N_G = \frac{v_S}{v_F} = \frac{g(\rho_p - \rho_w) d_p^2}{18 \mu v_F} \quad (11\text{-}50)$$

N_R = relative size group, dimensionless
N_G = gravity number, dimensionless
N_A = attraction number, dimensionless
N_{vdW} = van der Walls number, dimensionless
Pe = Peclet number (see Chap. 6, Eq. 6-91), dimensionless
D_L = diffusion coefficient (Chap. 7, Stokes–Einstein equation, Eq. 7-25), m^2/s
Ha = Hamaker constant, J

(*continued*)

Table 11-4 *(Continued)*

$\mathrm{Pe} = \dfrac{v_F d_c}{D_L} = \dfrac{3\pi\mu d_p d_C v_F}{k_B T}$	(11-40)	A_S = porosity function, dimensionless d_p = particle diameter, m d_c = collector diameter, m k_B = Boltzmann constant, 1.381×10^{-23} J/K T = absolute temperature, K $273 + °C$ v_F = filtration rate, m/s v_S = Stokes' settling velocity (see Chap. 10, Eq. 10-13), m/s ε = bed porosity, dimensionless γ = porosity coefficient, dimensionless ρ_p = particle density, kg/m^3 ρ_w = liquid density, kg/m^3 μ = liquid viscosity, kg/m-s
$N_A = \dfrac{N_{vdW}}{N_R \mathrm{Pe}} = \dfrac{\mathrm{Ha}}{3\pi\mu d_p^2 v_F}$	(11-51)	
$N_{vdW} = \dfrac{\mathrm{Ha}}{k_B T}$	(11-52)	
$\gamma = (1-\varepsilon)^{1/3}$	(11-53)	
$A_S = \dfrac{2(1-\gamma^5)}{2-3\gamma+3\gamma^5-2\gamma^6}$	(11-54)	

[a]The RT model does not consider η_I and η_G independent; they are shown here separately for convenience of comparison to the other models.

efficiency predicted by each model under comparable conditions is shown on Fig. 11-11b. The Hamaker constant is a parameter used in describing van der Waals forces. The theory necessary to calculate a value for the Hamaker constant is beyond the scope of this text, but the value ranges from 10^{-19} to 10^{-20} J (Hiemenz and Rajagopalan, 1997).

Fundamental filtration models can be used to examine the effect of important variables on filter performance, as shown in Example 11-6.

Example 11-6 Application of the TE Model

Use the TE model to examine the effect of media diameter (ranging from 0.4 to 2 mm in diameter) on the removal of 0.1-μm particles in a filter bed of monodisperse media under the following conditions: porosity $\varepsilon = 0.50$, attachment efficiency $\alpha = 1.0$, temperature $T = 20^{\circ}$C (293.15 K), particle density $\rho_p = 1050$ kg/m^3, filtration rate $v = 15$ m/h, bed depth $L = 1.0$ m, Hamaker constant Ha $= 10^{-20}$ J (10^{-20} kg · m^2/s^2), and Boltzmann constant $k_B = 1.381 \times 10^{-23}$ J/K (1.381×10^{-23} kg · m^2/s^2 · K).

Solution

1. Calculate N_R for a media diameter of 0.4 mm using Eq. 11-49:

$$N_R = \frac{d_p}{d_c} = \frac{1 \times 10^{-7}}{4 \times 10^{-4}} = 2.5 \times 10^{-4}$$

2. Calculate N_G using Eq. 11-50. The values of ρ_w and μ are available in Table C-1 in App. C:

$$N_G = \frac{g(\rho_p - \rho_w)d_p^2}{18\mu v_F}$$

$$= \frac{(1050 - 998 \text{ kg/m}^3)(9.81 \text{ m/s}^2)(1 \times 10^{-7} \text{ m})^2 (3600 \text{ s/h})}{18(1 \times 10^{-3} \text{ kg/m} \cdot \text{s})(15 \text{ m/h})}$$

$$= 6.76 \times 10^{-8}$$

3. Calculate Pe for a media diameter of 0.4 mm using Eq. 11-40:

$$\text{Pe} = \frac{3\pi\mu d_p d_c v}{k_B T}$$

$$= \frac{3\pi(1 \times 10^{-3} \text{ kg/m} \cdot \text{s})(1 \times 10^{-7} \text{ m})(4 \times 10^{-4} \text{ m})(15 \text{ m/h})}{(1.381 \times 10^{-23} \text{ kg} \cdot \text{m}^2/\text{s}^2 \text{ K})(293.15 \text{ K})(3600 \text{ s/h})}$$

$$= 3.89 \times 10^5$$

4. Calculate N_A using Eq. 11-51:

$$N_A = \frac{\text{Ha}}{3\pi\mu d_p^2 v} = \frac{(1 \times 10^{-20}\ \text{kg} \cdot\ \text{m}^2/\text{s}^2)(3600\ \text{s/h})}{3\pi(1 \times 10^{-3}\ \text{kg/m} \cdot \text{s})(1 \times 10^{-7}\text{m})^2(15\ \text{m/h})}$$

$$= 2.54 \times 10^{-2}$$

5. Calculate N_{vdW} using Eq. 11-52:

$$N_{\text{vdW}} = \frac{\text{Ha}}{k_B T} = \frac{1 \times 10^{-20}\ \text{kg} \cdot \text{m}^2/\text{s}^2}{(1.381 \times 10^{-23}\ \text{kg} \cdot\ \text{m}^2/\text{s}^2)(293.15\ \text{K})} = 2.47$$

6. Calculate γ using Eq. 11-53:

$$\gamma = (1 - \varepsilon)^{1/3} = (1 - 0.50)^{1/3} = 0.7937$$

7. Calculate A_S using Eq. 11-54:

$$A_S = \frac{2(1 - \gamma^5)}{2 - 3\gamma + 3\gamma^5 - 2\gamma^6}$$

$$= \frac{2[1 - (0.7937)^5]}{2 - 3(0.7937) + 3(0.7937)^5 - 2(0.7937)^6} = 21.46$$

8. Calculate η_I using Eq. 11-46:

$$\eta_I = (0.55)(21.46)(2.54 \times 10^{-2})^{1/8}\ (2.5 \times 10^{-4})^{1.675}$$

$$= 6.91 \times 10^{-6}$$

9. Calculate η_G using Eq. 11-47:

$$\eta_G = (0.22)(2.5 \times 10^{-4})^{-0.24}\ (2.47)^{0.053}\ (6.76 \times 10^{-8})^{1.11}$$

$$= 1.86 \times 10^{-8}$$

10. Calculate η_D using Eq. 11-48:

$$\eta_D = (2.4)(21.46)^{1/3}\ (2.50 \times 10^{-4})^{-0.081}$$

$$\times\ (2.47)^{0.052}\ (3.89 \times 10^5)^{-0.715} = 1.38 \times 10^{-3}$$

11. Calculate η using Eq. 11-41:

$$\eta = 6.91 \times 10^{-6} + 1.86 \times 10^{-8} + 1.38 \times 10^{-3} = 1.39 \times 10^{-3}$$

12. Calculate C/C_0 using Eq. 11-36:

$$\frac{C}{C_0} = \exp\left[\frac{-3(1-0.50)(1.39\times10^{-3})(1.0)(1\text{ m})}{2(4\times10^{-4}\text{ m})}\right] = 0.074$$

13. Set up a computation table to determine particle removal for other diameters. Repeat steps 1 through 12 for additional media sizes between 0.4 and 2.0 mm. These calculations are best done with a spreadsheet. The results are as follows:

Media Diameter (mm)	C/C_0	Log Removal
0.4	0.074	1.13
0.6	0.262	0.58
0.8	0.434	0.36
1.0	0.560	0.25
1.2	0.650	0.19
1.4	0.716	0.15
1.6	0.764	0.12
1.8	0.801	0.10
2.0	0.830	0.08

Comment

The initial removal of small particles is highly sensitive to media size. While these particles are removed relatively efficiently by 0.4-mm-diameter media, removal drops dramatically as the media size increases.

Attachment Efficiency

As particles approach the surface of the media, short-range surface forces begin to influence particle dynamics. The attachment efficiency varies from a value of zero (no particles adhere) to a value of 1.0 (every collision between a particle and collector results in attachment). The attachment efficiency is affected by London–van der Waals forces, surface chemical interactions, electrostatic forces, hydration, hydrophobic interactions, or steric interactions (Tobiason and O'Melia, 1988; O'Melia, 1985; O'Melia and Stumm, 1967). Laboratory studies have found values of attachment efficiency ranging from about 0.002 to 1.0 (Chang and Chan, 2008; Elimelech and O'Melia, 1990; Tobiason and O'Melia, 1988). A number of correlations have been developed to relate the attachment efficiency value to properties of the collectors, particles, and solution (Chang and Chan, 2008; Bai and Tien, 1999; Elimelech, 1992). A key property that makes attachment unfavorable is the presence of repulsive electrostatic forces.

In water treatment, the interest is not so much the ability to predict the value of the attachment efficiency when attachment conditions are unfavorable, but to modify the system so that attachment is as favorable as possible, that is, an attachment efficiency value very nearly 1.0. The most important factor in achieving high attachment efficiency is eliminating the repulsive electrostatic forces; that is, proper destabilization of particles by coagulation. The need for a high attachment efficiency is exactly why coagulation is a critical part of rapid filtration. Particle stability and destabilization by coagulation was discussed in Chap. 9.

Predicting Filter Performance

The RT model has been used to demonstrate the value of dual-media filter beds when poorly pretreated water enters the filter (O'Melia and Shin, 2001). A similar analysis is shown on Fig. 11-12a. When water is properly conditioned ($\alpha = 1.0$), both the monomedia and dual-media filters perform well. When the water is not properly conditioned ($\alpha = 0.25$), both filters perform worse, but the degradation of quality is much more dramatic with the monomedia filter, suggesting that dual-media filters are more robust during periods of inadequate chemical pretreatment.

Similarly, the TE model can be used to demonstrate the effect of specifying filter media with a low uniformity coefficient. The particle concentrations through three filter beds with different UC values, but the same filter effluent quality are shown on Fig. 11-12b. The monodisperse media (i.e., UC = 1.0) has a constant filter grain size through the depth of the bed, but the two polydisperse media have been stratified by backwashing,

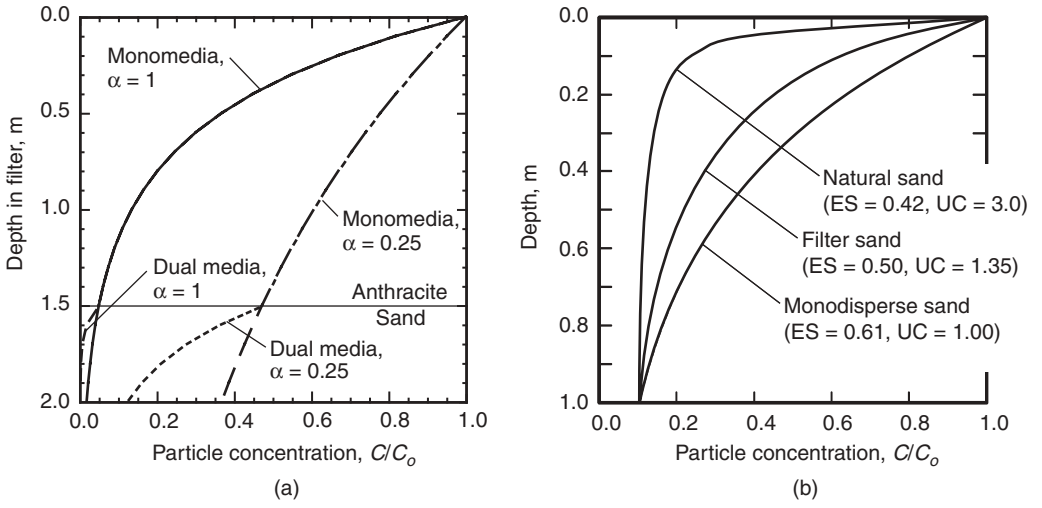

Figure 11-12
(a) Effect of attachment efficiency on effluent from monomedia and dual-media filters, as predicted by the RT model and (b) effect of media uniformity on solids penetration in filter bed, as predicted by the TE model.

sending the smallest grains to the top and the largest grains to the bottom. Stratification increases the removal efficiency near the top of the bed. As a result, nearly all of the particles are removed near the top of the bed with the natural sand (UC = 3.0), whereas the particles are distributed throughout the monodisperse bed. In addition, the rapid collection of particles at the top of the natural sand bed will lead to clogging and onset of straining as an additional removal mechanism, leading to rapid head loss buildup and short filter runs. Thus, a low uniformity coefficient leads to a more effective use of the entire depth of the filter bed, less straining and cake formation at the top of the bed, and longer filter runs.

As filtration progresses, the media bed physically changes due to the accumulation of particles. Thus, filtration efficiency changes with time, a phenomenon not addressed in the fundamental filtration models. More sophisticated models have been developed to incorporate time-dependent phenomena, such as ripening (Darby et al., 1992), but current models are unable to predict changes in particle removal or head loss when design or operating conditions change. To examine the change in filter performance as solids collect within the filter bed, phenomenological filter models have been developed.

Phenomenological Depth Filtration Models

The primary function of phenomenological filtration models is to explore the progression of a filter run and the change in performance as solids collect within the filter. Performance variables of interest include (1) the duration of ripening and water quality during ripening, (2) the water quality during the effective filtration cycle, (3) the time to breakthrough, and (4) the time to limiting head.

PHENOMENOLOGICAL MODEL DEVELOPMENT

The mathematical formulation of phenomenological filtration models is based on the same overall mass balance through the filter bed that was used for the fundamental filtration models, using Eq. 11-32 to describe the accumulation of solids in a differential element of depth in the filter bed, as shown on Fig. 11-9. Phenomenological models do not focus on the accumulation of particles on a single collector but instead consider the increase of mass within the differential element. The basic mass balance equation for phenomenological models is developed with the following simplifying assumptions: (1) although particles are present in the interstitial fluid and at the surface of the media, the accumulation of particles in the interstitial fluid is negligible compared to the accumulation of particles on the media; (2) the number of particles entering and exiting the element by diffusion is negligible; and (3) the generation or loss of particles due to reaction is ignored. Thus, the mass balance for a differential element is described by the expression

$$\frac{\partial \sigma}{\partial t} = -v_F \frac{\partial C}{\partial z} \tag{11-55}$$

where σ = specific deposit, mass of accumulated particles per filter bed volume, mg/L
t = time, s

Phenomenological models are empirical and based on experimental data using the specific deposit as a master variable. By combining Eqs. 11-27 and 11-55, the basic form of the phenomenological model can be developed as

$$\frac{\partial \sigma}{\partial t} = \lambda v_F C \tag{11-56}$$

As noted earlier, filter performance changes as a function of time as solids collect in the filter bed. Thus, the filtration coefficient is normally expressed as a function of the specific deposit. For instance, filter efficiency improves as a filter ripens, and the filtration capabilities of the clean media are quickly superseded by the filtration capabilities of the retained particles. Ripening can be viewed as a condition that increases the value of the filtration coefficient as solids are collected in the filter bed. Thus, the filtration coefficient could be expressed as follows (Iwasaki, 1937):

$$\lambda = \lambda_0 + k\sigma \tag{11-57}$$

where λ_0 = initial filtration coefficient, m^{-1}
k = filtration rate constant, $L/mg \cdot m$

As solids accumulate in the filter, the value of the filtration coefficient increases, leading to greater capture of solids and a lower concentration of particles in the filter effluent. Removal efficiency increases with depth during ripening and is dependent on the size and charge of particles in the water and other factors (Kim and Lawler, 2008; Kim et al., 2008). Consequently, the value of the filtration coefficient must be calculated as a function of depth because solids do not collect uniformly throughout the entire depth of the filter.

Breakthrough is a decrease of the filtration coefficient that causes an increase in effluent turbidity, which is opposite to what occurs when particles are being captured in the filter. A filtration coefficient that initially increases (ripening) and eventually decreases to zero (breakthrough) can be expressed in several forms, such as (Tien, 1989)

$$\lambda = \lambda_0 + k\sigma - \frac{k_T \sigma^2}{\varepsilon_0 - \sigma/\rho_P} \tag{11-58}$$

where k_T = breakthrough rate constant, $L^2/mg^2 \cdot m$
ε_0 = initial porosity, dimensionless

Filtration models must account for ripening and breakthrough and must also consider other processes such as detachment of previously attached particles. A number of filtration models have been proposed over the years and have been summarized elsewhere in the filtration literature (Tien, 1989; Tien and Payatakes, 1979).

A solution to a phenomenological model allows the particle concentration at any depth in the filter bed as well as the effluent concentration to be calculated at any point in time. Unfortunately, phenomenological model equations are complex and not easily solved. The rate of particle capture at any point in the filter bed is dependent on the quantity of previously captured solids, which in turn varies with bed depth (more solids collect at the top of the bed because the concentration of solids is higher near the top of the bed, in accordance with Eq. 11-56) and filtration time. Development of a phenomenological model involves the simultaneous solution of Eqs. 11-27 and 11-55 under conditions where λ is a function of the specific deposit, which in turn varies in both space and time. The filter rate coefficient λ is also site specific because of variations in local water quality, characteristics of the particles, characteristics of the media, stratification, and operating parameters. Because determining the filter rate coefficient is complex, phenomenological models are frequently solved numerically, although analytical solutions are possible depending on the complexity of the equation for λ.

STEADY-STATE PHENOMENOLOGICAL MODEL

A simplified phenomenological model can be developed to allow easier analysis of pilot data. The basic assumptions of a simplified phenomenological model are (1) the specific deposit is averaged over the entire filter bed, (2) solids accumulate at a steady rate over the entire filter run (the reduced accumulation of solids during ripening is ignored, under the legitimate assumption that the relatively small quantity of solids retained in the bed during ripening has little impact on the specific deposit over the entire filter run), and (3) head loss increases at a constant rate. With these assumptions, the specific deposit can be determined by performing a mass balance over the entire bed:

$$\sigma_t V = C_O Q t - C_E Q t \tag{11-59}$$

where σ_t = specific deposit at time t, mg/L
V = bed volume, m^3
C_O = influent concentration, mg/L
C_E = effluent concentration, mg/L

Dividing by the filter bed area and rearranging yields an expression for the specific deposit as a function of time:

$$\sigma_t = \frac{v_F (C_O - C_E) t}{L} \tag{11-60}$$

where L = filter bed depth, m

The specific deposit increases at a steady rate as solids accumulate in the filter bed. Pilot filters can be operated until breakthrough occurs, and the

value of the specific deposit at breakthrough can be related to the time to breakthrough by the expression

$$\sigma_B = \frac{v_F(C_O - C_E)t_B}{L} \tag{11-61}$$

where σ_B = specific deposit at breakthrough, mg/L
t_B = time to breakthrough, h

Equation 11-61 can be rearranged and expressed as a function of t_B:

$$t_B = \frac{\sigma_B L}{v_F(C_O - C_E)} \tag{11-62}$$

Specific deposit depends on process parameters (influent water quality, filtration rate, bed depth, media diameter, etc.). The value of the specific deposit at breakthrough can be recorded for a number of pilot filter runs in which these process parameters are varied. A regression analysis of the data can determine the dependence of the specific deposit at breakthrough, σ_B, on the process parameters (Kavanaugh et al., 1977). The dependence of the specific deposit varies because of site-specific conditions and can be determined only by analyzing pilot data.

Similarly, the rate of head loss buildup has been observed to depend on the rate of solids deposition in a filter. If $h_{L,O}$ is the clean-bed head loss determined from the Ergun equation (Eq. 11-13) and head loss increases at a constant rate, then the head loss at any time during the filtration run can be determined using the expression (Ives, 1967)

$$h_{L,t} = h_{L,O} + k_{HL}\sigma_t \tag{11-63}$$

where $h_{L,t}$ = filter head loss at time t, m
$h_{L,O}$ = initial head loss, m
k_{HL} = head loss increase rate constant, L · m/mg

Like the specific deposit, the head loss increase rate constant depends on site-specific conditions and process parameters. Some evidence suggests that filtration rate is an important factor in determining the type of deposit that forms. Higher filtration rates tend to cause particle to penetrate more deeply into the bed, spreading the deposit over a larger area of the bed. In addition, higher filtration rates lead to more compact deposits whereas lower filtration rates tend to form more open, porous deposits (Veerapnani and Weisner, 1997; Weisner, 1999). Compact deposits can be characterized by a higher fractal dimension (spheres have a fractal dimension of 3 whereas lines have a fractal dimension of 1). The rate of head loss increase as the deposit accumulates (i.e., the head loss increase rate constant k_{HL}) appears to be higher for deposits with a low fractal dimension; thus, low filtration rates cause a faster increase in head loss than high filtration rates for the same specific deposit. Quantitative models relating the rate of head loss increase to the characteristics of the deposit have not been successfully developed, and the head loss increase rate constant is best determined

through a pilot study. Incorporating Eq. 11-60 and rearranging yields an expression for the rate constant:

$$k_{HL} = \frac{(h_{L,t} - h_{L,O})L}{v_F(C_O - C_E)t} \tag{11-64}$$

Once the rate constant for head loss buildup is determined, it can be used to determine the specific deposit that can be accumulated before reaching the limiting head as follows:

$$t_{HL} = \frac{(H_T - h_{L,O})L}{k_{HL}v_F(C_O - C_E)} \tag{11-65}$$

where t_{HL} = time to limiting head, h
H_T = total available head, m

Once dependence of the specific deposit at breakthrough and the rate of head loss buildup on process parameters are determined, the phenomenological model can be used to determine the duration of filter runs and whether filter runs are limited by breakthrough or limiting head. Use of the simplified phenomenological model to analyze pilot data is shown in Example 11-7.

Example 11-7 Determination of optimum media size from pilot data

Four pilot filters with different effective sizes of anthracite (UC < 1.4, ρ = 1700 kg/m^3) were operated over multiple runs. The results are summarized in the table below. The media depth in each filter was 1.8 m, the filtration rate was 15 m/h, and the temperature was relatively constant at 20°C. Based on turbidity, you can assume the solids concentration was constant at 2.2 mg/L in the influent and negligible in the effluent.

Media ES (mm)	No. of Runs	Ave. Eff. Turbidity (NTU)	Ave. Time to Breakthrough (h)	Ave. Initial Head (m)	Ave. Final Head (m)
0.73	7	0.08	55	0.77	3.35
0.88	6	0.07	49	0.56	2.38
1.02	9	0.08	41	0.44	1.87
1.23	8	0.13	38	0.29	1.44

Determine: (a) the relationship between specific deposit at breakthrough (σB) and the media ES, (b) the relationship between the head loss rate constant (k_{HL}) and the media ES, and (c) the required available head and optimal media size if the full-scale system is to have a design run length of at least 48 h.

Solution

1. Any type of equation that relates media ES to σ_B and k_{HL} and results in a linear graph can be used. Often the relationships between the media ES and σ_B or k_{HL} can be described by a power function, and that type of equation is used in this example. Thus:

$$\sigma_B = b_1 (d)^{m_1} \quad \text{and} \quad k_{HL} = b_2 (d)^{m_2}$$

To find the value of the coefficients b and m, take the log of each equation and plot $\log(\sigma_B)$ and $\log(k_{HL})$ as a function of $\log(d)$. The slope of the straight line is m and the intercept is $\log(b)$:

$$\log(\sigma_B) = \log(b_1) + m_1 \log(d)$$

and

$$\log(k_{HL}) = \log(b_2) + m_2 \log(d)$$

2. Calculate the necessary values for the first effective size
   a. Calculate $\log(d)$

$$\log(d) = \log(0.73 \text{ mm}) = -0.137$$

   b. Calculate σ_B using Eq. 11-61

$$\sigma_B = \frac{v (C_O - C_E) t_B}{L} = \frac{(15 \text{ m/h})(2.2 - 0 \text{ mg/L})(55 \text{ h})}{1.8 \text{ m}}$$
$$= 1008 \text{ mg/L}$$

   c. Calculate $\log(\sigma_B)$

$$\log(\sigma_B) = \log(1008) = 3.00$$

   d. Calculate k_{HL} using Eq. 11-64

$$k_{HL} = \frac{(3.35 - 0.77 \text{ m})(1.8 \text{ m})}{15 \text{ m/h } (2.2 - 0 \text{ mg/L})(55 \text{ h})} = 0.00256 \text{ L} \cdot \text{ m/mg}$$

   e. Calculate $\log(k_{HL})$

$$\log(k_{HL}) = \log(0.00256) = -2.59$$

3. Repeat step 2 for the remaining effective sizes. The results are summarized in the following table:

ES	log(d)	σ_B	log (σ_B)	k_{HL}	log (k_{HL})
0.73	−0.137	1008	3.00	0.00256	−2.59
0.88	−0.056	898	2.95	0.00203	−2.69
1.02	0.0086	752	2.88	0.00190	−2.72
1.23	0.090	697	2.84	0.00165	−2.78

4. Plot log(σ_B) against log(d).

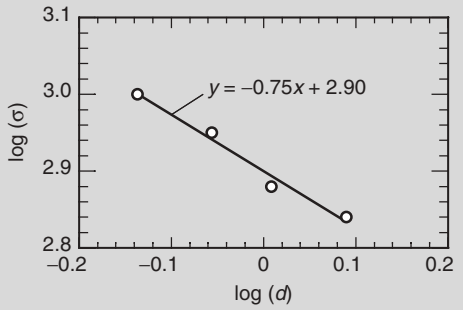

5. Perform a linear regression of the data (shown in the graph in step 4 using the Excel trendline function) and determine the slope and intercept of the regression line. From the graph in step 4, $m_1 = -0.75$ and $\log(b_1) = 2.90$. Therefore, $b_1 = 794$. The relationship between σ_B and d is

$$\sigma_B = 794\,(d)^{-0.75} \tag{1}$$

when the units of σ_B are mg/L and the units of d are mm.

6. Plot log(k_{HL}) against log(d).

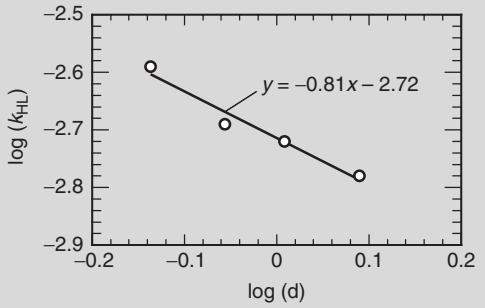

7. Perform a linear regression of the data (shown in the graph in step 6 using the Excel trendline function) and determine the slope and intercept of the regression line. From the graph in step 6, $m_2 = -0.81$ and $\log(b_2) = -2.72$. Therefore, $b_2 = 0.00191$. Thus, the relationship between k_{HL} and d is

$$k_{HL} = 0.00191\,(d)^{-0.81} \tag{2}$$

when the units of k_{HL} are L·m/mg and the units of d are mm.

8. Calculate the required size to reach 48 h before breakthrough by substituting Eq. 1 above into Eq. 11-62 and solving for the media size.

$$t_B = \frac{794\,(d)^{-0.75}\,L}{v_F(C_O - C_E)}$$

$$(d)^{-0.75} = \frac{t_B v_F(C_O - C_E)}{794L} = \frac{(48\text{ h})(15\text{ m/h})(2.2 - 0\text{ mg/L})}{794(1.8\text{ m})} = 1.108$$

$$d = (1.108)^{1/-0.75} = 0.87\text{ mm}$$

9. Calculate the required head to reach 48 h before reaching the limiting head by substituting Eq. 2 above into Eq. 11-65 and solving for the available head.

$$t_{HL} = \frac{(H_T - h_{L,O})\text{L}}{0.00181\,(d)^{-0.81}\,v_F(C_O - C_E)}$$

$$H_T = \frac{t_{HL}0.00181\,(d)^{-0.81}\,v_F(C_O - C_E)}{\text{L}} + h_{L,O}$$

$$= \frac{(48\text{ h})(0.00181)(0.87\text{mm})^{-0.81}(15\text{ m/h})(2.2 - 0\text{ mg/L})}{1.8\ m} + 0.53\,m$$

$$= 2.3\text{ m}$$

where the initial head loss was calculated with Eq. 11-13 (the Ergun equation; see Example 11-2).

OPTIMIZATION

For a given set of design and operating conditions, optimum water production occurs when the time to reach limiting head is equal to the time to breakthrough provided the run length is adequate. Phenomenological filtration models can be used to optimize filtration design by allowing the engineer to vary design parameters until the time to breakthrough and limiting head are equal. Optimization of the filter design presented in Example 11-7 for two conditions of available head with respect to media size is shown on Fig. 11-13. Increasing the media depth will tend to increase the time to reach breakthrough (t_B) but decrease the time to reach the limiting head (t_{HL}). For 2.5 m of available head, the optimum design is achieved at a media size of 1.0 mm. An increase in available head to 3.0 m would have no effect on the run length if the media stayed the same size but would increase the run length by about 5 h if the media effective size were decreased to 0.90 mm.

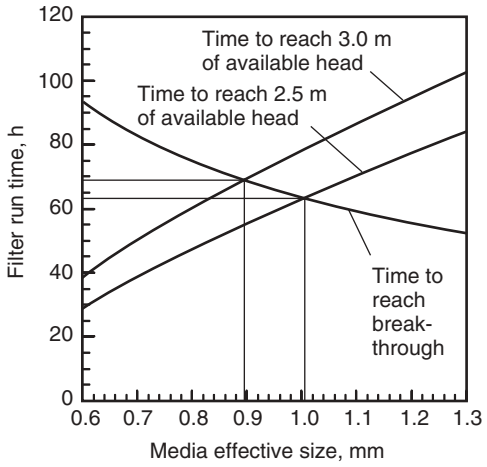

Figure 11-13
Optimization of media size with respect to time to breakthrough and time to limiting head.

The effect of significant design parameters on t_B and t_{HL} is summarized in Table 11-5. The effects summarized in Table 11-5 can be predicted from the theory presented earlier in the chapter and have generally been observed in actual filter operation. These design variables will influence filter performance, and thus t_B and t_{HL}, based on the rate of particulate capture and the rate of head loss increase. Some of the design variables, such as media size, media depth, and flow rate, are subject to designer selection. The limits of media size should be chosen to minimize interlayer mixing, which tends to decrease porosity and thereby lead to a rapid increase in head loss (decrease in t_{HL}) (Cleasby and Woods, 1975). Other variables, such as influent solids concentration, will depend upon the location of the filter in the process scheme. Variables such as floc strength and deposit

Table 11-5
Effect of design parameters on time to breakthrough and limiting head loss

Parameter	Effect of Parameter Increase on	
	Time to Breakthrough, t_B	Time to Limiting Head Loss, t_{HL}
Effective size	Decrease	Increase
Media depth	Increase	Decrease
Filtration rate	Decrease	Decrease
Influent particle concentration	Decrease	Decrease
Floc strength	Increase	Decrease
Deposit density	Decrease	Decrease
Porosity	Decrease	Increase

density are difficult to control, but the use of polymers can be employed to improve floc strength.

Particle Detachment

Particle removal in granular filters is not an irreversible process, and detachment of particles may occur during the filtration cycle. Several studies have examined the breakthrough phenomenon and noted that it may be due to a decrease in particle capture or an increase in detachment, with evidence suggesting that the latter may be the dominant cause (Moran et al., 1993). Detachment occurs when there are perturbations to the system (Bergendahl and Grasso, 2003) but may occur at a low rate during steady-state filtration in the absence of perturbations. Perturbations may include changes in hydraulic forces or changes in water quality, including ionic strength and pH (Amirtharajah and Raveendran, 1993; Raveendran and Amirtharajah, 1995).

Detachment occurs when the forces shearing the particles away from the media grain are greater than the adhesive forces holding the particle. The primary forces between particles and media grains include van der Waals forces, electric double-layer interactions, Born repulsion, and hydration and hydrophobic forces (Raveendran and Amirtharajah, 1995). Under constant-flow (shear) conditions, detachment increases as pH increases or ionic strength decreases. Under constant chemical conditions, detachment increases as hydraulic shear increases. Models suggest that the shear stress from hydraulic perturbations has a greater effect on large particles than on smaller colloids (Bergendahl and Grasso, 2003). In addition, experimental evidence suggests that solids aggregate on the filter media (in a manner analogous to the aggregation of solids during flocculation) and that the aggregated flocs can then detach from the media (Darby and Lawler, 1990; Kau and Lawler, 1995; Moran et al., 1993).

Experimental research has not produced a quantitative model describing particle attachment and detachment mathematically. It is evident, however, that changes in filtration rate or influent water quality can have negative effects on filter performance and lead to the detachment of previously retained particles as well as changes in the ability to retain new particles, resulting in higher effluent turbidity. For these reasons, granular filters perform best when operated under constant conditions and when any changes are made gradually.

11-6 Rapid Filter Design

Preliminary design of rapid filters consists of the following:

1. Setting performance criteria, such as effluent turbidity, filter run length, recovery, and unit filter run volume (UFRV)
2. Selecting process design criteria, such as required level of pretreatment; filter media type, size, and depth; filtration rate; number of filters; and available head

3. Selecting a method for flow distribution and control
4. Selecting major process components, including backwashing systems, underdrains, wash troughs, and process piping

These topics are considered in the following sections.

Performance Criteria

The primary performance criteria for rapid filter design are the effluent water quality, the length of the filter run, and the recovery (i.e., the ratio of net to total water filtered). Filter design must also consider nonperformance criteria, such as minimizing capital and operation and maintenance (O&M) costs, reliability, and ease of maintenance.

EFFLUENT WATER QUALITY

Filter performance is primarily monitored by measuring effluent turbidity. To be in compliance with current U.S. regulations, the turbidity must be measured in the combined filter effluent at least every 4 h and at least 95 percent of the measurements must be below 0.3 NTU (maximum 1 NTU) (U.S. EPA, 2006). Most utilities set a design turbidity goal below the regulated limits, with a typical goal being 0.1 NTU. Additional information about the measurement and interpretation of turbidity values is presented in Chap. 2. Facilities can get additional credit for *Cryptosporidium* removal by achieving lower turbidity levels or by achieving low levels in the effluent from each individual filter.

A second method of measuring effluent water quality is particle counts. Particle counters provide both the number and size distribution of particles in water. Some utilities have installed particle counters and set water quality goals for particles, but there are no standard methods for the measurement of particles or regulatory requirements for the number of particles in filtered water. Additional information about particle counters is presented in Chap. 2.

FILTER RUN LENGTH

The length of the filter run dictates how often backwashes must be performed and has an impact on recovery. Since operators either perform backwashes manually or supervise automated backwash procedures, the frequency of backwashing has a direct impact on the amount of labor involved in filter operation. Typically, the minimum desirable filter run length is about 1 day, with filter designs that produce a filter run length between 1 and 4 days being common. Design parameters that can affect the length of a filter run are presented in Table 11-5.

RECOVERY

Recovery is the ratio between the net and total quantity of water filtered. Portions of the filtered water are used for backwashing and discharged as filter-to-waste volume, so the net water production is lower than the total

volume of water processed through the filter. Recovery is evaluated using the concepts of unit filter run volume (UFRV) and unit backwash volume (UBWV) (Trussell et al., 1980). The UFRV is the volume of water that passes through the filter during a run, and the UBWV is the volume required to backwash the filter, defined as

$$\text{UFRV} = \frac{V_F}{a} = v_F t_F \tag{11-66}$$

$$\text{UBWV} = \frac{V_{\text{BW}}}{a} = v_{\text{BW}} t_{\text{BW}} \tag{11-67}$$

$$\text{UFWV} = \frac{V_{\text{FTW}}}{a} = v_F t_{\text{FTW}} \tag{11-68}$$

where UFRV = unit filter run volume, m^3/m^2
UBWV = unit backwash volume, m^3/m^2
UFWV = unit filter-to-waste volume, m^3/m^2
V_F = volume of water filtered during one filter run, m^3
V_{BW} = volume of water required to backwash one filter, m^3
V_{FTW} = volume of water discharged as filter-to-waste, m^3
v_F = filtration rate (superficial velocity), m/h
v_{BW} = backwash rate, m/h
t_F = duration of filter run, h
t_{BW} = duration of backwash cycle, h
t_{FTW} = duration of filter-to-waste period, h
a = filter cross-sectional area, m^2

The ratio of net to total water filtered is the recovery:

$$r = \frac{V_F - V_{\text{BW}} - V_{\text{FTW}}}{V_F} = \frac{\text{UFRV} - \text{UBWV} - \text{UFWV}}{\text{UFRV}} \tag{11-69}$$

where r = recovery, expressed as a fraction

Filters should be designed for a recovery of at least 95 percent. Typical wash water quantities are about 8 m^3/m^2 (200 gal/ft^2). Thus, to achieve a recovery greater than 95 percent, a UFRV of at least 200 m^3/m^2 (5000 gal/ft^2) is required. Calculation of the parameters for net water production is demonstrated in Example 11-8.

Utility operators sometimes use excessive backwash rates or time in the belief that cleaning the media thoroughly will result in longer filter runs or lower effluent turbidity. Excessive backwashing, however, is counterproductive because it lowers the recovery and can result in longer ripening periods, which further reduce recovery.

Process Design Criteria

Design criteria are established to meet the performance requirements, given the source water quality and site-specific constraints.

Example 11-8 Calculation of parameters for net water production

A filter is operated at a rate of 12.5 m/h for 72 h, of which 30 min was discharged as filter-to-waste volume. After filtration, it is backwashed at a rate of 40 m/h for 15 min. Calculate the UFRV, UBWV, UFWV, and recovery.

Solution

1. Calculate UFRV using Eq. 11-66:

$$\text{UFRV} = (12.5\ \text{m/h})(72\ \text{h}) = 900\ \text{m} = 900\ \text{m}^3/\text{m}^2$$

2. Calculate UBWV using Eq. 11-67:

$$\text{UBWV} = (40\ \text{m/h})(0.25\ \text{h}) = 10\ \text{m} = 10\ \text{m}^3/\text{m}^2$$

3. Calculate UFWV using Eq. 11-68:

$$\text{UFWV} = (12.5\ \text{m/h})(0.5\ \text{h}) = 6.25\ \text{m} = 6.25\ \text{m}^3/\text{m}^2$$

4. Calculate recovery using Eq. 11-69:

$$r = \frac{(900 - 10 - 6.25)\ \text{m}^3/\text{m}^2}{900\ \text{m}^3/\text{m}^2} = 0.982 = 98.2\%$$

FILTER TYPE

Classifications of rapid filters were presented on Fig. 11-3 (by level of pretreatment) and in Table 11-1 (by type of media). The level of pretreatment is typically based on raw-water quality. In borderline cases, pilot studies can verify whether a lower level of pretreatment is effective (i.e., direct filtration instead of conventional treatment).

The selection of monomedia versus dual-media filters is also based on raw-water quality and pilot study data. Deep-bed monomedia anthracite filters have a low rate of head loss accumulation, a high capacity for solids retention, and long filter runs. Dual-media filters, however, can provide a more robust design when filters are subjected to influent water that has not been properly conditioned, as was shown with the RT model on Fig. 11-12a. Thus, monomedia filters may be appropriate in situations when the raw-water quality is fairly constant and predictable, and dual-media filters may be more appropriate for variable water supplies. Deep-bed dual-media filters might be an attractive option when robustness and long filter runs are needed with variable water supplies.

FILTRATION RATE

Filtration rate influences the required area of the filter beds, clean-bed head loss, rate of head loss accumulation, distribution of solids collection in

the bed, effluent water quality, and run length. Filters are typically designed to treat the maximum plant capacity at the design filtration rate with at least one filter out of service for backwashing. A low filtration rate increases the capital cost because it increases the required area of the filter beds, whereas a high filtration rate can increase the clean-bed head loss and decrease the length of the filter runs. Typically, the highest filtration rate that yields good filter performance is recommended. In filtering floc resulting from alum or ferric coagulation with polymeric coagulant aids, reasonable filter run lengths with no degradation of effluent quality can generally be achieved up to 25 m/h (10 gpm/ft^2). Filter effluent quality tends to degrade at filtration rates above 12.5 m/h (5 gpm/ft^2) with weak chemical floc such as alum floc without polymer or poorly flocculated biological floc. Higher filtration rates tend to increase solids penetration (if media size is properly selected), and the rate of head loss accumulation may be slower at higher rates because of more efficient use of the filter bed.

Filtration rates are often subject to regulatory limits. For instance, West Coast states restrict the filtration rate to 15 m/h (6 gpm/ft^2) or less, unless pilot testing demonstrates a higher rate is justified (Kawamura, 1999). Most rapid-filtration plants have design filtration rates between 5 and 15 m/h (2 and 6 gpm/ft^2), although some high-rate rapid filters have been constructed with filtration rates as high as 33 m/h (13.5 gpm/ft^2).

NUMBER AND DIMENSIONS OF FILTERS

The number of filters is influenced by the overall capacity of the plant, the maximum dimensions of a single filter, the effect of filtration rate changes during backwashing, and economic considerations. Most water treatment plants have a minimum of four filters, although small plants may have as few as two.

A small number of filters can reduce cost by minimizing the number of components, but a large number of filters minimizes the filtration rate change on the remaining filters when one is taken out of service for backwash. With only two filters, the filtration rate in one filter would double when the other was backwashed. As noted in Sec. 11-5, significant changes in the filtration rate can have adverse effects on filter performance by causing particle detachment and increasing effluent turbidity.

The maximum dimensions of a single filter are generally determined by the economic sizing of the filter backwash facility and possible difficulties in providing uniform distribution of backwash water over the entire filter bed. The practical maximum size of a typical high-rate gravity filter is about 100 m^2 (1100 ft^2).

AVAILABLE HEAD

The head for filtration is the difference between the clean-bed head loss and the available head in the structure. Because rapid filters typically operate

by gravity, the available head is dependent on the elevation of the filter building relative to upstream and downstream structures (sedimentation basins and clearwells). Selection of the available head involves a trade-off between longer filter runs (greater available head) and economics (smaller available head). Due to construction costs, filter designs rarely provide more than 2 to 3 m (6.5 to 10 ft) of available head through the filter bed.

FILTER MEDIA

The selection of filter media is critical to meeting the performance criteria established for the treatment plant. Selection of filter media involves a trade-off between filtration efficiency (smaller media captures particles better) and head loss (larger media minimizes head loss).

The primary design criteria for filter media are the ES and UC. As noted earlier, a low UC is important for effective utilization of the entire filter bed. The ES must be selected in concert with other design parameters, such as filtration rate and filter depth. Factors such as clean-bed head loss as calculated in Sec. 11-4 must be considered along with effluent quality.

Filter depth and media size are interrelated. Some design engineers recommend a rule-of-thumb relationship, the ratio of depth to effective size (L/d ratio), to be between 1000 and 2000. As described in Secs. 11-4 and 11-5, head loss and particle removal are not simple inverse relationships of media diameter. Thus, the L/d ratio can provide some general guidance on the adequacy of a particular design, but it cannot be used to predict that two filters with the same L/d ratio will perform identically, particularly if they are composed of different media.

Pilot Testing

As a result of many years of successful operation of rapid filters, it is frequently possible to design an effective rapid-filtration system using the principles presented in this chapter without the use of pilot testing. In situations where higher filtration rates are warranted, pilot testing may be necessary to verify acceptable performance or satisfy regulatory agencies.

A typical rapid-filtration pilot plant is shown on Fig. 11-14. The pilot equipment typically consists of a feed pump, acrylic columns with an inside diameter of 0.1 to 0.15 m (4 to 6 in), and associated piping, valves, and instrumentation. In general, the diameter of the column should be at least 50 times the diameter of the media (Lang et al., 1993). The most common variables to be considered in a filtration pilot study are media size, media depth, and filtration rate. In addition, mono- and dual-media filters are often compared in pilot studies. For each pilot experiment, it is important to collect data on (1) clean-bed head loss, (2) filtration rate, (3) duration and magnitude of ripening, (4) influent and effluent turbidity, (5) water temperature, (6) time to breakthrough, and (7) head loss at the end of the filter run. It is normally desirable to collect some of these data continuously, particularly the turbidity, filtration rate, and head loss data.

Figure 11-14
Typical rapid granular filter pilot plant and associated facilities. The filters are the tall Plexiglas columns near the front of the photograph.

Flow Control

Flow control is an important part of any filter system. Filter flow control can be accomplished in a variety of ways, and texts and design manuals describe four or five different control strategies (Cleasby and Logsdon, 1999; Kawamura, 2000). All systems for flow control have advantages and disadvantages but must accomplish three objectives: (1) control the filtration rate of individual filters, (2) distribute flow among individual filters, and (3) accommodate increasing head loss. Figure 11-15 shows several options for filter control systems.

Three basic methods are used for controlling filtration rates and distributing the flow to individual filters: (1) modulating control valve, (2) influent weir flow splitting, and (3) declining-rate filtration (no active flow control or distribution). The features of these methods are described in Table 11-6.

As noted earlier, the total available head in a gravity rapid filter system is fixed by the water elevation in the upstream and downstream structures (i.e., sedimentation basins and clearwells). The head loss through the filter bed increases as the filter collects solids, so provisions must be made to accommodate the variation in head loss. Three basic strategies are used: (1) maintain constant head above the filter (e.g., constant water level) and vary the head in the filter effluent by modulating a control valve;

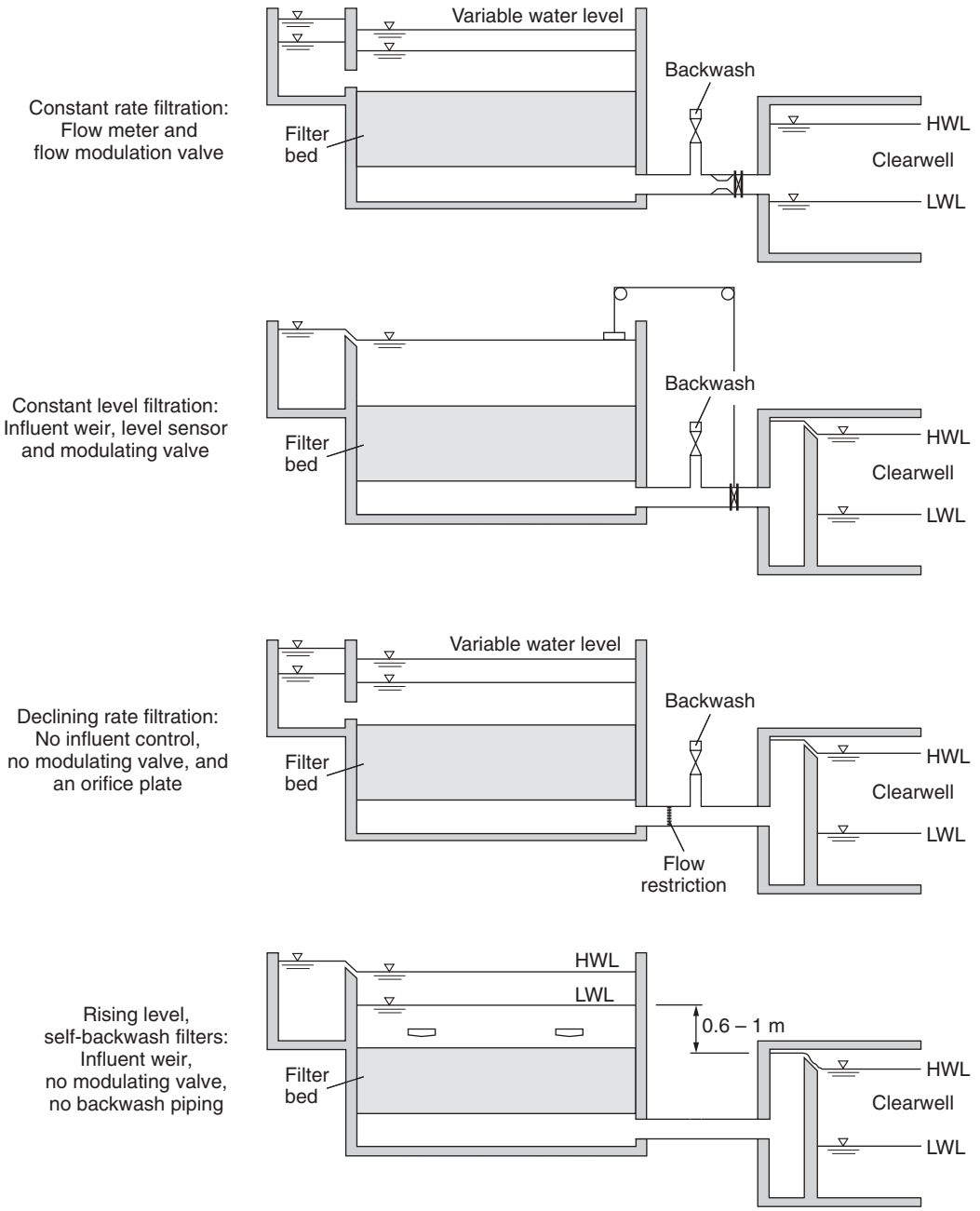

Figure 11-15
Rapid granular filter flow control strategies.

Table 11-6
Filter control options for distributing flow to filters and controlling filtration rate

	Modulating Control Valve	Influent Weir Flow Splitting	Declining Rate Filtration
Description	Effluent piping from each filter has a flowmeter and modulating control valve. The control system calculates a flow setpoint for each filter (from total flow and number of filters in service, or an influent level indicator) and automatically adjusts the control valve until the signal from the flowmeter matches the setpoint.	Water from a common influent channel flows to each filter over a weir. Water splits equally to all operating filters. When a filter is removed from service for backwashing, the flow is automatically distributed to the remaining filters.	Water from a common influent channel flows to each filter without any devices to measure or control the flow. All filters operate at the same head loss but different filtration rates. The flow is greatest in the cleanest filters and declines as solids accumulate. The common water level rises as all filters accumulate solids and then falls after the dirtiest (i.e., longest operating) filter is backwashed. After backwash, the filter that had been producing the lowest flow now produces the highest flow.
Advantages	Maximum flexibility and control. No need for influent weirs or orifices that can cause turbulence that can break fragile floc and degrade filter performance.	Simple and effective. No sophisticated instrumentation required. Total flow always divided evenly with each filter having the same filtration rate. Filtration rate changes gradually as water level rises or drops.	Simple. No instrumentation required. May be appropriate in developing countries or remote locations.
Disadvantages	Greatest complexity. Without proper maintenance, components can break down and lead to poor filter control. Valve movement in discrete steps can repeatedly overshoot target position, resulting in the valve "hunting" for the right position and causing large swings in the filtration rate, which can cause particle detachment and an increase in effluent turbidity (see Sec. 11-5).	Floc may break up and degrade filter performance if floc is fragile or if drop over weir is large (drop can be minimized by proper design and floc can be strengthened by using polymers during coagulation or flocculation).	No indication of the flow rate in any individual filter is provided. No way to control the filtration rate. The filtration rate at the beginning of a filter run may greatly exceed the design filtration rate. The high filtration rate during the filter-to-waste (FTW) period can waste water. Flow restrictors in FTW piping can reduce water loss but may cause particle detachment during increase in filtration rate with the FTW period is over.

(2) maintaining constant head in the filter effluent and vary the head upstream of the filter (allowing the water level to rise); and (3) maintaining nearly constant head loss and allowing the filtration rate to decline as solids accumulate in the bed (declining-rate filtration). Declining rate filtration was described in Table 11-6, and the features of the other two methods are described in Table 11-7.

It should be evident from Tables 11-6 and 11-7 that all flow control methods have advantages and disadvantages. No method is clearly superior

Table 11-7
Filter control options for accommodating the increase in head loss in a rapid granular filter during filtration

	Constant Level	Rising Water Level
Description	The water column above the filter is maintained near the maximum level. When head loss in the filter bed is low (immediately after backwash), an effluent valve is maintained in a nearly closed position. As head loss builds up in the filter, the valve gradually opens so that the total head loss across the filter bed and effluent valve stays constant. The effluent valve is controlled by an effluent flowmeter or a level transmitter. Head loss is monitored with a differential-pressure transmitter.	Filter effluent piping is configured to keep the filter bed submerged, typically with a filter effluent control weir with an elevation just above the top of the filter bed. When head loss in the filter bed is low, the water level is just above the top of the filter bed. As head loss builds up in the filter, the water level in the filter box gradually increases.
Used with (see Table 11-6)	Influent weir flow splitting. Modulating control valve.	Influent weir flow splitting.
Advantages	The filter box can be shorter (minimizing construction costs) than for rising water level systems because no head is lost over an effluent control weir, and even more height can be saved if there is no influent flow splitting weir. Minimizes cascade over the influent weir, when one is present.	Simple. No individual flow meters or modulating control valves on filters. Changes in filtration rate occur gradually because it takes time for the water level in the filter box to rise or fall.
Disadvantages	With no effluent control weir, poor design can lead to potential for negative pressure in the filter bed (see section on negative pressure in filter beds).	The influent weir must be above the maximum water level in the filter boxes to feed all filters equally. If the influent water cascades into the filter box from a large height, the top of the filter bed may be disturbed or the floc may be broken up by turbulence.

to the others. Selection is typically made on the basis of designer and owner preferences. Cost, complexity, and reliability are important issues. Whichever method is used, proper design is important because poor flow control can have a significant negative impact on filter performance.

Backwashing Systems

Backwashing is an indispensable part of rapid filtration. Improper or inadequate backwashing is one of the most frequent causes of problems in filters. Backwash criteria are established based on the flow rates necessary to fluidize the media and carry away deposited solids. The design equations for calculating these backwash rates were presented in Sec. 11-4. Alternatives for backwashing and backwash water delivery systems are discussed below.

ALTERNATIVES FOR BACKWASHING

Backwashing consists of upflowing water and a supplemental scouring system. The typical options for supplemental scouring systems are (1) fixed-nozzle surface wash, (2) rotating-arm surface wash, and (3) air scour. Supplemental scouring causes vigorous agitation of the bed and causes collisions and abrasion between media grains that break deposited solids loose from the media grains. Once the solids are separated from the media grains, the upflowing wash water can flush the solids from the filter. Design criteria for water-jet-type surface wash systems and air scour washing systems are shown in Table 11-8.

SURFACE WASH SYSTEMS

Surface wash systems typically have water nozzles on a rotating header or on a fixed pipe grid located just above the surface of the bed. Subsurface

Table 11-8
Typical design criteria for supplemental backwash systems

Criteria	Units	Fixed-Nozzle Surface Wash	Rotating-Arm Surface Wash	Air Scour
Surface wash water flow rate	m/h gpm/ft^2	7–10 2.8–4	1.2–1.8 0.5–0.7	— —
Air flow rate	m^3/m^2 · h scfm/ft^2	— —	— —	36–72 2–4
Pressure at discharge point	bar psi	0.5–0.8 7.2–11.6	5–7 73–100	0.3–0.5 4.3–7.3
Duration of washing	min	4–8	4–8	8–15
Backwash water flow rate	m/h gpm/ft^2	30–60 12–24	30–60 12–24	15–45 6–18

agitators or dual-arm agitators (with one set of nozzles above the bed and a second set located near the interface in a dual- or multimedia bed) are also available but are not common. Surface wash systems typically start operation 1 to 2 min before the backwash water starts flowing and continue for 5 to 10 min after the bed is fluidized. As the media fluidizes, it rises above the level of the nozzles, so the surface wash system is able to provide vigorous agitation of the fluidized media. Surface wash systems are effective for cleaning traditional filters with depths of 0.6 to 0.9 m (2 to 3 ft) but are less effective for cleaning deep-bed filters.

AIR SCOUR SYSTEMS

Air scour systems are necessary for cleaning deep-bed filters. Air and water are introduced simultaneously at the bottom of the filter bed for a portion of the backwash cycle followed by a water-only wash for the remainder of the cycle. The method of air introduction depends on the type of underdrain and support system used. Most modern underdrain systems can introduce air through the underdrains along with the water. When the filter design includes support gravel, however, air must be introduced through a piping system located just above the support gravel to prevent dislodging the gravel.

The most effective air scouring occurs when the water is flowing between 25 and 50 percent of the minimum fluidization velocity (Amirtharajah, 1993). At this water flow rate, the air forms cavities within the media that subsequently collapse (a phenomenon that has been called *collapse pulsing*), causing a substantial amount of agitation of the bed. With no water flow, air moves through the media as bubbles or channels with little movement of the media. At water flow rates above 75 percent of the minimum fluidization velocity, the air moves with the water as bubbles.

Air scour provides such vigorous agitation that media can be lost if air is flowing while waste wash water is being discharged from the filter. Thus, the common procedure for using air scour is to (1) drain the water to a level about 150 mm (6 in.) above the top of the media, (2) start the water air at appropriate rates for collapse pulsing, (3) continue the air scour while the water level gradually rises in the filter box, (4) terminate the air flow rate just before the water level reaches the lip of the wash water troughs, (5) increase the backwash water rate to a fluidization velocity and continue to wash the filter for several more minutes to flush solids from the bed, and (6) terminate backwash water slowly to allow dual-media filters to restratify. This procedure typically allows several minutes for air scour, which is sufficient for cleaning the bed. Additional details of the air scour process are available in Amirtharajah (1993).

BACKWASH WATER DELIVERY SYSTEMS

Backwashing requires a large volume of water to flow through the filter in a short time. Backwash rates typically range from 30 to 60 m/h (12 to

24 gpm/ft^2) for 10 to 20 min. Backwash water can be delivered to the filter through one of three methods: (1) backwash pumps, (2) an elevated backwash water tank, or (3) a head difference between the effluent channel and filter box. These systems are described in Table 11-9. Most filters require between 2 and 4 m (6.6 and 13 ft) of static head at the filter bottom, although many backwash systems are designed to provide up to 10 m (33 ft) of head at the pump or elevated tank, with the remaining head being dissipated by delivery piping, a throttling valve, and a flow controller to ensure a relatively constant backwash rate.

Table 11-9
Backwash water delivery systems

Water Supply	Backwash Pumps	Elevated Tank	Effluent Channel (Self-Backwashing Filter)
Description	Pumps, sized to provide the entire backwash flow, withdraw water from the filter effluent channel or finished water clearwell and provide it directly to the filter bottom.	Small pumps withdraw water from the filter effluent channel or finished water clearwell and send it to an elevated tank. The minimum water level in the tank is typically 9–12 m (30–40 ft) above the filter media. During backwash, water flows from the tank to the filters by gravity.	Filter effluent flows to a common effluent channel whose water elevation is controlled by a weir set several feet above the top of the media. During backwash, the water level in the filter box drops so that the head in the effluent channel is sufficient to provide the necessary backwash flow. This type of filter is often called a self-backwashing filter.
Advantages	Provides the maximum amount of control over backwash flow rates.	Smaller pumps are required because the volume of water required for backwash can be pumped to the tank over a period of hours.	Simplicity of design and operation; no pumps required.
Disadvantages	Large pumps are required.	Backwash flow rate can decline as water level in the elevated tank declines.	Less control over backwash flow rates. Deep filter box is required to provide sufficient head for filtering (maximum water level in filter to water level in effluent channel) and sufficient head for backwashing (water level in effluent channel to minimum water level in filter).

Filter System Components

Filters can be designed with a wide variety of configurations and various alternatives for the positioning of influent and effluent channels and piping. Detailed design of the structural aspects of filters is beyond the scope of this text, and students are referred to several references for detailed design, such as Kawamura (1975a,b,c, 1999, 2000). The primary components of a filter, other than the media, control system, and backwashing systems, are the underdrains and wash troughs.

FILTER SUPPORT MEDIA AND UNDERDRAINS

The function of filter underdrains is to support the filter media, collect and convey filtered water away from the filter system, and distribute backwash water and air. The underdrains must capture and distribute water uniformly to avoid localized variations in filtration rate or backwash rate that would jeopardize the effectiveness of the filter. Historically, a common design was a grid of perforated pipes overlain by several layers of gravel. The perforated pipe collects filtered water and distributes backwash water, and the gravel prevents the filter media from entering the perforations and provides additional distribution of backwash water. The gravel is installed in several layers, each 75 to 150 mm (3 to 6 in.) thick. The gravel on the bottom is typically 40 to 60 mm (1.5 to 2.5 in.) in diameter, and each overlying layer has stones of smaller diameter, with the top layer having an effective size of 0.8 to 2.0 mm (known as torpedo sand). Each layer is able to physically retain the overlying layer (recall from Fig. 11-8 that smaller grains can be physically retained by larger grains if the ratio of sizes is larger than about 0.15). A wide variety of other systems have been used, including false bottoms with strainers, underdrain blocks, precast concrete underdrains, teepee-type underdrains, and porous plates. Examples of underdrains are shown on Fig. 11-16. Uniform backwash flow distribution, durability, and cost are the three most important factors in selecting filter underdrains.

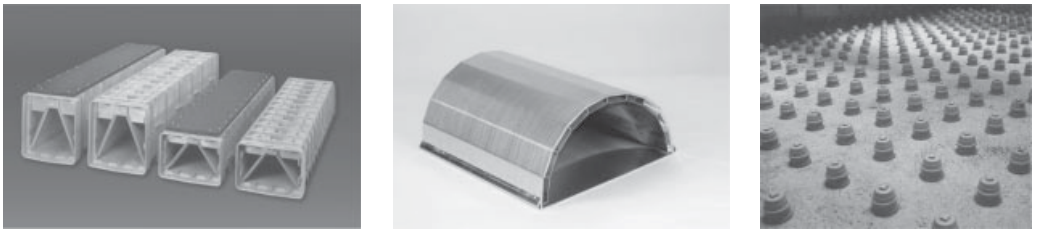

(a) (b) (c)

Figure 11-16
Typical filter underdrains: (a) Type S and SL with and without integral media support (IMS) cap (courtesy F. B. Leopold Company, Inc.), (b) direct retention underdrain system (courtesy Johnson Screens), and (c) nozzle-type underdrain system (courtesy of Ondeo-Degremont).

Modern underdrains typically have porous plates or fine mesh screens that can retain the filter media directly without the layers of gravel. Eliminating the gravel reduces the height of the filter box by about 0.5 m (1.6 ft). In addition, gravel can be dislodged by surges in backwash water or air scour.

To achieve an even distribution of backwash flow, (1) the orifice openings should be small enough to introduce a controlling loss of head and (2) the flow velocity in the pipe or channel in the underdrain system should be reasonably low and uniform throughout the entire filter area. Head loss in the underdrain system during backwash ranges from 0.1 to 3 m (0.3 to 10 ft) depending on the type of underdrain and backwash rates. For a false-bottom-type underdrain system, the required head loss is low (0.1 m for some systems) because the pressure is constant throughout the plenum if the inlet is properly designed. Perforated pipe grid systems use small orifices to create the necessary head loss to provide even distribution of backwash water.

WASH TROUGHS

Wash troughs provide a channel to collect the waste washwater so that dislodged suspended matter will be carried away without losing filter media. Backwash troughs are nearly universal in filtration plants in the United States but are typically not used in Europe, where waste washwater flows over a single overflow weir or side-channel weirs.

Wash troughs are generally of two basic types: (1) troughs with a shallow but wide cross section and a slight V-shaped bottom and (2) deeper troughs with a U-shaped cross section. The bottom of the wash trough should not be flat because froth and suspended matter are often trapped under the trough bottom and may never be washed out. Typical wash troughs are shown on Fig. 11-17. If the troughs are located close to the top of the filter bed, it may be difficult to provide sufficient depth to fluidize the media without losing media. In these cases, troughs can be modified to retain media while allowing suspended solids to flow to the wash troughs (Kawamura, 2000; Kawamura et al., 1997).

The troughs should have enough capacity to carry the maximum expected wash rate without flooding. A uniform flow over the lip of the trough can be guaranteed if the trough lips behave as free-flowing weirs along their entire length. Weirs should also provide a free-fall to the main collection outlet gullet. The bottom of the trough may be either horizontal or sloping. Spacing and dimensions of troughs can be obtained from standard design texts (Kawamura, 2000) or from manufacturer's literature.

Negative Pressure in Filter Beds

During filtration, the hydraulic gradient (head loss per unit depth) can be greater near the top of the bed because of the greater collection of solids near the top of the bed (Darby and Lawler, 1990). If the hydraulic gradient is greater than the static head gradient, low or even negative pressure

(a) (b)

Figure 11-17
Typical filter washwater troughs: (a) plastic adjustable type and (b) cast-in-place concrete type (see also Fig. 1-1e in Chap. 1).

(below atmospheric pressure) can develop in the filter bed. The pressure within a filter bed and the potential for negative pressure development are depicted on Fig. 11-18. Negative pressure can cause bubbles to form as dissolved gases (oxygen and nitrogen) and come out of solution. Bubbles can be trapped by the media and cause a dramatic increase in head loss, a phenomenon called air binding.

Air binding can be avoided with proper filter design. A weir in the effluent channel that maintains sufficient water depth over the media can prevent the problem, but with proper understanding of the hydraulics of the filtration process, it is not necessary to provide an excessive water depth (Monk, 1984).

Residual Management

Filters produce two waste streams. The filter-to-waste water is water that has been fully treated through the water treatment plant but does not meet effluent requirements such as turbidity. Because filter-to-waste water is fully treated, it may be recycled to the head of the plant for retreatment instead of being sent to the waste washwater recovery system. The second waste stream is the waste washwater produced from filter backwashing, which contains the accumulated solids from a filter run and can have significant concentrations of microorganisms such as *Giardia* and *Cryptosporidium*. Waste washwater is regulated by the Filter Backwash Recycling Rule (U.S. EPA, 2001) and should typically be treated before being recycled to the head of the plant or discharged to a receiving stream. Additional details on the treatment and ultimate disposition of filter waste streams are discussed in Chap. 21.

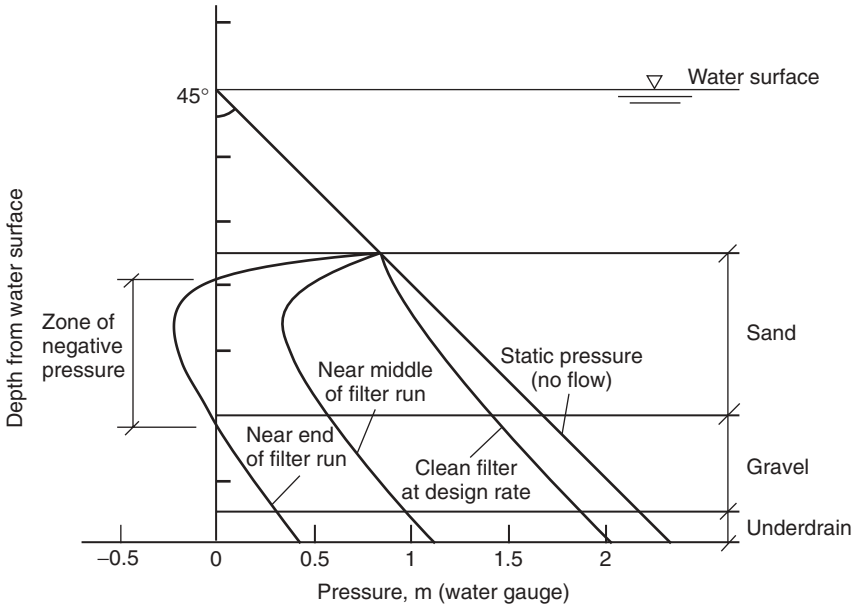

Figure 11-18
Pressure development within filter bed during filtration. (Adapted from Kawamura, 2000).

11-7 Rapid Filter Design Example

A new water treatment plant is to be built to treat water from a river in Arkansas. The average turbidity in the river is typically about 40 NTU but will frequently spike to 150 NTU during storm events. The plant is to have a capacity of 230,000 m^3/d (60 mgd). The owners and engineers have set the target effluent turbidity to be 0.1 NTU. Other treatment plants upstream of the proposed site have been successful at treating the water with dual media sand/anthracite filters. Pilot testing similar to that presented in Example 11-7 has been conducted.

The process design criteria that need to be determined are:

1. Type of filtration process (conventional, direct, or contact filtration)
2. Type of filter bed (monomedia or dual media)
3. Type of flow control
4. Media size (ES and UC)
5. Media depth
6. Filtration rates with all filters in service and with one out of service
7. Available head
8. Number and size of filters
9. Backwash rate
10. UFRV and recovery

Solution

Pretreatment requirements for the filtration process can be influenced by raw water quality, regulatory agency requirements, and the experience and preference of the operators. In this case, the turbidity spikes to 150 NTU dictate that the appropriate rapid granular filtration process is conventional filtration (see Fig 11-3). Based on successful pilot testing, deep-bed monomedia filters containing 1.8 m (6 ft) of anthracite are selected.

As noted earlier, several options are available for flow control in filters and no one method has clear advantages over the other methods. Selection is based on engineer and owner preferences with respect to cost, complexity, and reliability. For this design, the engineers have chosen the influent weir split, constant level flow control system.

The principles presented in this chapter demonstrate that media effective size, media depth, filtration rate, and available head are interrelated. None of these design parameters can be set without considering the impact of the others. The goal for selecting these parameters is to minimize capital and operating costs while achieving the effluent turbidity goal. The regulatory limit on turbidity is 0.3 NTU but a typical goal is to keep effluent turbidity below 0.1 NTU. Many combinations of size, depth, and rate can achieve this turbidity goal. Capital costs are reduced by minimizing the required filter area, which is accomplished by operating at the highest possible filtration rate. The cost of media does not change significantly as the size changes. The depth of the bed is only a portion of the overall structure depth, so an increase in media depth causes only a moderate increase in capital cost. However, capital costs increase almost linearly as the filter area increases. Operating costs are minimized by decreasing the frequency of backwashing; thus, long filter runs are desirable.

Increasing the filtration rate will moderately reduce the time to breakthrough but significantly reduce the time to reach the available head. The reduced time to reach the available head at a higher rate is almost entirely due to the higher clean-bed head loss. Clean-bed head loss is also sensitive to media diameter. Thus, increasing the media diameter can compensate for the reduced run length resulting from a higher filtration rate. As noted earlier, smaller media captures particles better, so an increase in media effective size might reduce effluent quality. Equation 11-36 demonstrates that filter effluent turbidity improves as the media depth increases, so an increase in media effective size can be compensated for by increasing the media depth.

Using data from the pilot plant shown in Example 11-7 and the optimization graph shown on Fig 11-13, the engineers design the system with 2.5 m (8.2 ft) of available head. To get the longest filter runs at this condition, the optimal media effective size is about 1.0 mm. From the other pilot information, the filtration rate is 15 m/h (6.1 gpm/ft^2) and the media depth is 1.8 m (6 ft). With this filter bed design, filter runs of about 62 h are expected. The uniformity coefficient is specified to be below 1.4 to minimize stratification after backwashing.

With the media specifications and filtration rate set, the number of filters and filtration area can be determined. The required filter area is based on the capacity and filtration rate:

$$A = \frac{Q}{v_F} = \frac{230{,}000\ \text{m}^3/\text{d}}{(15\ \text{m/h})\ (24\ \text{h/d})} = 640\ \text{m}^2\ (6900\ \text{ft}^2)$$

Capital costs are minimized by using the lowest possible number of filters (reducing valves, piping connections, etc). Because the largest practical size of a filter is about 100 m^2 (1100 ft^2), the required filter area could be met with seven filters. It is necessary to operate at full capacity while one filter is backwashing or out of service for maintenance, so eight filters are required. The area of each filter is

$$A_F = \frac{230{,}000\ \text{m}^3/\text{d}}{(15\ \text{m/h})\ (24\ \text{h/d})\ (7)} = 91\ \text{m}^2\ (980\ \text{ft}^2)$$

The dimensions of individual filters are determined by options for components such as underdrains and wash troughs. For this plant, filters were configured to have two cells separated by a central gullet (the channel that provides water flow), with each cell being 10 m × 4.55 m (32.8 ft × 15 ft).

The effective filtration rate when all filters are in service is

$$v_F = \frac{230{,}000\ \text{m}^3/\text{d}}{(91\ \text{m}^2)\ (24\ \text{h/d})\ (8)} = 13.2\ \text{m/h}\ (5.4\ \text{gpm/ft}^2)$$

The slightly lower filtration rate when all filters are in service will have a positive effect on the length of filter runs.

Backwash flow requirements are determined using principles shown in Example 11-4. A 1.8-m (6-ft) bed of 1.0 mm anthracite with a density of 1700 kg/m^3 and porosity of 0.50 can be expanded by 25 percent at a temperature of 20°C using a normal backwash flow rate of 38.6 m/h (15.8 gpm/ft^2). The required backwash flow rate is

$$Q_B = v_{\text{BW}} A_F = (38.6\ \text{m/h})(91\ \text{m}^2) = 3500\ \text{m}^3/\text{h}\ (15{,}400\ \text{gpm})$$

Backwash pumps are frequently specified with additional capacity to accommodate occasional as more vigorous backwashing or changes in temperature. Twenty-five percent additional capacity is specified in this plant.

The unit filter run volume at design capacity is determined with Eq. 11-66:

$$\text{UFRV} = v_F t_F = (6\ \text{m/h})(62\ \text{h}) = 372\ \text{m}^3/\text{m}^2\ (9100\ \text{gal/ft}^2)$$

Because a deep-bed monomedia filter is specified, collapse-pulse backwashing will be necessary. The expected volume of backwash water based on a backwash flow rate of 12 m/h for 5 min followed by a flow of 38.6 m/h for 10 min is 676 m^3 (23,900 ft^3). Including a filter-to-waste period of 30 min

(found during the pilot study), the net water recovery is determined from Eqs. 11-66 to 11-69:

$$\text{UFWV} = v_F t_{FTW} = (6\ \text{m/h})(0.5\ \text{h}) = 3\ \text{m}^3/\text{m}^2\ (74\ \text{gal/ft}^2)$$

$$\text{UBWV} = \frac{V_{\text{BW}}}{a} = \frac{676\ \text{m}^3}{91\ \text{m}^2} = 7.4\ \text{m}^3/\text{m}^2\ (182\ \text{gal/ft}^2)$$

$$r = \frac{372 - 7.4 - 3}{372} \times 100 = 97.2\%$$

The UFRV and recovery meet typical goals for granular media filters. The design parameters for this filter system are summarized in Table 11-10.

11-8 Other Filtration Technologies and Options

This chapter has focused on gravity-driven rapid filtration because that is the most common granular filtration technology used in water treatment. Several other filtration options, however, are used in specific applications. The following filtration options are briefly introduced in this section: pressure filtration, biologically active filtration, slow sand filtration, greensand

Table 11-10
Summary of design criteria for rapid filter design example

Parameter	Units	Value
Filter type	—	Conventional, deep-bed monomedia
Flow control	—	Influent weir split, constant level
Number	—	8
Inside dimensions	m · m	10 × 4.55 × 2 cells
Media surface area (each filter)	m^2	91
Media surface area (total)	m^2	728
Maximum available head	m	2.5
Filtration rate (at plant design flow rate)		
One filter off-line	m/h	15
All filters in service	m/h	13.2
Filter media		
Type	—	Anthracite
Depth	m	1.8
Effective size	mm	1.0
Uniformity coefficient	—	<1.4
Density	—	1700
Backwash criteria		
Maximum rate	m/h	48.2
Normal rate	m/h	38.6
Duration	min	15

filtration, diatomaceous earth filtration, and bag or cartridge filtration. Membrane filtration is discussed in Chap. 12.

Pressure Filtration

Pressure filtration is largely similar to gravity-driven rapid filtration with the exception that the filter is housed in a pressure vessel. Filter media used, pretreatment requirements, mechanisms for filtration, backwashing requirements, and other features of gravity-driven rapid filtration are applicable to pressure filters. Design equations and procedures are similar. An example of a pressure filter system is shown on Fig. 11-19. The primary advantage of a pressure filtration system is that the water remains under continuous pressure; that is, any excess pressure in the influent water (beyond that needed to overcome the head loss in the filter bed and piping) is available in the filtered water. Because of this, the filter effluent can be delivered to the point of use without additional pumping facilities.

A key disadvantage of pressure filters is that it is not easy to observe the filtration process, backwash process, or condition of the filter bed. Sudden changes in pressure can disturb the media and lead to channeling and poor filtration. Because poor filter conditions might be difficult to detect and compromise filtration effectiveness, some state regulatory agencies do not allow pressure filters to be used for surface water treatment, where prevention of waterborne illness is a primary concern (GLUMRB, 2007). Pressure filters can be suitable for groundwater applications. An example of an appropriate use for pressure filters is for iron and manganese removal from well water (see Chap. 20). The well pump can supply the head for the filter and deliver the water to the distribution system. Pressure filters are also used in tertiary wastewater treatment, swimming pools, and industrial applications.

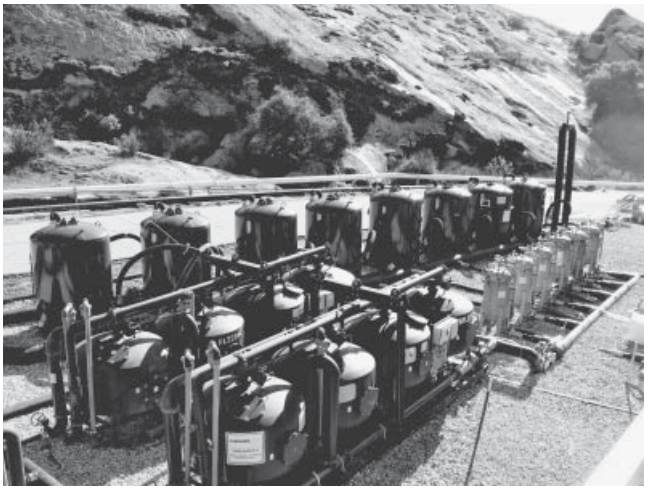

Figure 11-19
Typical pressure filters. The vessels in the left foreground are pressure filters, right foreground are cartridge filters, and background are GAC contactors.

Biologically Active Filtration

Biologically active filtration, or biofiltration, incorporates biological activity into the granular filtration process. Heterotrophic bacteria colonize the surface of the media, forming a biofilm that is able to degrade some organic compounds and micropollutants, such as phenol, trichlorobenzene, ozonation by-products, ammonia, and odor-causing compounds such as geosmin and MIB. Biofiltration can improve water quality by decreasing the potential for bacterial regrowth in distribution systems, decreasing DBP formation during final disinfection, decreasing chlorine demand, and decreasing chlorine potential (Urfer et al, 1997).

Biofiltration is frequently used after ozonation because ozone can break down large recalcitrant humic acid molecules to smaller, more biologically degradable compounds. Without biofiltration, this increase in biodegradable organic matter (BOM) may encourage regrowth in the distribution system. With biofiltration, DOC removal of 35 to 40 percent may be possible, as shown on Fig 11-20. Thus, ozonation and biofiltration might be considered as a coupled process.

In Europe, dedicated biofilters using GAC media are sometimes installed following a conventional filtration process. In the United States, granular media filters are typically configured to accomplish both biodegradation and particle filtration in a single process. A thorough review of the use of biofiltration in water treatment is provided in Urfer et al. (1997).

Several factors affect the removal of BOM with biological filtration. These include (1) BOM type and concentration, (2) filter media type (i.e., GAC, anthracite, and/or sand), (3) water temperature, and (4) and empty bed contact time (EBCT) through the filter. Depending on these factors, steady-state biological performance will be reached within a maximum period of 1 to 2 months.

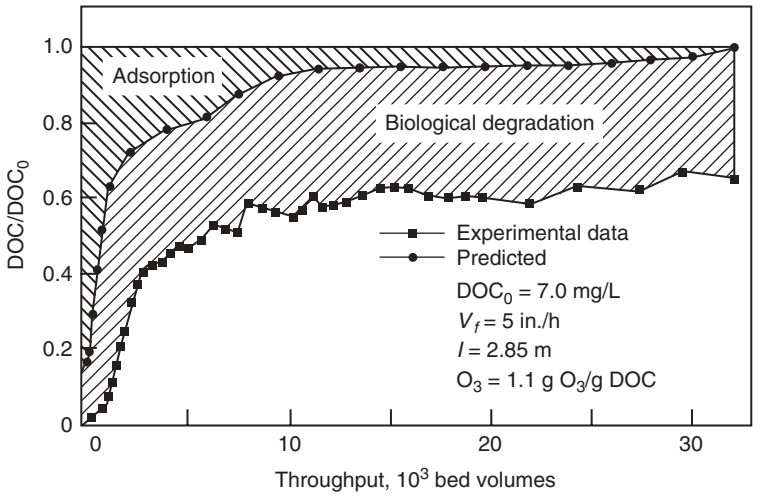

Figure 11-20
DOC removal by adsorption and biodegration during biofiltration of an ozonated humic acid solution (Adapted from Sontheimer and Hubele, 1987).

BIOFILTRATION MEDIA

Sand, anthracite, and GAC have all been used as biofilter media and some studies suggest that they all perform similarly. Other studies suggest that GAC can be a more effective biofiltration media in some situations. The advantages of GAC appear to be that its irregular surface may provide a better attachment surface for bacteria, it may adsorb potentially inhibitory chemicals and thereby protect the biofilm, it may adsorb slowly biodegradable compounds that may then be degraded by the bacteria, and it can degrade oxidant residuals in the top few centimeters of the bed, thereby protecting the remaining biofilm from inadvertent exposure to oxidants such as chlorine or ozone. Because of these advantages, GAC may be able to establish a biofilm more rapidly, work better at colder temperatures, and be more robust following upsets or inadvertent oxidant exposure.

Results from studies comparing GAC and anthracite as biofilter media are shown on Fig. 11-21. Data shown on Fig. 11-21a were gathered under relatively warm temperature conditions of 10 to 15°C. The anthracite–sand filter performed as well as the GAC–sand filter for removal of oxalate, a common by-product of ozonation, regardless of EBCT. Similar performance in warm conditions was reported by Price et al. (1993) and Krasner et al. (1993). On the other hand, under cold temperature conditions as shown on Fig. 11-21b, the GAC–sand biofilter was still capable of removing a fraction of the oxalate (albeit with high EBCT values), while no removal was achieved with the anthracite–sand biofilter. The removal of total

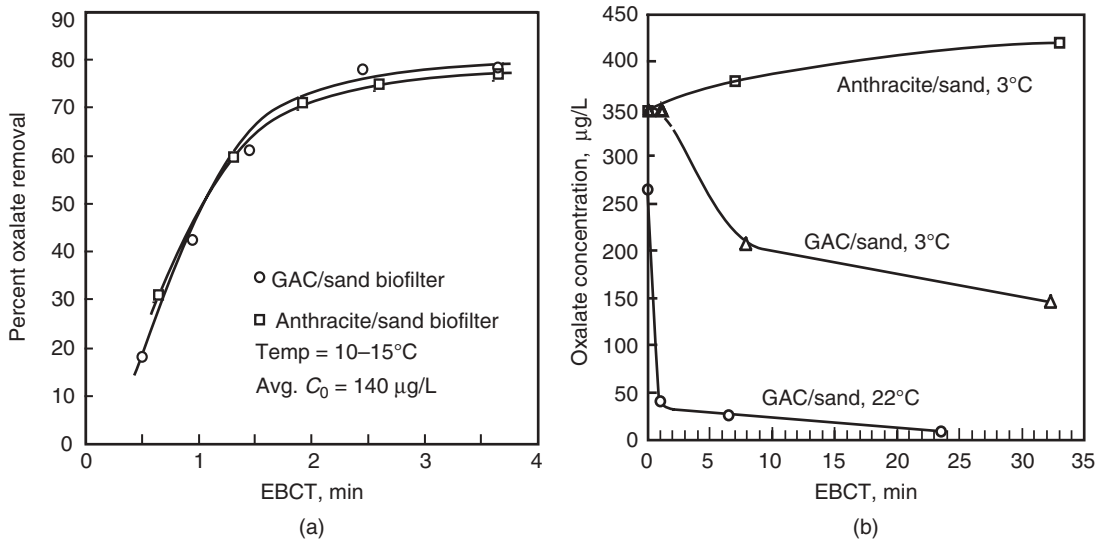

Figure 11-21
Impact of media type and EBCT on the removal of oxalate with biofiltration (a): under warm temperature conditions (Adapted from Coffey et al., 1997) and (b) under cold temperature conditions (Adapted from Emelko et al., 1997).

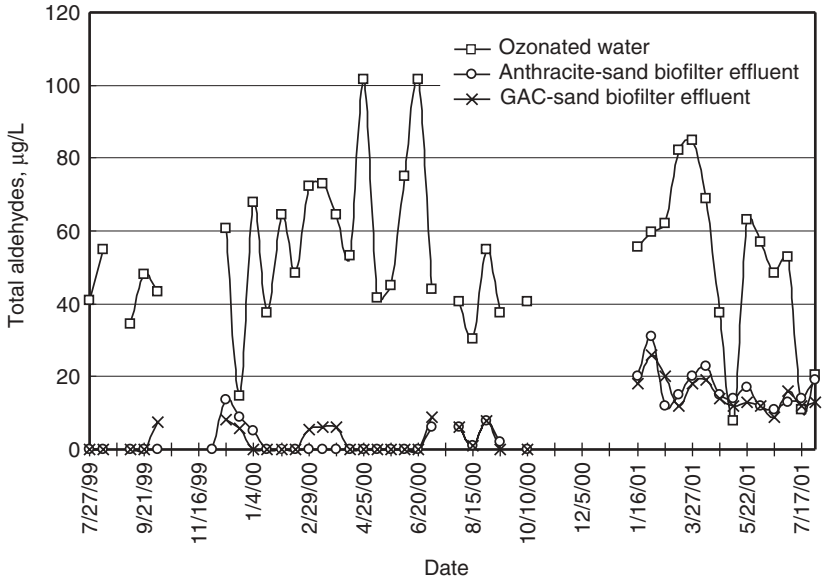

Figure 11-22
Removal of aldehydes with biological filtration at a full-scale water treatment plant (temperature = 12 to 24°C) (Data Courtesy of the Alameda County Water District, Fremont, California).

aldehydes (another common by-product of ozonation) with biofiltration in a full-scale water treatment plant in Fremont, California, is shown on Fig. 11-22. The 3-year operational data confirm that under relatively warm temperature conditions, anthracite–sand biofilters perform as well as GAC–sand biofilters.

BIOFILM MAINTENANCE AND BACKWASHING

A biofilm will establish itself in granular media as long as conditions (substrate, oxygen, temperature, etc.) are favorable. A key requirement is to prevent exposure to inhibitory substances; thus, the primary factor in operating a biofilter is to ensure that the filter influent has no chlorine or ozone residual.

Biofilters develop head loss similar to conventional filters, requiring backwashing on a regular basis. Numerous studies have indicated that biofilms adhere more strongly to filter media than nonbiological particles and that no major losses of biomass occur with proper backwashing procedures for particle removal. There are two types of concerns about backwashing of biological filters: (1) whether backwashing (especially with air scour) causes excessive detachment of the biomass off the filter media and (2) whether biofilters must be backwashed exclusively with nonchlorinated water to maintain their viability. Evaluations of these issues has concluded that rigourous backwashing does not adversely impact biofiltration performance (Miltner et al., 1995; Ahmad and Amirtharajah, 1995; Ahmad et al., 1998). While AOC removal was impaired immediately after backwashing with chlorinated water, its removal was back to normal levels

within a few hours of filter run. Amirtharajah (1993) concluded that air scour helped control the long-term buildup of head loss in a biofilter, which was confirmed by Teefy (2001) who noted that occasional backwashing with chlorinated water was necessary at a full-scale water treatment plant to prevent excessive biological growth, which otherwise results in shorter filter runs. The biofiltration performance shown on Fig. 11-22 was achieved with filters backwashed with chlorinated water approximately every third wash.

FILTRATION PERFORMANCE

Biological filters will generally achieve good turbidity removal, and many studies have observed no difference in turbidity removal between biological and prechlorinated filters. In other cases, differences in particle counts were observed. Bacterial counts in filter effluent may be higher with biofiltration; but postdisinfection will be provided in either case. The rate of head loss buildup may be higher in biologically active filters, leading to somewhat shorter filter runs if the length of the filter run is limited by the available head. Temperature is also an important factor with respect to biological activity and will vary through the year depending upon the climate. For example, biological activity is usually high in summer months but then drops in the winter months (Servais and Joret, 1999).

DESIGN OF BIOFILTERS

When used for both biological activity and particle removal, design of the filtration aspects of a biofilter is essentially identical to that presented earlier in this chapter for rapid filters. Contact time, expressed as empty bed contact time (EBCT), is a primary design variable for biofiltration. Removal of BOM generally increases as EBCT increases. Removal of ozone by-products can generally be accomplished with an EBCT of 2 to 4 min, and most biofilters in the United States have EBCT between 1 and 15 min. An appropriate value for the EBCT can be determined during pilot testing.

Slow Sand Filtration

Slow sand filtration is substantially different from rapid filtration. Some of the most significant differences are that slow sand filters use sand media that does not need to be as uniform in size as in rapid filters, do not need coagulation pretreatment, and do not need backwashing. While these differences suggest that slow sand filters are simpler to build and operate than rapid filters, another key difference is that the filtration rate is 50 to 100 times lower, which means that slow sand filters require that much more land to treat the same amount of water. Other differences between rapid filtration and slow sand fitration are summarized in Table 11-11.

In slow sand filtration, the low filtration rate and the use of smaller, less uniform sand causes particles to be removed in the top few centimeters of the bed. The surface of the bed forms a mat of material, called a *schmutzdecke*. The schmutzdecke forms an additional filtration layer, physically straining smaller particles from the influent water. In addition, the schmutzdecke

Table 11-11
Comparison between rapid and slow sand granular filtration design criteria[a]

Process Characteristic	Slow Sand Filtration	Rapid Filtration
Filtration rate	0.08–0.25 m/h (0.03–0.10 gpm/ft^2)	5–15 m/h (2–6 gpm/ft^2)
Media effective size	0.15–0.30 mm	0.50–1.2 mm
Media uniformity coefficient	<2.5	<1.4
Bed depth	0.9–1.5 m (3–5 ft)	0.6–1.8 m (2–6 ft)
Required head	0.9–1.8 m (3–6 ft)	1.8–3.0 m (6–10 ft)
Run length	1–6 months	1–4 days
Ripening period	Several days	15 min–2 h
Pretreatment	None required	Coagulation
Dominant filtration mechanism	Straining, biological activity	Depth filtration
Regeneration method	Scraping	Backwashing
Maximum raw-water turbidity	10 NTU	Unlimited with proper pretreatment

[a]Values represent typical ranges. Some filters are designed and operated outside of these ranges.

forms a complex biological community that degrades some organic matter. Because particles are physically strained at the surface of the filter bed, destabilization by coagulation pretreatment is not necessary.

A typical configuration for a slow sand filter is illustrated on Fig. 11-23. Filter effluent passes through a support layer of graded gravel about 0.3 to 0.6 m (1 to 2 ft) deep and is collected in an underdrain system constructed of perforated pipes or concrete blocks. The water level in the structure is several feet above the top of the media, with the maximum water level dictating the available head. The filtration rate is controlled by valves in either the influent or effluent piping.

OPERATING CYCLE FOR SLOW SAND FILTRATION

As with rapid filtration, slow sand filtration operates over a cycle with two stages, consisting of a filtration stage and a regeneration stage. Head loss builds slowly during a filter run that lasts weeks or months. Head loss builds slowly because of the low filtration rate and because the microorganisms degrade some of the accumulated particles. Slow sand filters typically never reach breakthrough and are always terminated when the head loss reaches the available head in the system, typically 0.9 to 1.8 m (3 to 6 ft). Instead of being backwashed when the available head is reached, the filter is drained and the top 1 to 2 cm (0.4 to 0.8 in.) of media is scraped off, hydraulically

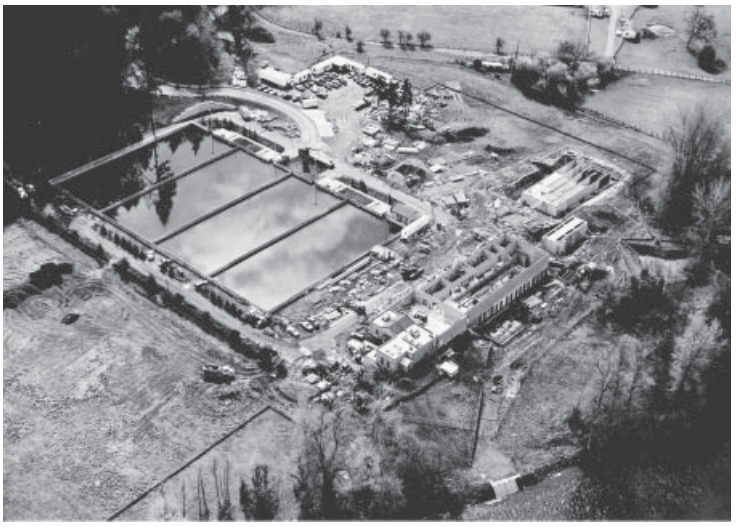

Figure 11-23
Typical slow sand filter.

cleaned, and stockpiled onsite. The filter is then placed back in service. The operation and scraping cycle can be repeated many times, often over a period of several years, before the sand must be replenished. When the sand reaches a minimum depth of 0.5 m (20 in.), the stockpiled sand is replaced in the filter to restore the original depth.

A filter with new media typically has a ripening period that can last several days, during which the schmutzdecke forms and the effluent quality improves. Filter-to-waste piping is provided to allow filtered water to be returned to the source during the ripening period. After several filter runs and scrapings, the microbial community can become established deeper in the bed and the ripening period can be shorter or nonexistent.

ADVANTAGES AND USE OF SLOW SAND FILTRATION

The primary advantage of slow sand filtration is that the filters are simple to operate and can run without constant supervision. Operators do not need to have knowledge of coagulation chemistry. Simple operational requirements are particularly attractive to small utilities that do not have the resources for full-time, highly trained treatment plant operators. The simplicity may make slow sand filtration appropriate in developing countries.

With no pretreatment, slow sand filters cannot adequately treat poor-quality surface waters. Slow sand filtration should be used only when source waters have turbidity less than 10 NTU, color less than 15 color units, and no colloidal clay (GLUMRB, 2007). While most slow sand filter plants treat water with less than 10 NTU of turbidity (Slezak and Sims, 1984), some research suggests that the upper limit should be 5 NTU (Cleasby et al., 1984).

For small facilities that have high-quality source water but want to avoid the use of coagulants, membrane filtration (see Chap. 12) or cartridge or bag filters should also be considered.

Slow sand filtration continues to be used successfully in Europe, including facilities supplying large communities such as London and Amsterdam (Joslin, 1997). However, it has been largely superseded by rapid filtration in the United States. A survey conducted in the early 1980s (Slezak and Sims, 1984) identified fewer than 50 operating slow sand filtration plants in the United States [for comparison, there are more than 50,000 community water systems in the United States (U.S. EPA, 2001)]. Most of the facilities listed in Slezak and Sims's (1984) survey were more than 50 years old and served populations of less than 10,000.

DESIGN OF SLOW SAND FILTERS

Slow sand filters can be housed in steel, fiberglass, or reinforced concrete structures. Details of slow sand filter design can be found in the literature, such as Hendricks et al. (1991), Visscher (1990), and Seelaus et al. (1986).

Greensand Filtration

Greensand filtration combines oxidation and filtration in a single granular media filtration process. The filtration media is coated with a layer of manganese dioxide, which oxidizes soluble iron, manganese, hydrogen sulfide, and other reduced species. The underlying media can be sand, anthracite, or naturally occurring glauconite mineral. After oxidation, iron and manganese precipitate and can be removed by the filter. The manganese dioxide coating must periodically be regenerated by feeding an oxidant to the filter; typically, potassium permanganate is used. Continuous regeneration can be practiced by feeding potassium permanganate continuously.

The design of the filtration process using greensand media is essentially identical to rapid filtration. The media is typically specified with an effective size of about 0.3, uniformity coefficient < 1.6, and depth similar to rapid filtration. Filtration rates typically range from 7.5 to 12.5 m/h (3 to 5 gpm/ft^2). Greensand filters can be designed as either gravity or pressure rapid filters. Additional information about the use of greensand filtration for iron and manganese removal is presented in Chap. 20.

Diatomaceous Earth Filtration

Diatomaceous earth (DE) filtration, also known as precoat filtration, uses a thin cake (2 to 5 mm) of fine granular material as a filter medium. Particle removal occurs primarily at the surface of the cake, with straining as the predominant removal mechanism.

Diatomaceous earth (also known as Fuller's earth) is the microscopic remnants of the siliceous shells of diatoms, occurs in natural deposits, and is almost pure silica. DE used for filter media typically has a diameter between 4 and 30 μm (Baumann, 1978). Smaller sizes produce higher

quality effluent but at the expense of more head loss. The properties and characteristics of precoat media are covered in *ANSI/AWWA B101-01 Standard for Precoat Filtering Media* (AWWA, 2001b).

The DE filtration cycle has three stages: precoat, filtration, and backwash (AWWA, 1988). In the first stage, a slurry of DE is fed into the filter vessel and deposited on the septum, which is a porous plate or screen designed to support the precoat material. After precoat is complete, raw water enters the filtration vessel and filtration occurs across the precoat layer. Additional DE (called body feed) is added to the influent water during filtration. The body feed reduces the rate at which head loss builds up by maintaining the porosity of the cake and extends the length of the filter run. Run lengths range from 10 min to 30 days (Baumann, 1957).

Backwash starts after the pressure drop reaches the limiting head, typically 2 to 3 bars (29 to 44 psi). During backwash, water is pumped through the septum in reverse and the filter cake and all accumulated solids slough off. In some instances, a surface wash or agitation system is used to break up an encrusted filter cake, particularly in high-pressure filters. After backwash is complete, the entire cycle begins again.

DE filtration is not used extensively in drinking water treatment (AWWA, 1988), but some small utilities have used it for compliance with the SWTR and subsequent surface water treatment rules. DE filters strain particles larger than about 1 μm, so they can achieve high removal of *Giardia* and *Cryptosporidium* without coagulation. Under the SWTR and LT1ESWTR, precoat filters receive filtration credit for 2 log removal of *Giardia* and *Cryptosporidium* if the filtered water turbidity is equal to or less than 1 NTU (U.S. EPA, 1989, 2002). DE filters are less effective for particles smaller than 1 μm and should only be used for high-quality source waters (turbidity of 10 NTU or less). Additional information on precoat filtration is available in the published literature (AWWA, 1988; Baumann, 1965).

Bag and Cartridge Filtration

Bag and cartridge filtration are not granular filtration processes and therefore do not really belong in this chapter. They are, however, considered as alternatives for compliance for surface water treatment regulations and are discussed briefly here.

Bag and cartridge filters are filter elements installed inside a pressure vessel. Cartridge filters are typically a self-supporting filter element with either a pleated-fabric or string-wound construction. The flow is from the outside of the cartridge to the inside. Bag filters are a nonrigid, fabric filter with the flow from the inside of the bag to the outside. Although some cartridge filters are backwashable, both cartridge and bag filters are typically considered to be disposable media and are discarded when the head loss exceeds the available head. Thus, they are only suitable for small systems treating relatively high-quality water. Cartridge filter vessels are shown in Fig. 11-19.

Problems and Discussion Topics

11-1 Samples of filter media was sifted through a stack of sieves and the weight retained on each sieve is recorded below. For a given sample (A, B, C, D, or E, to be selected by instructor), determine the effective size and uniformity coefficient for the media.

Sieve Designation	Sieve Opening, mm	Weight of Retained Media, g				
		A	B	C	D	E
8	2.36	0				4
10	2.00	35	0			11
12	1.70	178	11		0	60
14	1.40	216	315		4	227
16	1.18	242	242		16	343
18	1.00	51	116	0	33	216
20	0.85	12	55	23	75	40
25	0.71	5	26	217	285	16
30	0.60	3	14	325	270	3
35	0.50	0	2	151	121	1
40	0.425		0	71	21	0
45	0.355			49	8	
50	0.300			4	3	
Pan	—			20	4	

11-2 Explain why a low uniformity coefficient is important in rapid filtration.

11-3 Explain (a) the process of ripening, (b) how ripening affects recovery, or net water production, and (c) how to minimize the duration of ripening.

11-4 A filter is designed with the following specifications. The anthracite and sand have density of 1700 and 2650 kg/m^3, respectively, and the design temperature is 10°C. For a given sample (A, B, C, D, or E; to be selected by instructor), calculate the clean-bed head loss.

Item	A	B	C	D	E
Bed type	Mono-media	Mono-media	Dual media	Dual media	Dual media
Filtration rate (m/h)	8	15	15	10	10
Anthracite specifications:					
Effective size (mm)		1.0	1.0	1.2	1.6
Depth (m)		1.8	1.5	1.4	1.2
Sand specifications:					
Effective size (mm)	0.55		0.5	0.55	0.55
Depth (m)	0.75		0.3	0.4	0.7

11-5 For the media specification given in Problem 7-4 (C, D, or E to be selected by instructor), determine if the two media layers are matched to each other.

11-6 A filter contains 0.55-mm sand that has a density of 2650 kg/m^3. Calculate the effective size of 1550 kg/m^3 anthracite that would be matched to this sand.

11-7 In dual-media filter containing sand and anthracite, which material will be the top layer? Why?

11-8 Using the sieve analysis from Problem 11-1, determine the clean-bed head loss through a stratified filter bed by calculating the head loss contribution from each layer of media. Assume that the media stratifies into layers based on grain size, that the depth of each layer is proportional to the mass of media retained on each sieve pan, that the grain diameter of the media in each layer is equal to the arithmetic average of two adjacent sieve pans (i.e., the layer formed by the 178 g of media in sample A that passed through the 2.0-mm pan and was retained on the 1.70-mm pan has an average size of 1.85 mm), and that the total head loss is the sum of the head loss from each layer. In addition, assume that the sand that passed through the smallest pan has an average grain diameter of 0.1 mm. The total bed depth is 0.9 m, the filtration rate is 10 m/h, and the temperature is 15°C.

a. Calculate the total clean-bed head loss using the entire sand sample in Problem 11-1, including the material smaller than the smallest sieve pan.

b. Calculate the total clean-bed head loss assuming that the top 5 percent of the filter bed has been scraped to remove fines.

c. Discuss the importance of scraping the surface of rapid-filter beds after media installation and the impact it has on clean-bed head loss.

11-9 Compare the clean-bed head loss at 15°C through a rapid filter with a filtration rate of 15 m/h to that through a slow sand filter with a filtration rate of 0.15 m/h for media with the following specifications: effective size 0.5 mm, density 2650 kg/m^3, depth 1 m, and porosity 0.42. What implications do these calculations have on the significance of clean-bed head loss in the design of rapid and slow sand filters?

11-10 Given a backwash flow rate of 45 m/h and temperature of 20°C, calculate the largest (a) sand particle (density = 2650 kg/m^3) and (b) floc solid particle (density = 1050 kg/m^3) that can be washed from a filter bed.

11-11 Calculate and plot the size of particles that will be washed from a filter as a function of backwash velocity ranging from 10 to

100 m/h at 20°C for (a) sand particles (density = 2650 kg/m^3), (b) anthracite particles (density = 1650 kg/m^3), and (c) floc solid particles (density = 1050 kg/m^3). In addition, calculate the minimum fluidization velocities for 0.5-mm sand (porosity 0.40) and 1.0-mm anthracite (porosity 0.50) and indicate these velocities on your graph. What is an appropriate range for the backwash velocity for dual-media filters? Assuming the backwash troughs are placed high enough, will any media be lost with backwash velocities in this range?

11-12 A monomedia anthracite filter is designed with the following specifications: effective size 1.1 mm, uniformity coefficient 1.4, and density 1650 kg/m^3.

a. Calculate backwash rate to get a 25 percent expansion at the design summer temperature of 22°C.

b. Calculate the expansion that occurs at the backwash rate determined in part (a) at the minimum winter temperature of 3°C.

c. Discuss the implications of these results on backwash operations for plants that experience a large seasonal variation in water temperature.

11-13 Using the Yao filtration model, examine the effect of filtration rate on filter performance for particles with diameters of 0.1, 1.0, and 10 μm. Assume a monodisperse media of 0.5 mm diameter, porosity 0.42, particle density 1020 kg/m^3, filtration rate 10 m/h, filter depth 1 m, temperature 20°C, and attachment efficiency 1.0. Plot the results as C/C_O as a function of filtration rate over a range from 1 to 25 m/h. Comment on the effect of filtration rate and particle size on filter performance.

11-14 Using the Tufenkji and Elimelech filtration model, examine the effect of water temperature on filter efficiency for particles with diameters of 0.1, 1.0, and 10 μm. Assume a monodisperse media of 0.5 mm diameter, porosity 0.42, particle density 1020 kg/m^3, filtration rate 10 m/h, filter depth 1 m, and attachment efficiency 1.0. Plot the results as $\log(C/C_O)$ as a function of temperature over a temperature range of 1 to 25°C. What implications do these calculations have on filtration in cold climates? Is temperature more important for filtration of certain particle sizes?

11-15 Using the Rajagopalan and Tien filtration model, calculate and plot the concentration profile of 4 μm particles (i.e., the size of *Cryptosporidium* oocysts), through monodisperse filter with 0.5-mm-diameter media under filtration conditions typical of rapid filtration (v = 10 m/h) and slow sand filtration (v = 0.1 m/h). Assume porosity 0.40, particle density 2650 kg/m^3, filter depth

1 m, and temperature 20°C. Assume an attachment efficiency of 1.0 for the rapid filter and 0.05 for the slow sand filter. Explain why rapid and slow sand filtration should be modeled with different values for the attachment efficiency. Plot the results as C/C_O as a function of depth. Using these results, comment on the methods used to restore the filtration capacity of slow sand and rapid filters (i.e., scraping vs. backwashing).

11-16 The results of pilot filter experiments are summarized in the tables below. For each set of experiments, the independent variable was either the media effective size or the media depth, as given in the second column below. For a given set of experiments (A, B, C, or D, to be selected by instructor), determine equations for how the specific deposit at breakthrough (σ_B) and the head loss rate constant (k_{HL}) each depend on the independent variable. Also determine the optimal value of the independent variable and the corresponding filter run duration. For all problems, assume $C_O = 2.0$ mg/L and $C_E = 0$ mg/L.

a. Design conditions: $v_F = 15$ m/h, media = anthracite, depth = 1.75 m, max available head = 2.8 m.

A Filter	Media ES, mm	Time to Breakthrough, h	Initial Head Loss, m	Head Loss When Breakthrough Occurred, m
1	0.8	112	0.65	4.6
2	1.0	85	0.39	2.9
3	1.1	72	0.33	2.4
4	1.2	71	0.30	2.0
5	1.4	58	0.24	1.5

b. Design conditions: $v_F = 15$ m/h, media = GAC, depth = 2.0 m, max available head = 3.0 m.

B Filter	Media ES, mm	Time to Breakthrough, h	Initial Head Loss, m	Head Loss When Breakthrough Occurred, m
1	0.83	54	0.65	6.1
2	1.05	43	0.40	4.3
3	1.25	38	0.33	2.9
4	1.54	32	0.22	2.0

c. Design conditions: $v_F = 33.8$ m/h, media = anthracite, ES = 1.55 mm, max available head = 3 m (adapted from pilot results for the LADWP Aqueduct Filtration Plant).

C Filter	Media ES, m	Time to Breakthrough, h	Initial Head Loss, m	Head Loss When Breakthrough Occurred, m
1	0.6	4.0	0.16	1.0
2	1.0	6.7	0.30	1.7
3	1.8	11.9	0.50	3.2
4	2.0	13.4	0.58	3.6
5	2.2	14.5	0.65	4.1

d. Design conditions: $v_F = 25$ m/h, media = anthracite, ES = 1.50 mm, max available head = 3 m (adapted from pilot results for the Bull Run water supply)

D Filter	Media ES, m	Time to Breakthrough, h	Initial Head Loss, m	Head Loss When Breakthrough Occurred, m
1	2.0	41	0.43	1.8
2	2.3	49	0.51	2.0
3	2.5	55	0.51	2.5
4	3.0	65	0.63	2.9

11-17 For the filter design selected in Problem 11-16, what is the UFRV at the design condition? If the filters are designed to be backwashed at 40 m/h for 15 min, what are the UBWV and recovery, assuming there is no filter-to-waste period?

11-18 A filter has been designed to have a run length of 48 h while operating at a filtration rate of 12 m/h. The design backwash rate is 40 m/h, backwash duration is 15 min, and filter-to-waste duration is 10 min. The plant operator decides to clean the filters more thoroughly and backwashes at a rate of 55 m/h for 25 min. As a result, ripening takes longer and the filter-to-waste duration is 50 min. Calculate the UFRV, UBWV, UFWV, and recovery (a) as designed and (b) as operated. What is the percent increase in the volume of treated water lost as waste backwash water and filter-to-waste water?

11-19 Explain (a) the importance of flow control in proper filtration operation and (b) the main types of flow control systems.

11-20 Discuss (a) the impact of rapid variations in filtration rate on filter performance, (b) causes of rapid variations in filtration rate, and (c) design features and operational methods for preventing rapid variations in filtration rate.

11-21 Discuss factors that influence the selection of the number of filters in a treatment plant design.

11-22 Discuss the benefits and salient features of air scour.

References

Ahmad, R., and Amirtharajah, A. (1995) ''Detachment of Biological and Nonbiological Particles from Biological Filters During Backwashing,'' pp. 1057–1085, in *Proceedings of the AWWA Annual Conference*, Anaheim, CA, Volume on Water Research, American Water Works Association, Denver, CO.

Ahmad, R., Amirtharajah, A., Al-Shawwa, A., and Huck, P. M. (1998) ''Effects of Backwashing on Biological Filters,'' *J. AWWA*, **90**, 12, 62–73.

Ahmed, N., and Sunada, D. (1969) ''Nonlinear Flow in Porous Media,'' *J. Hydr. Div. ASCE*, **95**, 6, 1847–1857.

Akgiray, Ö., and Saatçi, A. M. (2001) ''A New Look at Filter Backwash Hydraulics,'' *Water Sci. Technol. Water Supply*, **1**, 2, 65–72.

Amirtharajah, A. (1988) ''Some Theoretical and Conceptual Views of Filtration,'' *J. AWWA*, **80**, 12, 36–46.

Amirtharajah, A. (1993) ''Optimum Backwashing of Filters with Air Scour: A Review,'' *Water Sci. Technol.*, **27**, 10, 195–211.

Amirtharajah, A., and Raveendran, P. (1993) ''Detachment of Colloids from Sediments and Sand Grains,'' *Colloids Surfaces A: Physicochem. Eng. Aspects*, **73**, 211–227.

ASTM (2001a) *C136-01 Standard Test Method for Sieve Analysis of Fine and Coarse Aggregates*, American Society for Testing and Materials, Philadelphia, PA.

ASTM (2001b) *E11-01 Standard Specification for Wire Cloth and Sieves for Testing Purposes*, American Society for Testing and Materials, Philadelphia, PA.

AWWA (1988) *Precoat Filtration*, AWWA Manual M30, American Water Works Association, Denver, CO.

AWWA (1996) *ANSI/AWWA B604-96 Standard for Granular Activated Carbon*, American Water Works Association, Denver, CO.

AWWA (2001a) *ANSI/AWWA B100-01 Standard for Filtering Material*, American Water Works Association, Denver, CO.

AWWA (2001b) *ANSI/AWWA B101-01 Standard for Precoat Filtering Media*, American Water Works Association, Denver, CO.

Bai, R. B., and Tien, C. (1999) ''Particle Deposition under Unfavorable Surface Interactions,'' *J. Colloid Interface Sci.*, **218**, 2, 488–499.

Baker, M. N. (1948) *The Quest for Pure Water; The History of Water Purification from the Earliest Records to the Twentieth Century*, American Water Works Association, New York.

Baumann, E. R. (1957) ''Diatomite Filters for Municipal Installations,'' *J. AWWA*, **49**, 2, 174–186.

Baumann, E. R. (1965) ''Diatomite Filters for Municipal Use,'' *J. AWWA*, **57**, 2, 157–180.

Baumann, E. R. (1978) Precoat Filtration, p. 845, in R. L. Sanks (ed.), *Water Treatment Plant Design for the Practicing Engineer*, Ann Arbor Science, Ann Arbor, MI.

Bergendahl, J. A., and Grasso, D. (2003) ''Mechanistic Basis for Particle Detachment from Granular Media,'' *Environ. Sci. Technol.*, **37**, 10, 2317–2322.

Carman, P. C. (1937) ''Fluid Flow through Granular Beds,'' *Trans. Inst. Chem. Eng.*, **15**, 150–165.

Chang, Y-I., and Chan, H-C. (2008) ''Correlation Equation for Predicting Filter Coefficient under Unfavorable Deposition Conditions,'' *J. AICHE*, **54**, 5, 1235–1253.

Chang, M., Trussell, R. R., Guzman, V., Martinez, J., and Delaney, C. K. (1999) ''Laboratory Studies on the Clean Bed Headloss of Filter Media,'' *Aqua (Oxford)*, **48**, 4, 137–145.

Clark, M. M. (1996) *Transport Modeling for Environmental Engineers and Scientists*, Wiley-Interscience, New York.

Cleasby, J. L., and Fan, K.-S. (1981) ''Predicting Fluidization and Expansion of Filter Media,'' *J. Environ. Eng.*, **107**, EE3, 455–471.

Cleasby, J. L., Hilmoe, D. J., and Dimitracopoulos, C. J. (1984) ''Slow Sand and Direct In-line Filtration of a Surface Water,'' *J. AWWA*, **76**, 12, 44–55.

Cleasby, J. L., and Logsdon, G. S. (1999) Granular Bed and Precoat Filtration, Chap. 8, in R. D. Letterman (ed.), *Water Quality and Treatment: A Handbook of Community Water Supplies*, McGraw-Hill, New York.

Cleasby, J. L., and Woods, C. F. (1975) ''Intermixing of Dual Media and Multi-Media Granular Filters,'' *J. AWWA*, **67**, 4, 197–203.

Coffey, B. M., Huck, P. M., Bouwer, E. J., Hozalski, R. M., Pett, B., and Smith E. F. (1997) The Effect of BOM and Temperature on Biological Filtration: An Integrated Comparison at Two Treatment Plants, paper presented at the American Water Works Association Annual Conference, Denver, CO.

Darby, J. L., Attanasio, R. E., and Lawler, D. F. (1992) ''Filtration of Heterodisperse Suspensions. Modeling of Particle Removal and Head Loss,'' *Water Res.*, **26**, 6, 711–726.

Darby, J. L., and Lawler, D. F. (1990) ''Ripening in Depth Filtration. Effect of Particle Size on Removal and Head Loss,'' *Environ. Sci. Technol.*, **24**, 7, 1069–1079.

Darcy, H. (1856) *Les fontaines publiques de la vile de Dijon* [in French], Victor Dalmont, Paris.

Dharmarajah, A. H., and Cleasby, J. L. (1986) ''Predicting the Expansion Behavior of Filter Media,'' *J. AWWA*, **78**, 12, 66–76.

Elimelech, M. (1992) ''Predicting Collision Efficiencies of Colloidal Particles in Porous Media,'' *Water Res.*, **26**, 1, 1–8.

Elimelech, M., and O'Melia, C. R. (1990) ''Kinetics of Deposition of Colloidal Particles in Porous Media,'' *Environ. Sci. Technol.*, **24**, 10, 1528–1536.

Emelko, M. B., Huck, P. M., and Smith, E. F. (1997) Full-Scale Evaluation of Backwashing Strategies for Biological Filtration, paper presented at the American Water Works Association Annual Conference, Atlanta, GA.

Ergun, S. (1952) ''Fluid Flow through Packed Columns,'' *Chem. Eng. Prog.*, **48**, 2, 89–94.

Fair, G. M., Geyer, J. C., and Okun, D. A. (1971) *Elements of Water Supply and Wastewater Disposal*, Wiley, New York.

Fair, G. M., and Hatch, L. P. (1933) ''Fundamental Factors Governing the Streamline Flow of Water through Sand,'' *J. AWWA*, **25**, 11, 1551–1565.

Forchheimer, P. (1901) ''Wasserbewegung durch Boden'' [in German], *Forschtlft ver. D. Ing*., **45**, 1782–1788.

Fuller, G. W. (1933) ''Progress in Water Purification,'' *J. AWWA*, **25**, 11, 1566–1576.

GLUMRB (Great Lakes Upper Mississippi River Board). (2007) *Recommended Standards for Water Works (Ten State Standards)*, Health Research Inc., Albany, NY.

Hendricks, D. W., Barrett, J. M., and AWWA Research Foundation (1991) *Manual of Design for Slow Sand Filtration*, American Water Works Association Research Foundation, Denver, CO.

Hiemenz, P. C., and Rajagopalan, R. (1997) *Principles of Colloid and Surface Chemistry*, Marcel Dekker, New York.

Ives, K. J. (1967) ''Deep Filters,'' *Filtration Separation*, **4**, 3/4, 125–135.

Iwasaki, T. (1937) ''Some Notes on Sand Filtration,'' *J. AWWA*, **29**, 10, 1592–1602.

Joslin, W. R. (1997) ''Slow Sand Filtration: A Case Study in the Adoption and Diffusion of a New Technology,'' *J. N. Engl. Water Works Assoc.*, **111**, 3, 294–303.

Kau, S. M., and Lawler, D. F. (1995) ''Dynamics of Deep-Bed Filtration: Velocity, Depth, and Media,'' *J. Environ. Eng.*, **121**, 12, 850–859.

Kavanaugh, M., Evgster, J., Weber, A., and Boller, M. (1977) ''Contact Filtration for Phosphorus Removal,'' *J. WPCF*, **49**, 10, 2157–2171.

Kawamura, S. (1975a) ''Design and Operation of High-Rate Filters—Part 1,'' *J. AWWA*, **67**, 10, 535–544.

Kawamura, S. (1975b) ''Design and Operation of High-Rate Filters—Part 2,'' *J. AWWA*, **67**, 11, 653–662.

Kawamura, S. (1975c) ''Design and Operation of High-Rate Filters—Part 3,'' *J. AWWA*, **67**, 12, 705–708.

Kawamura, S. (1999) ''Design and Operation of High-Rate Filters,'' *J. AWWA*, **91**, 12, 77–90.

Kawamura, S. (2000) *Integrated Design and Operation of Water Treatment Facilities*, Wiley, New York.

Kawamura, S., Najm, I. N., and Gramith, K. (1997) ''Modifying a Backwash Trough to Reduce Media Loss,'' *J. AWWA*, **89**, 12, 47–59.

Kim, J., and Lawler, D. F. (2008) ''Influence of particle characteristics on filter ripening,'' Separation Sci. and Technol., **43**, 7, 1583–1594.

Kim, J., Nason, J. A., and Lawler, D. F. (2008) ''Influence of Surface Charge Distributions and Particle Size Distributions on Particle Attachment in Granular Media Filtration,'' *ES&T*, **42**, 7, 2557–2562.

Kozeny, J. (1927a) Ueger Kapillare Leutung des Wassers im Boden (On Cappillary Conduction of Water in Soil), *Sitzungsbericht Akad. Wiss.* **136**, 271–306, Wein, Austria.

Kozeny, J. (1927b) ''Ueger Kapillare Leutung des Wassers im Boden (On Cappillary Conduction of Water in Soil),'' *Wasserkraft Wasserwirtschaft*, **22**, 67–78.

Krasner, S. W., Sclimenti, M. J., and Coffey, B. M. (1993) ''Testing Biologically Active Filters for Removing Aldehydes Formed During Ozonation,'' *J. AWWA*, **85**, 5, 62–71.

Lang, J. S., Giron, J. J., Hansen, A. T., Trussell, R. R., and Hodges, W. E. J. (1993) ''Investigating Filter Performance as a Function of the Ratio of Filter Size to Media Size,'' *J. AWWA*, **85**, 10, 122–130.

Levich, V. G. (1962) *Physicochemical Hydrodynamics*, Prentice-Hall, Englewood Cliffs, NJ.

Miltner, R. J., Summers, R. S., and Wang, J. Z. (1995) ''Biofiltration Performance: Part 2, Effect of Backwashing,'' *J. AWWA*, **87**, 12, 64–70.

Monk, R. D. G. (1984) ''Improved Methods of Designing Filter Boxes,'' *J. AWWA*, **76**, 8, 54–59.

Moran, M. C., Moran, D. C., Cushing, R. S., and Lawler, D. F. (1993) ''Particle Behavior in Deep-Bed Filtration: Part 2—Particle Detachment,'' *J. AWWA*, **85**, 12, 82–93.

O'Melia, C. R. (1985) ''Particles, Pretreatment, and Performance in Water Filtration,'' *J. Environ. Eng.*, **111**, 6, 874–890.

O'Melia, C. R., and Shin, J. Y. (2001) ''Removal of Particles Using Dual Media Filtration: Modeling and Experimental Studies,'' *Water Sci. Technol.: Water Supply*, **1**, 4, 73–79.

O'Melia, C. R., and Stumm, W. (1967) ''Theory of Water Filtration,'' *J. AWWA*, **59**, 11, 1393–1411.

Poiseuille, J. (1841) *Reserches Experimentales sur le Mouvement des Liquides dans les Tubes de tres Petits Dimetres* [in french], Comptes Rendus de l'Academie des Sciences, Paris, France.

Price, M. L., Enos, A. K., Bailey, R., Hermanowicz, S. W., and Jolis, D. (1993) ''Evaluation of Ozone-Biological Treatment for Reduction of Disinfection By-Products and Production of Biologically Stable Water,'' *Ozone Sci. Eng.*, **15**, 2, 95–130.

Rajagopalan, R., and Tien, C. (1976) ''Trajectory Analysis of Deep-Bed Filtration with the Sphere-in-Cell Porous Media Model,'' *AIChE J.*, **22**, 3, 523–533.

Raveendran, P., and Amirtharajah, A. (1995) ''Role of Short-Range Forces in Particle Detachment During Filter Backwashing,'' *J. Environ. Eng.*, **121**, 12, 860–868.

Seelaus, T. J., Hendricks, D. W., and Janonis, B. A. (1986) ''Design and Operation of a Slow Sand Filter,'' *J. AWWA*, **78**, 12, 35–41.

Servais, P., and Joret, J. C. (1999) BOM in Water Treatment, in M. Prevost (ed.), *Biodegradable Organic Matter in Drinking Water*, American Water Works Association Research Foundation, Lewis Publisher, Boca Raton, FL.

Slezak, L. A., and Sims, R. C. (1984) ''The Application and Effectiveness of Slow Sand Filtration in the United States,'' *J. AWWA*, **76**, 12, 38–43.

Streeter, V. L., and Wylie, E. B. (1979) *Fluid Mechanics*, McGraw-Hill, New York.

Sontheimer, H., and Hubele, C. (1987) The Use of Ozone and Granular Activated Carbon in Drinking Water Treatment, pp. 7–8, in P. M. Huck and P. Toft (eds.), *Treatment of Drinking Water Organic Contaminants*, Pergamon Press, Oxford, UK.

Teefy, S. (2001) Personal communication, Alameda County Water District, Fremont, CA.

Tien, C. (1989) *Granular Filtration of Aerosols and Hydrosols*, Butterworths, Boston.

Tien, C., and Payatakes, A. C. (1979) ''Advances in Deep Bed Filtration,'' *AIChE J.*, **25**, 5, 737–759.

Tobiason, J. E., and O'Melia, C. R. (1988) ''Physicochemical Aspects of Particle Removal in Depth Filtration,'' *J. AWWA*, **80**, 12, 54–64.

Trussell, R. R., and Chang, M. (1999) ''Review of Flow through Porous Media as Applied to Head Loss in Water Filters,'' *J. Environ. Eng.*, **125**, 11, 998–1006.

Trussell, R. R., Chang, M. M., Lang, J. S., and Hodges, W. E., Jr. (1999) ''Estimating the Porosity of a Full-Scale Anthracite Filter Bed,'' *J. AWWA*, **91**, 12, 54–63.

Trussell, R. R., Trussell, A., Lang, J. S., and Tate, C. (1980) ''Recent Developments in Filtration System Design,'' *J. AWWA*, **73**, 12, 705–710.

Tufenkji, N., and Elimelech, M. (2004) ''Correlation Equation for Predicting Single-Collector Efficiency in Physicochemical Filtration in Saturated Porous Media,'' *Environ. Sci. Technol.*, **38**, 2, 529–536.

Urfer, D., Huck, P. M., Booth, S. D. J., and Coffey, B. M., (1997) ''Biological filtration for BOM and Particle Removal: A critical Review,'' *J. AWWA*, **89**, 12, 83–98.

U.S. EPA (1989) ''National Primary Drinking Water Regulations: Filtration and Disinfection; Turbidity, *Giardia lamblia*, Viruses, *Legionella*, and Heterotrophic Bacteria; Final Rule,'' *Fed. Reg.*, **54**, 124, 27486.

U.S. EPA (2001) *Factoids: Drinking Water and Ground Water Statistics for 2000*, U.S. Environmental Protection Agency, Office of Water, Washington, DC.

U.S. EPA (2002) ''National Primary Drinking Water Regulations: Long Term 1 Enhanced Surface Water Treatment Rule; Final Rule,'' *Fed. Reg.*, **67**, 9, 1812.

U.S. EPA (2006) ''National Primary Drinking Water Regulations: Long Term 2 Enhanced Surface Water Treatment Rule; Final Rule,'' *Fed. Reg.*, **71**, 3, 654–786.

Veerapaneni, S. and Wiesner, M.R.. (1997) ''Deposit Morphology and Head Loss Development in Porous Media,'' *Environ. Sci. Technol.*, **31**, 10, 2738–2744.

Visscher, J. T. (1990) ''Slow Sand Filtration: Design, Operation, and Maintenance,'' *J. AWWA*, **82**, 6, 67–71.

Wiesner, M.R.. (1999) ''Morphology of Particle Deposits,'' *J. Environ. Eng.*, **125**, 12, 1124–1132.

Yao, K.-M., Habibian, M. T., and O'Melia, C. R. (1971) ''Water and Waste Water Filtration: Concepts and Applications,'' *Environ. Sci. Technol.*, **5**, 11, 1105–1112.